N84- 26165

DOE/NASA/0205-8
NASA CR-174660

FULL SCALE PHOSPHORIC ACID FUEL CELL STACK TECHNOLOGY DEVELOPMENT

FINAL TECHNICAL REPORT

L. Christner, M. Farooque
Energy Research Corporation
3 Great Pasture Road
Danbury, CT 06810

MARCH 1984

NOTICE

ENERGY RESEARCH CORPORATION

LIST OF CONTRIBUTORS

J. Ahmad

B. Baker

T. Benjamin

L. Christner

M. Farooque

M. George

D. Kelley

H. Maru

S. Perkari

M. Puskar

A. Skok

B. Snitzer

EXECUTIVE SUMMARY

The present program was directed at improving the technology base for phosphoric acid fuel cells. The initial emphasis was placed on an atmospheric pressure operation, but later the emphasis was shifted to a pressurized operation. The following areas were investigated:

- Materials Evaluation and Development
- Component Fabrication Development
- Endurance Testing of New Components and Materials
- Development of Catalysts for Pressurized Operation
- Facility Construction for Pressurized Testing

Significant progress was achieved during the program in improving the technology of critical cell components. Bipolar plate samples were fabricated with different resin contents and samples were heat-treated at various temperatures between 900 and 2700°C to improve their corrosion resistance. Physical properties of these plates were characterized and their corrosion behavior was investigated at atmospheric as well as elevated pressure. This effort has provided a strong data base for optimization of bipolar plates. Different carbon support materials and heat-treatments were investigated to impart improved cathode stability for pressurized operation. Initial performance improvements of 25 to 40 mV were obtained by the addition of vanadium, tantalum or chromium to the standard platinum-on-carbon cathode. Stability of these "alloy" catalysts, however, needs to be improved. Short stacks assembled with heat treated plates were operated for up to 22,000 hours. After termination of the contract, one of the stacks continued further operation under in-house funds. These and other highlights of the program are summarized below.

- Bipolar plate samples containing graphite powder and 30 to 80 wt% phenolic resin were molded and heat-treated from 900 to 2700°C. Heat-treatment beyond 900°C resulted in a glassy-carbon/graphite composite with increasingly improved corrosion resistance. Porosity measurements, however, revealed that while there was a gradual

increase in porosity between 900 to 1600°C, a rapid increase in porosity accompanied the heat treatments at temperatures beyond ~1600°C. Although the transition point was not accurately defined in this program, it appears that the magnitude of residual porosity can be controlled to a certain extent by improved mixing (e.g, by commercial compounding) and/or other manufacturing changes.

- Corrosion measurements on these bipolar plates at 1 atm showed that corrosion rates decreased 3 orders of magnitude when heat-treatment temperature was increased from 900°C to 2700°C. Tests of corrosion at elevated pressure agreed with the atmospheric pressure behavior and suggested that the only apparent effect of pressure would be to raise the corrrosion potential and lower the operating acid concentration. Both of these effects raised the corrosion rates significantly. Temperature also had a very strong effect on the corrosion rate. The apparent activation energy was in the range of 55 to 65 kcal/mol.

- Development of cost effective fabrication processes for full-scale cell components continued during this program. Improvements in the molding operation culminated in the demonstration of a 45 second pressing cycle for the bipolar plate.

- A selectively wetproofed anode backing was developed to provide an acid inventory control member (AICM). This member can help with acid expansion and storage during startup and transients. The member was reproducibly manufactured by simple stamp printing. Operation of a short stack with this member showed satisfactory performance.

- Eight multicell stacks with heat-treated plates (3 to 23 cells) were endurance tested during this program. Six of these stacks exceeded one year of continuous operation. Among these six, two stacks exceeded 2-1/2 years of continuous operation. This testing demonstrates a significant confidence level in component durability and stacking concepts.

- Various platinum loadings of the anode and cathode were investigated in several laboratory-scale cells. A short stack, containing half the standard platinum loading on both the anodes as well as cathodes, showed decay rates no greater than those observed with standard platinum loadings. Feasibility of lower platinum loadings (total Pt 0.35 mg/cm^2) was therefore demonstrated.

- The investigation of alternate cathode catalyst supports included heat-treated Vulcan XC-72 and Shawinigan acetylene black. The as-received Shawinigan, and the heat-treated carbons showed improved corrosion resistance and a somewhat better endurance (as compared with the standard carbon) in a limited number of laboratory-scale tests.

•   Additions of vanadium, tantalum and chromium metals to the standard platinum-on-carbon catalyst showed 25 to 40 mV improved performance during the initial period which is equivalent to a 5% improvement in the heat rate. A dissolution of the additives at operating conditions after several thousand hours operation, however, diminished the improvements to a certain degree. Stabilization of these additives is therefore needed. The results obtained so far suggest that chromium is the most stable additive of the three.

•   A pressurized facility for testing short stacks with full size cells was designed and constructed during the program.

ENERGY RESEARCH CORPORATION

TABLE OF CONTENTS

ENERGY RESEARCH CORPORATION

TABLE OF CONTENTS (concluded)

LIST OF FIGURES

LIST OF FIGURES (continued)

LIST OF FIGURES (concluded)

LIST OF TABLES

ENERGY RESEARCH CORPORATION

LIST OF TABLES (concluded)

THIS PAGE INTENTIONALLY LEFT BLANK

SECTION 1

MATERIALS EVALUATION AND DEVELOPMENT

The materials effort for this program focused on the development and evaluation of the bipolar plate. It is the backbone of the fuel cell stack and must be an impermeable, acid resistant separator for the fuel and oxidant. ERC's previous programs, EC-77-C-03-1404 and DEN3-67, had determined that some thermoplastic and thermosetting resins were marginally resistant to 100% H_3PO_4 at 185°C and 1 atm pressure. Preliminary testing of the bipolar plates heat-treated at 900°C in nitrogen were shown to be an order of magnitude more resistant than nonheat-treated plates. The present program was structured to extend these initial results by evaluating the effects of material composition (resin/graphite ratio), final heat-treatment temperature, sample geometry and test conditions on the physicochemical properties of the bipolar plates. This effort was divided into the following areas which will be discussed in this section.

- Corrosion Measurements
- Analysis of Possible Poisons
- Physical Properties Measurements

1.1 Corrosion Measurements

The out-of-cell corrosion measurements on bipolar plates were performed at atmospheric pressure as well as at elevated pressures. However, the bulk of the results reported below were obtained at atmospheric pressure while the apparatus for the pressurized measurements was being developed.

1.1.1 Equipment

Atmospheric pressure tests were performed in the cell used on ERC Contract DEN3-67 (see Figure 1.1). The aparatus consisted of a Teflon beaker

ENERGY RESEARCH CORPORATION

Item No.	Description
1	BOTTLE
2	COVER
3	WORKING ELECTRODE TUBE
4	ELECTRODE HOLDER
5	REF ELECTRODE TUBE
6	PLUG
7	TOP PLUG
8	CENTER PLUG
9	FRAME
10	SET COLLAR
11	ELECTRODE ROD
12	TUBE
13	TUBE
14	THERMOMETER
15	SCREWS
16	SAMPLE ELECTRODE
17	NUTS
18	OUTER JAR
19	SET SCREWS
20	THERMO-COLLAR

SECTION AA

SECTION BB

D0927
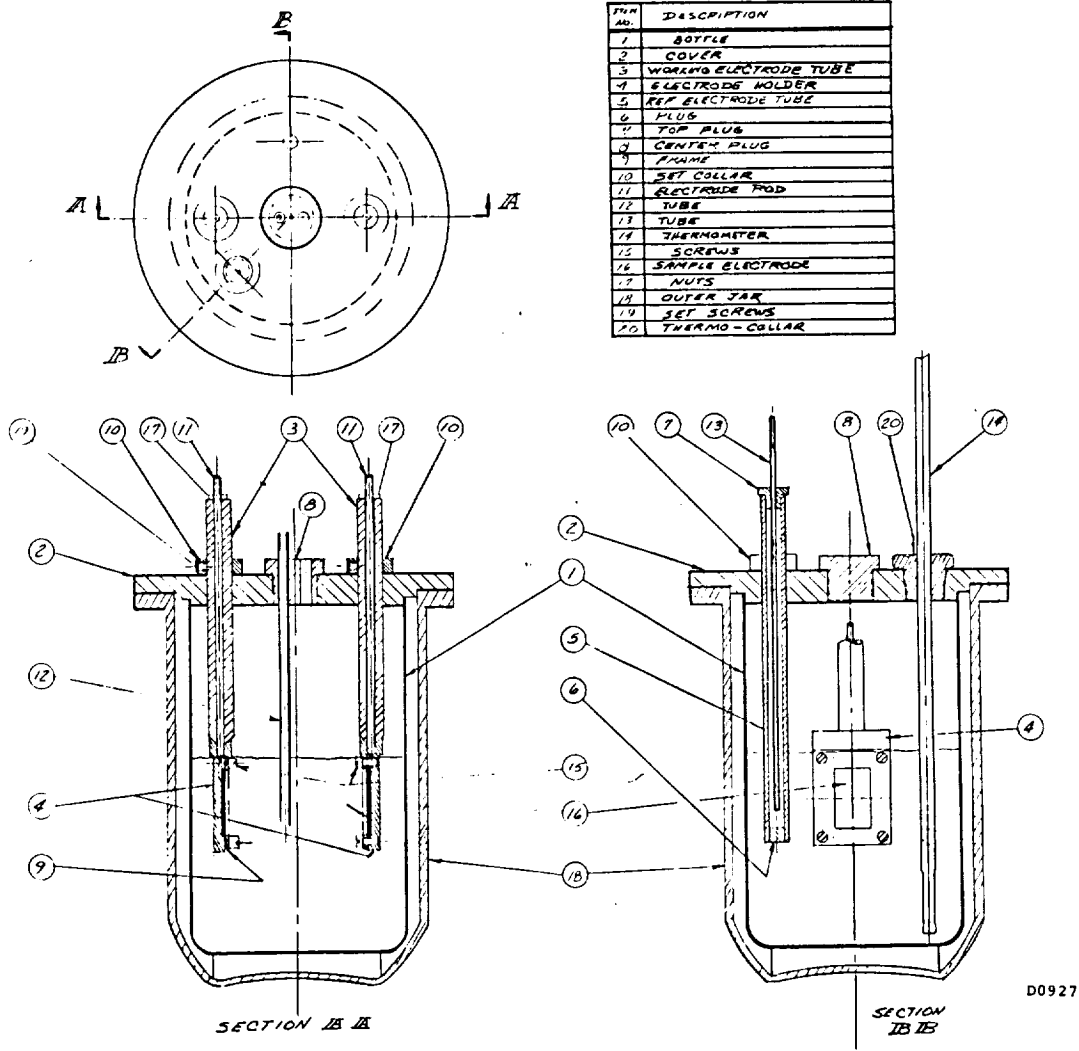
FIGURE 1.1   CROSS-SECTIONAL VIEWS OF THE CORROSION CELL
(1 atmosphere)

ENERGY RESEARCH CORPORATION

cut to fit in a Pyrex reaction kettle with a Teflon plate cover. Teflon was used to make the body of the cell and its fittings, and a standard reversible hydrogen electrode was used as the reference. Test samples were mounted on Teflon supports with only one surface of the sample exposed to the electrolyte. A Pt black counter-electrode of the same size was used to ensure uniform current distribution. Electrical connections were accomplished via a 0.32 cm diameter stainless steel rod covered with heavy wall Teflon tubing. The gold connecting wire was also covered with heat shrinkable Teflon. The central plug provided a flexibililty for choosing the proper cell environment.

The vessel for pressurized corrosion testing was purchased from Berghof, Inc. It is a Teflon lined pressure vessel with appropriate penetrations for gases and electrical connections as shown in Figure 1.2. The cell design as shown in Figure 1.3 uses Teflon for all structural components.

A special reference electrode must be used for controlling the potential since it will be working in 100 to 103% H_3PO_4 at 180 to 205°C and 343 to 1013 kPa. No reference electrodes are commercially available to operate in this environment. Furthermore, a H_2 bubbling reference electrode can not be easily adapted for this use. Therefore, a dynamic hydrogen electrode was used for this application. A sketch of this electrode is shown in Figure 1.4. It consists of two platinum black electrodes (A and B). On electrode (A), H_2 is evolved under a constant current of approximately 1 mA/cm^2. Since O_2 is evolved on Electrode B (anode) it is kept approximately 1.5 cm higher than the hydrogen electrode (A). This avoids diffusion of oxygen to the H_2 evolving electrode. Both electrodes are housed in a Teflon tube (E) which has a Luggin capillary (D) at the bottom. The top of this tube is filled with a platinum black catalyst (C) which is used to recombine the electrolytic hydrogen and oxygen. The water formed by this reaction maintains the acid concentration in the reference electrode chamber and also prevents accumulation of H_2 in the pressurized vessel. This reference electrode was frequently calibrated at 1 atm against a reversible hydrogen electrode and also against a calomel electrode giving only 2 mV hydrogen overpotential through the calibration period.

A number of special concerns had to be addressed to ascertain the reliability of the data collected from these two corrosion cells. Acid

PRESSURE GAUGE

TRAP FOR H_3PO_4 VAPOR

THERMOCOUPLE PORT

ELECTRICAL CONNECTIONS

GAS CONNECTION

PRESSURE VESSEL

TEFLON WALL

D1917
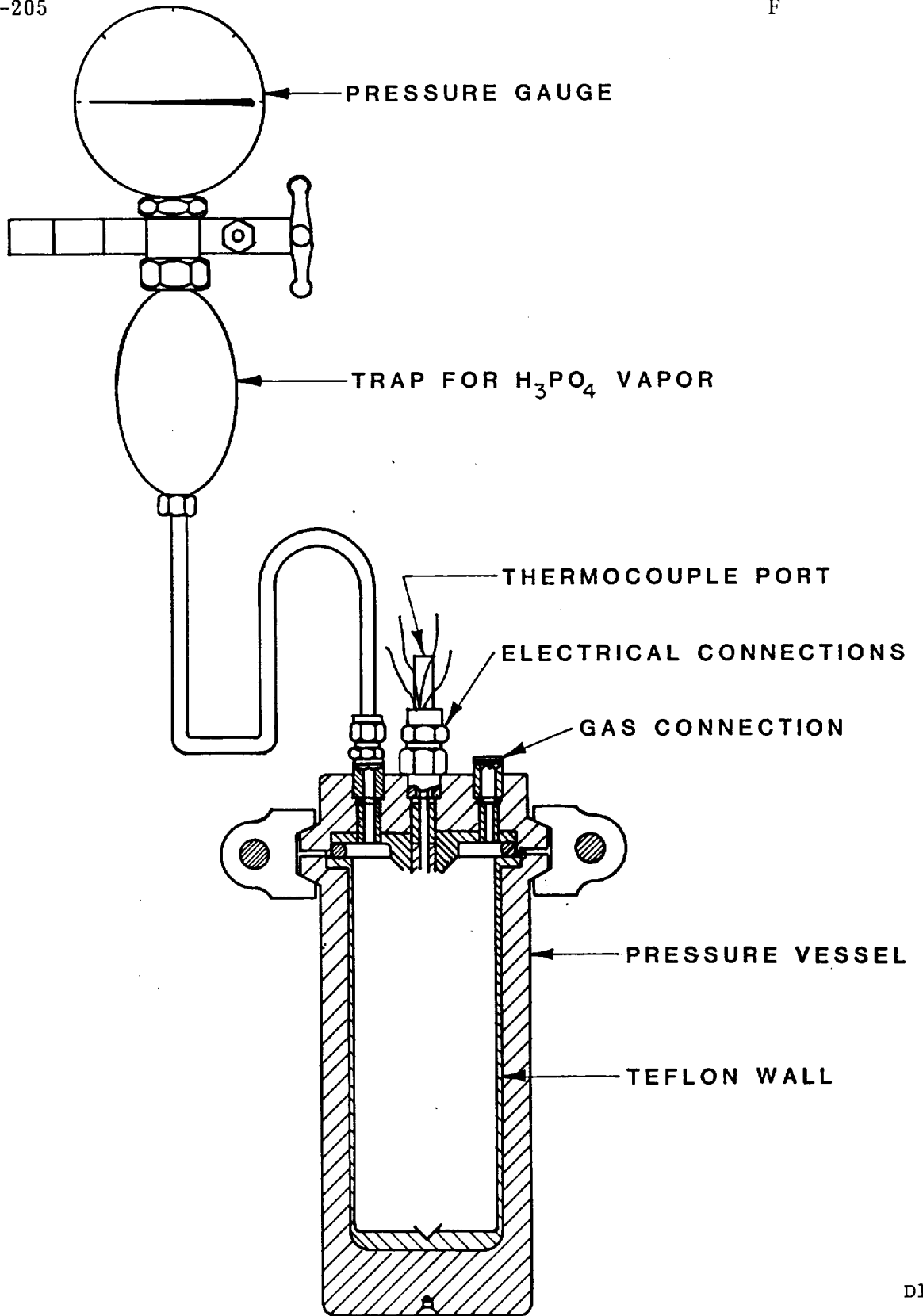
FIGURE 1.2   PRESSURE VESSEL FOR CORROSION STUDIES

A) TEFLON CELL BODY	G) ROD FOR WIRE WINDING
B) DYNAMIC HYDROGEN ELECTRODE	H) WIRE SEAL
C) GOLD SCREEN (Current Collector)	I) TOP COVER OF PRESSURIZED VESSEL
D) WORKING ELECTRODE CAVITY	J) CONNECTION WIRES COVERED WITH
E) LUGGIN CAPILLARY	HEAT SHRINKABLE TEFLON
F) COUNTER ELECTRODE CAVITY	K) Pt BLACK CATALYST
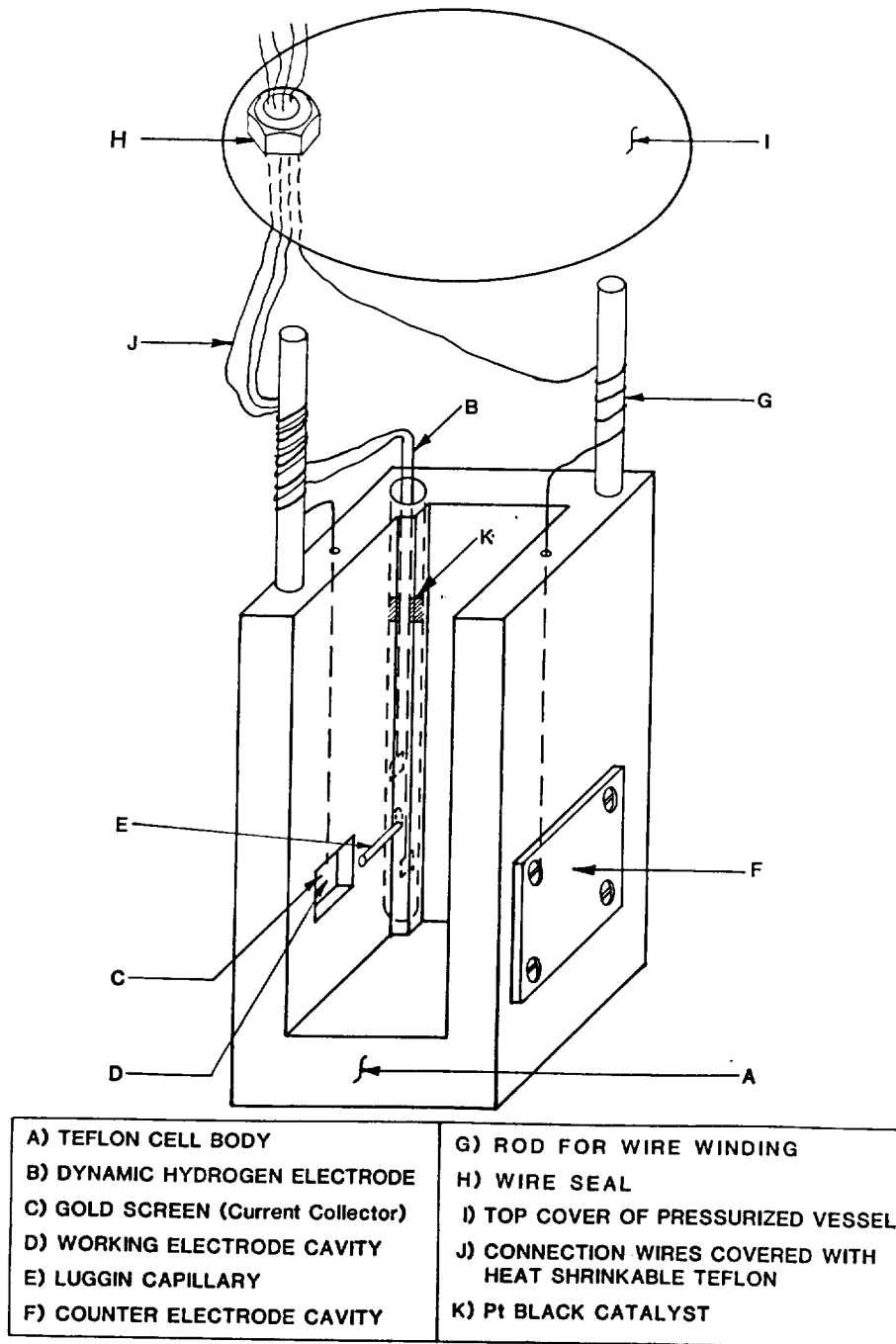
D1860-1

FIGURE 1.3   CELL DESIGN FOR PRESSURIZED CORROSION STUDY

A. H$_2$ Evolving Electrode
B. O$_2$ Evolving Electrode
C. Catalyst Bed
D. Luggin Tip
E. Teflon Tube
F. Power Supply
G. Ammeter
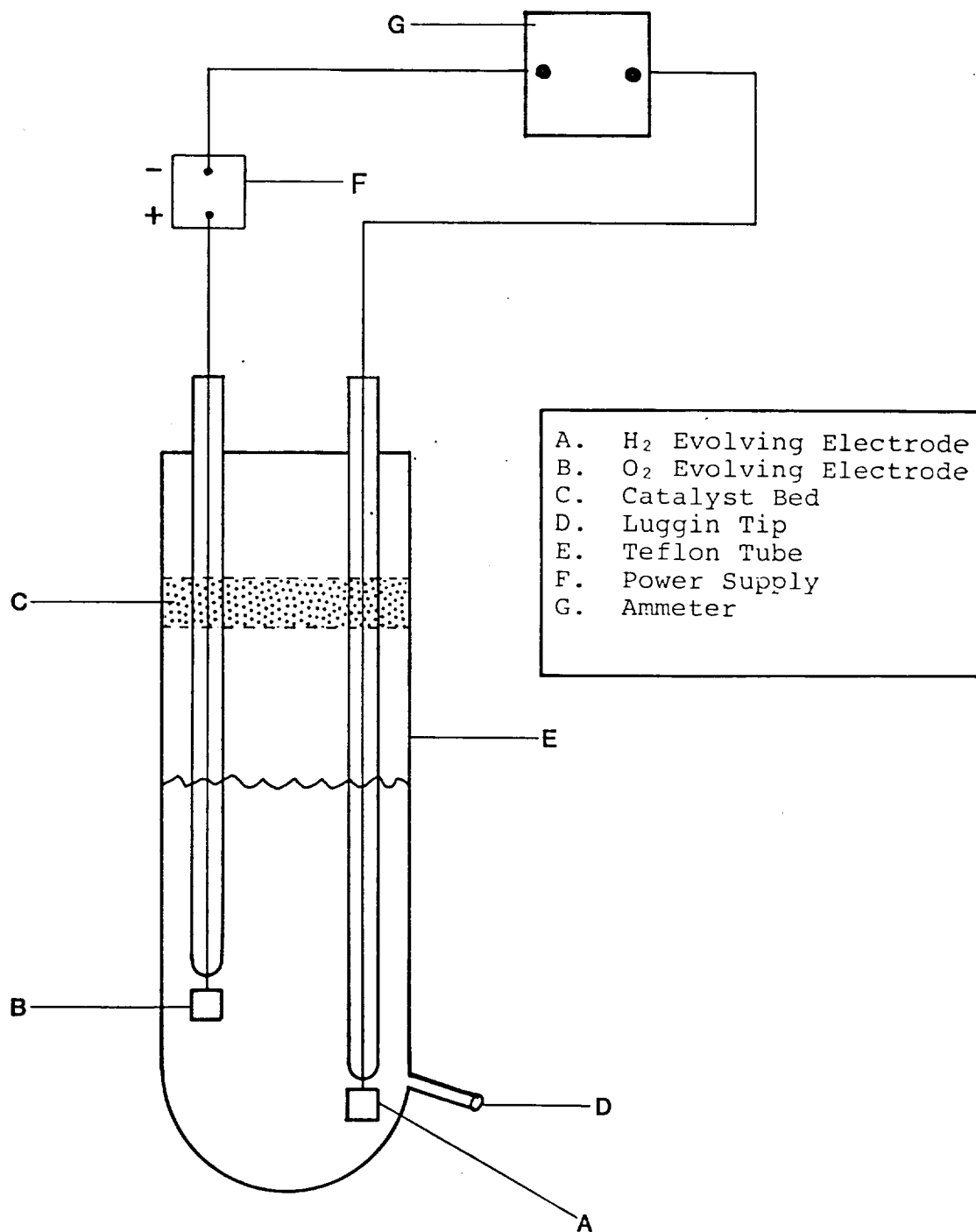
FIGURE 1.4   DYNAMIC HYDROGEN ELECTRODE (Reference Electrode)
FOR THE PRESSURIZED CORROSION STUDY

D1861R

ENERGY RESEARCH CORPORATION

concentrations before and after the experiments were checked and found to vary only a small amount (i.e., 1 to 2 wt%). Samples were corroded for varying lengths of time and Tafel slopes measured. The Tafel slopes changed as a function of time, unless the material was precorroded at or above 0.8V for at least 24 hours. Even with this pretreatment, the corrosion current varied by as much as a factor of three for similarly prepared material. This variability does not seem to be related to the experimental technique. Samples could be removed, washed and returned to the corrosion cell without any change in the corrosion rate. It therefore appears that the variability is primarily related to the chemical properties of the samples.

1.1.2 Materials

Most of the materials being studied were molded composites of thermo-setting phenolic resins and Asbury A-99 graphite which were heated to various temperatures in nitrogen. Another portion of the study evaluated the corrosion of heat-treated and nonheat-treated carbon blacks. The composite materials were dry blended and hot pressed into flat sheets before being cut into small pieces. The carbon blacks were mixed with 5 to 10% Teflon and rolled into sheets.

1.1.3 Corrosion Data At 1 Atmosphere

An examination of the corrosion characteristics of individual components in the bipolar plate (heat-treated phenolic resin and the graphite filler particles) was reported in ERC's DEN3-67 Final Report. A plot of their current/voltage relationship is shown in Figure 1.5. Heat-treated resin and graphite appear to have similar stable corrosion rates which are considerably lower than those for nonheat-treated molded plates. The heat-treatment to higher temperatures dramatically decreases the corrosion rate as indicated in Figures 1.6 and 1.7. Decreasing the rate by three orders of magnitude from 4×10^{-2} to 3×10^{-5} mA/cm^2 should provide sufficient corrosion protection for 40,000 hours of operation. These materials, however, have increased porosity when heat-treated
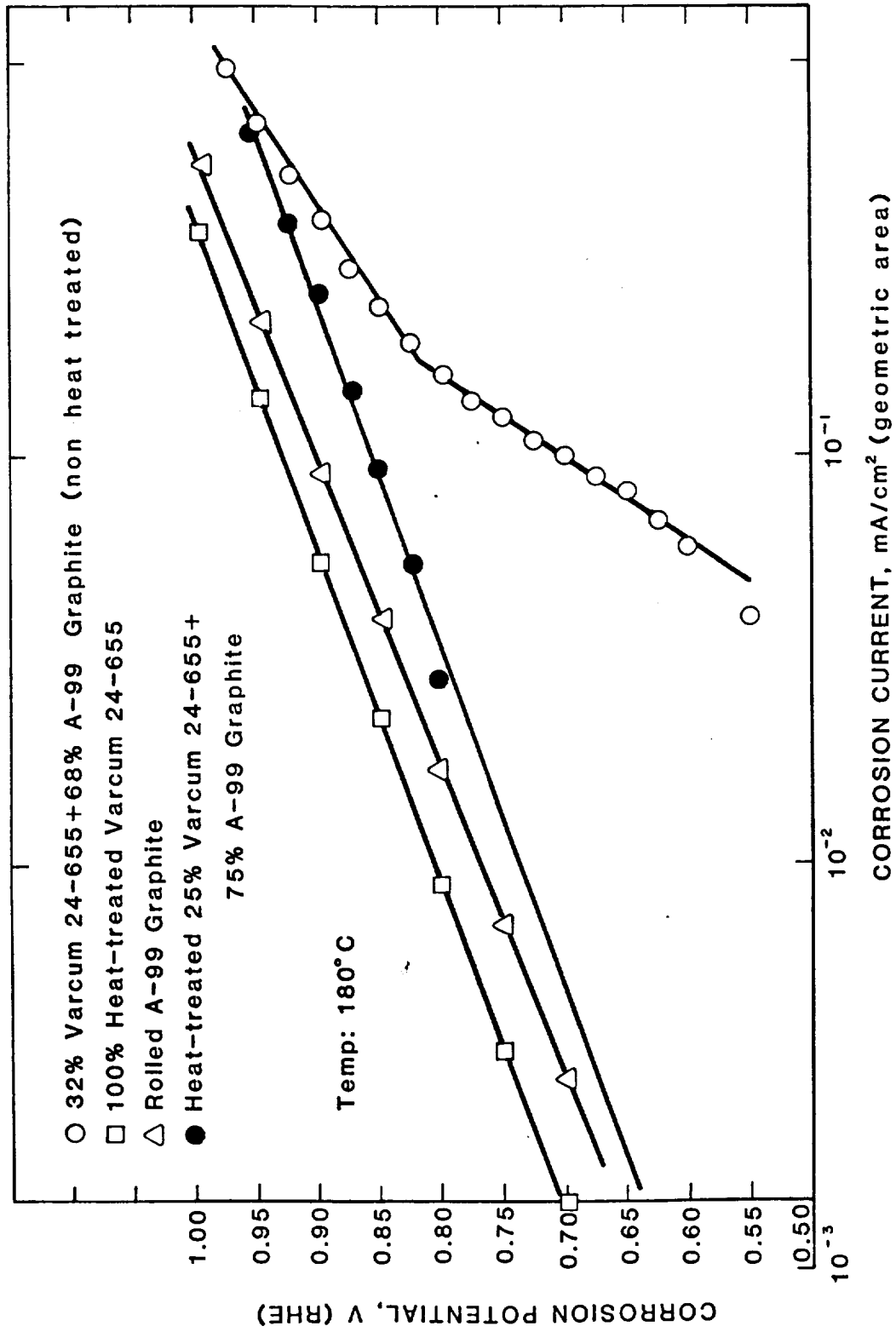
FIGURE 1.5   POLARIZATION CURVES OF VARIOUS BIPOLAR PLATE MATERIALS
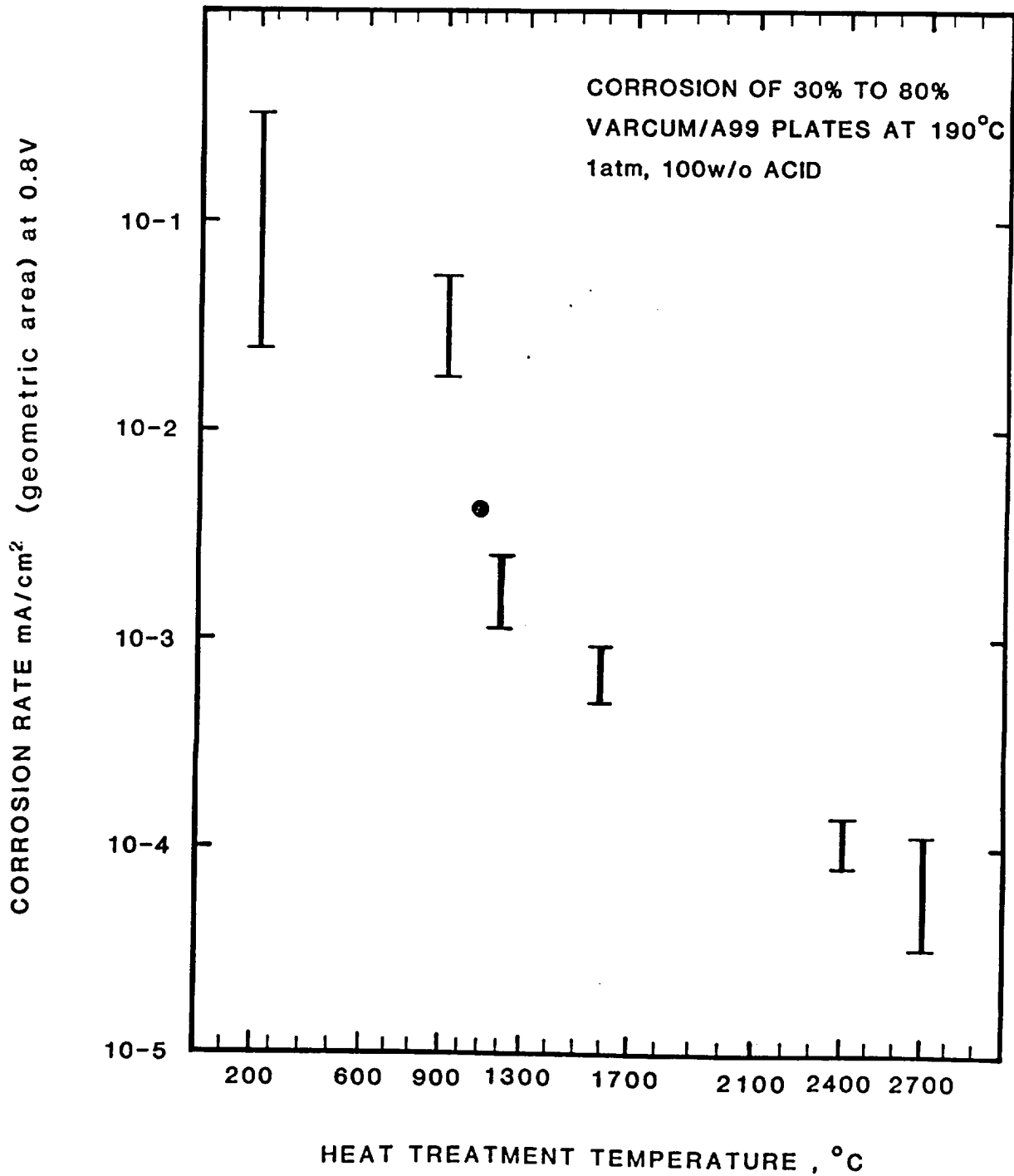
D1332aR1

FIGURE 1.6 EFFECT OF HEAT-TREATMENT TEMPERATURE ON CORROSION RATE
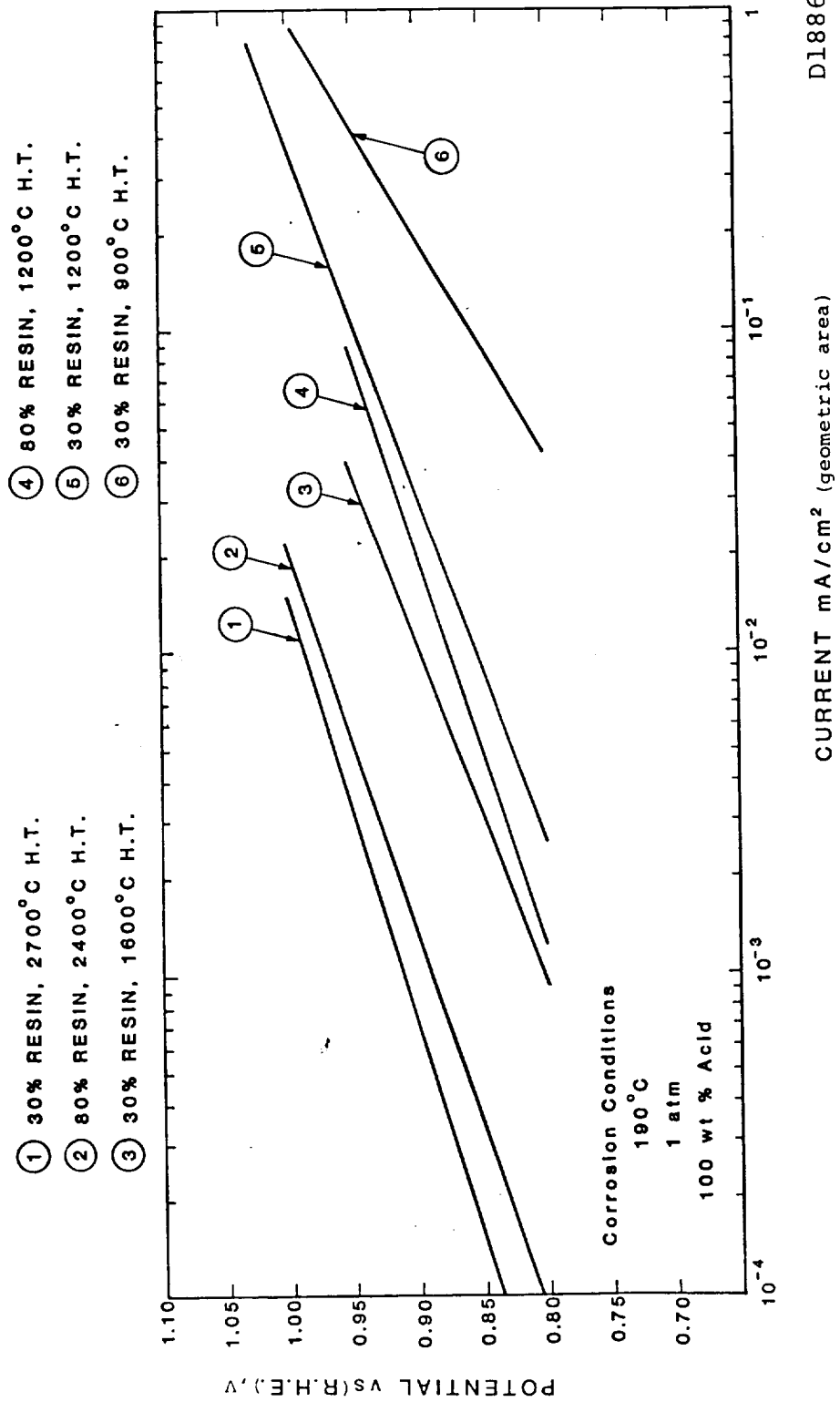
FIGURE 1.7   POLARIZATION PLOTS FOR CORROSION OF RESIN/GRAPHITE
COMPOSITE MATERIALS AT DIFFERENT TEMPERATURES

ENERGY RESEARCH CORPORATION

above 1600°C. This will be discussed in a later section, but the porosity is important when considering what the best heat-treatment temperature might be. Based on our present state of information, 1600 or 2700°C should be used for pressurized operation, while 900°C is satisfactory for atmospheric conditions.

The corrosion conditions have a strong influence on the measured rate. As expected, temperature and potential have the greatest effect on the corrosion rate. Activation energies in the range of 50 to 65 kcal/mol were measured for Asbury A-99 graphite (Figure 1.8, Table 1.1) and the heat-treated graphite/resin composites (Table 1.2).

In addition to the controlled variables, the samples probably had some variability in themselves. To evaluate this possiblity, samples were cut from a single large plate and tested individually. The results shown in Figure 1.9 demonstrate that the measured corrosion rate at 0.9V and 190°C in 100 wt% H_3PO_4 for the 900°C heat-treated graphite/resin composite is 0.12 to 0.31 mA/cm^2 and is independent of the location within the large plate. The corrosion rate decreased and leveled off after approximately 100 hours for most samples but required 1,000 hours for Sample B1. The reason for the decreasing corrosion rate is not clearly understood at this time, but is generally observed for all the corrosion experiments performed in this laboratory.

1.1.4 Study of Pressure, Temperature, and Acid Concentration Effects on Corrosion

The corrosion rates of 900 and 1200°C heat-treated 30 wt% resin bipolar plate materials were evaluated at utility fuel cell operating conditions (voltage 0.7 to 1.0 (RHE), pressure 343 to 689 kPa, and temperature 180 to 205°C). The polarization plot at 689 kPa pressure along with the plots at two other pressures are compared in Figure 1.10. Similarly, the polarization plots obtained for the 1200C heat-treated 30 wt% resin at various pressures are compared in Figure 1.11. The results indicate that the effect of applied pressure on the corrosion rate of the bipolar plate was not very significant. The increase in the applied pressure decreases the carbon corrosion overpotential resulting in a lower

FIGURE 1.8   CORROSION OF A-99 GRAPHITE AS A FUNCTION OF TEMPERATURE

TABLE 1.1 KINETIC PARAMETERS OF A-99 GRAPHITE CORROSION

MATERIAL COMPOSITION	TEMPERATURE, °C	BETWEEN 0.6 AND 1.2V (RHE)			ACTIVATION ENERGY, ΔE kcal/mol
		Tafel Slope, $\frac{RT}{\alpha F} \times 2.303$ mV/decade	Transfer Coeff., $\overset{\rightarrow}{\alpha}$	Exchange Current Density, i_0 $(mA/cm^2) \times 10^7$	
90% A-99 Graphite + 10% Teflon	190	142	0.65	1.4	63
	183	125	0.72	0.15	
	173	110	0.8	2.2×10^{-2}	
	165	93	0.94	4.5×10^{-4}	

ENERGY RESEARCH CORPORATION

TABLE 1.2 KINETIC PARAMETERS OF VARIOUS HEAT-TREATED SAMPLES AT 190°C
(Acid Conc. = 100 to 102% H$_3$PO$_4$) 1 atm.

| SAMPLE COMPOSITION (w/o) | | DENSITY g/cm^3 | HEAT-TREATMENT TEMPERATURE, °C | EXCHANGE CURRENT DENSITY i$_o$, mA/cm^2 | TRANSF. COEFF. α | TAFEL SLOPE mV/DECADE | | COMPOSITION CURRENT @ 0.8V, mA/cm^2 |
% VARCUM 29-703	% A-99 GRAPHITE					STEP TAFEL	SWEEP TAFEL	
30	70	1.899	900	3.3×10^{-7}	0.68	135	-	4.3×10^{-2}
40	60	1.870	900	4.4×10^{-8}	0.77	119	149	2.3×10^{-2}
80	20	1.620	900	7.9×10^{-9}	0.88	104	127	2.7×10^{-2}
30	70	1.826	1200	5.0×10^{-11}	1.04	89	123	2.5×10^{-3}
80	20	1.617	1200	2.0×10^{-12}	1.18	78	110	1.2×10^{-3}
30	70	1.848	1600	2.8×10^{-11}	1.01	91	115	9.0×10^{-4}
80	20	1.610	1600	1.2×10^{-10}	0.93	99	147	5.0×10^{-4}
30	70	1.625	2400	9.4×10^{-17}	1.53	60	131	1.4×10^{-4}
80	20	1.588	2400	1.0×10^{-10}	0.86	106	110	8.0×10^{-5}
30	70	1.852	2700	2.6×10^{-14}	1.22	75	104	3.3×10^{-5}
80	20	1.607	2700	1.2×10^{-11}	0.94	98	96	1.2×10^{-4}

mA/cm^{2}*

(mils/yr†)

A1 0.312†† (70)	A6	B1	B6	C1 0.219 (49)
A2	A7	B2	B7	C2
A3	A8 0.124 to 0.267 (28 to 60)	B3	B8 0.229 (52)	C3
A4	A9	B4	B9	C4
A5 0.300 (68)	A10	B5· 0.276†† (63)	B10	C5 0.312 (71)

*190°C, 100 to 102% H_3PO_4, 0.9V (RHE), 100 hours

†Based on composite density = 1.7 g/cm^3

††0.7V (RHE) for 112 hours, then 0.9V (RHE) for 98 hours
Data at 210 hours total time.

D2136

FIGURE 1.9   CORROSION UNIFORMITY OF 900°C HEAT-TREATED
              FLAT PLATE (49 v/o (35 w/o) Varcum 29-703/
              A-99 Graphite, Plate 3310)

FIGURE 1.10   POLARIZATION PLOTS OF 900°C HEAT-TREATED
SAMPLE AT VARIOUS PRESSURES AND 190°C
TEMPERATURE
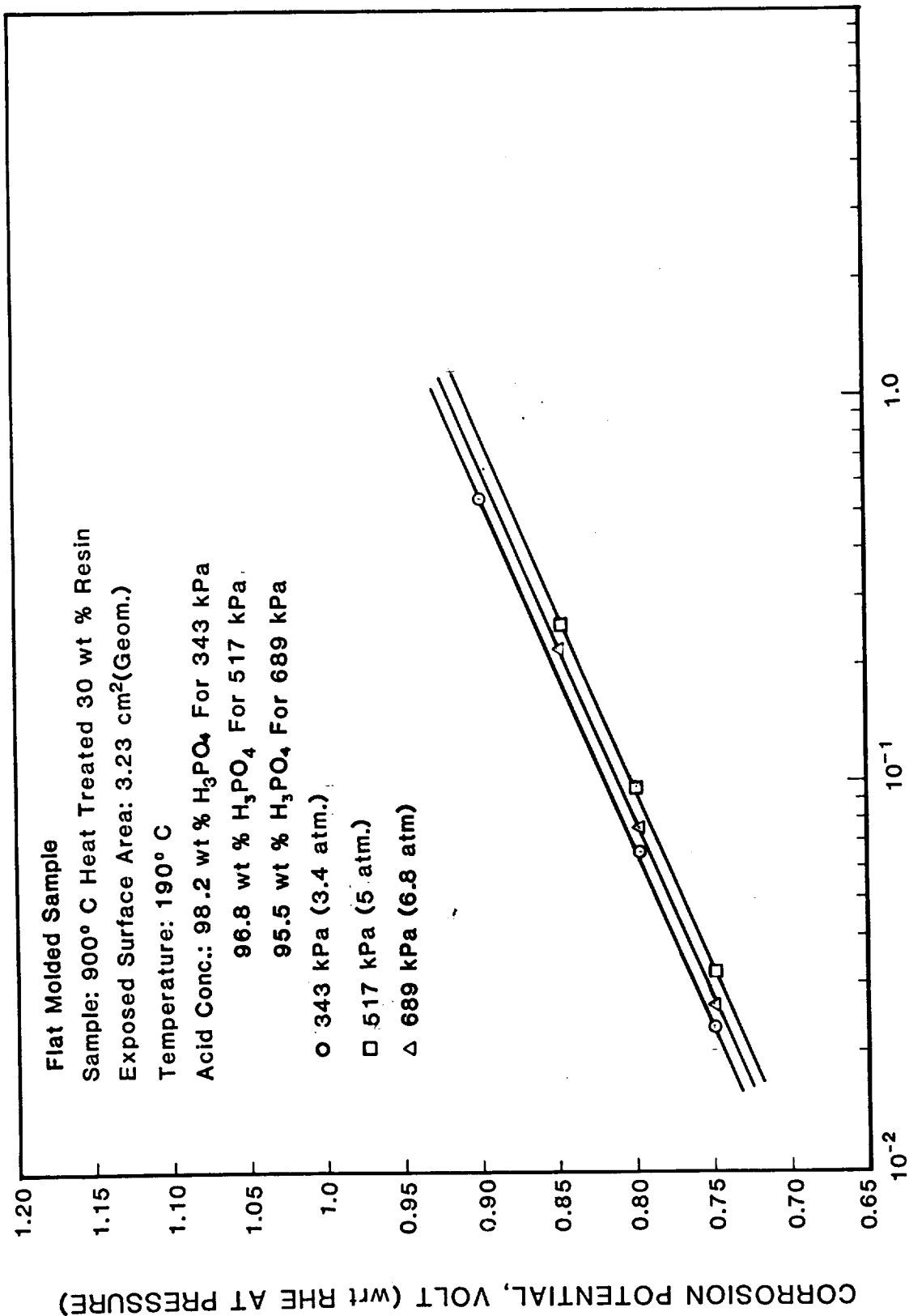
CORROSION CURRENT mA/cm^2 (Geom.)
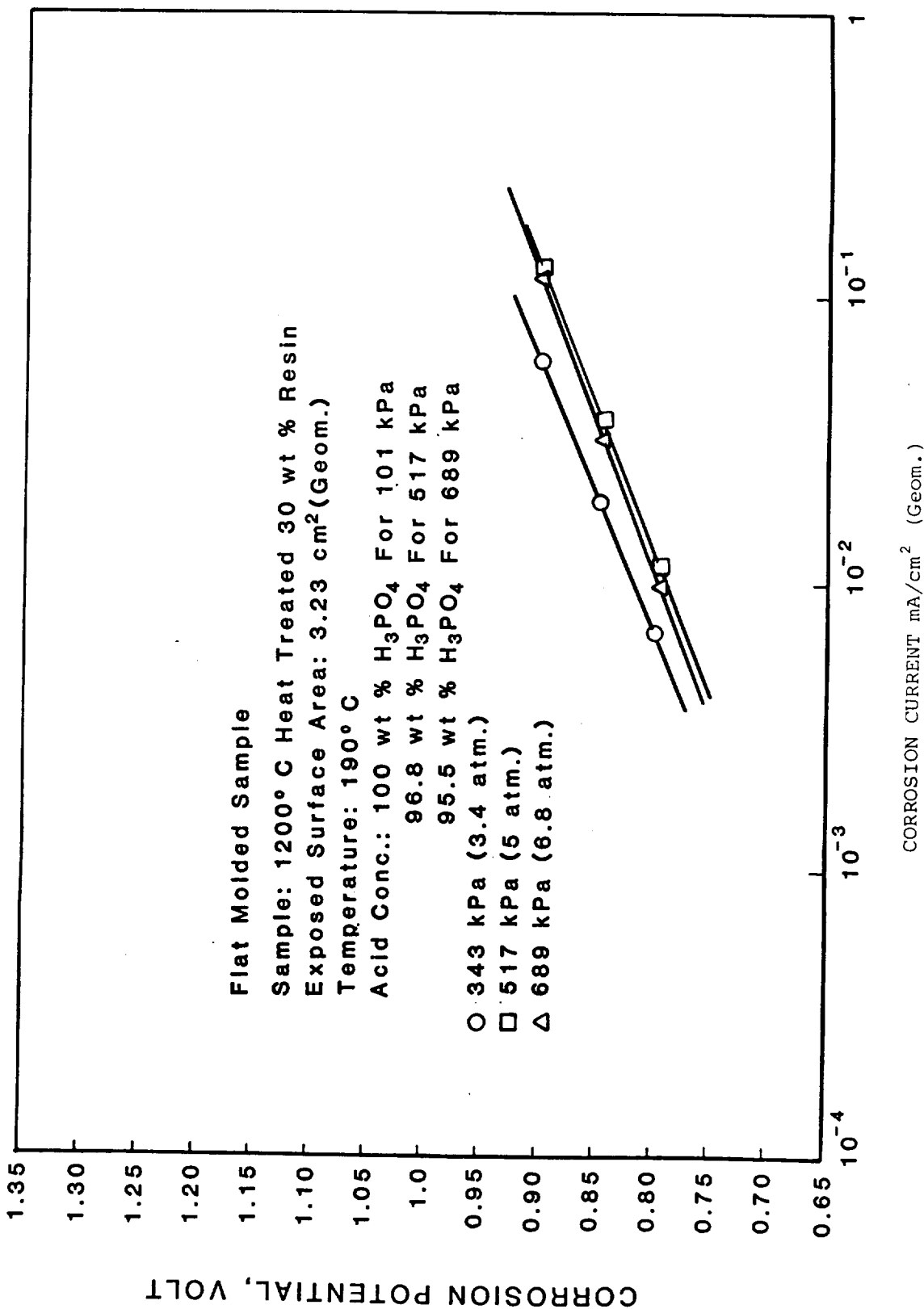
FIGURE 1.11   POLARIZATION PLOTS OF 1200°C HEAT-TREATED
              SAMPLE AT VARIOUS PRESSURES AND 190°C
              TEMPERATURE

ENERGY RESEARCH CORPORATION

corrosion current, but the lower acid concentration at high pressure causes the corrosion current to increase. The net effect of these variables on the corrosion rate at the same cathode potential (wrt RHE at pressure) was not significant. To ascertain this the 1200°C heat-treated 30 wt% resin sample was also corroded at 1 atm pressure. The obtained polarization plot is compared with the plots obtained under pressurized conditions (Figure 1.11). This comparison also indicates that the net effect of pressurization on the corrosion rate at the same cathode potential (wrt RHE at pressure) was not significant.

The corrosion currents and Tafel slopes obtained for the 900 and 1200°C heat-treated samples at various pressures and temperatures are tabulated in Table 1.3. Tafel slopes for 900 and 1200°C heat-treated materials vary between 95 to 110 mV/decade at 190 to 200°C. Tafel slopes for the 900°C heat-treated materials at different temperatures and pressures were found to be about 10 mV/decade higher than the 1200°C heat-treated material. The corrosion current for the 1200°C heat-treated sample at 0.8V (RHE at pressure), 517 kPa (5 atm) and 190°C was about an order of magnitude less than the 900°C heat-treated sample. The experimental data also shows that a decrease in the experimental temperature by 10°C at 517 kPa (5 atm) pressure and 0.8V (RHE at pressure) caused a decrease in the corrosion rate by a factor of ~2. These results suggest that in a fuel cell using 1200°C heat-treated 30 wt% bipolar plate, lowering the operating temperature by 10°C will cause lower corrosion equivalent to decreasing the cathode potential by 30 mV at constant temperature.

Determination for the 1200°C heat-treated 80 wt% resin sample is being continued to obtain the corrosion data at various pressures and temperatures.

A second 1200°C heat-treated 30 wt% resin sample was examined. The corrosion current of the sample is compared with the 900°C heat-treated 30 wt% and previously tested 1200°C heat-treated 30 wt% sample in Figure 1.12. The corrosion current of this sample at 0.8V (wrt RHE at pressure), 190°C and 343 kPa in 98 wt% of acid in 6.6 x 10^{-3} mA/cm^2 (geom.).

The experiments for 900 and 1200°C heat-treated 30 wt% resin samples were terminated after passing 1600 and 906 coulombs respectively, i.e., 5% and 2.5% of the samples were corroded. These samples were inspected visually and

ENERGY RESEARCH CORPORATION

TABLE 1.3 CORROSION RATES OF HEAT-TREATED BIPOLAR PLATE MATERIALS
AT VARIOUS TEMPERATURES AND PRESSURES

SAMPLE I.D.	CORROSION CURRENT (GEOM) mA/cm² 0.8V (RHE)						TAFEL SLOPE mV/DECADE					
	190°C			200°C			190°C			200°C		
	100%	96.8%	95.5%									
	343 kPa	517 kPa	689 kPa	343 kPa	517 kPa	689 kPa	343 kPa	517 kPa	689 kPa	343 kPa	517 kPa	689 kPa
900°C Heat-treated 30 wt% resin + 70 wt% A-99 Graphite	6.4×10^{-2}	9.28×10^{-2}	7.43×10^{-2}	2.48×10^{-1}	2.26×10^{-1}	2.1×10^{-1}	110	105	105	110	110	105
1200°C Heat-treated 30 wt% resin + 70 wt% A-99 Graphite	6.6×10^{-3}	1.25×10^{-2}	1.2×10^{-2}	2×10^{-2}	2.8×10^{-2}	3.56×10^{-2}	100	95	95	100	95	95
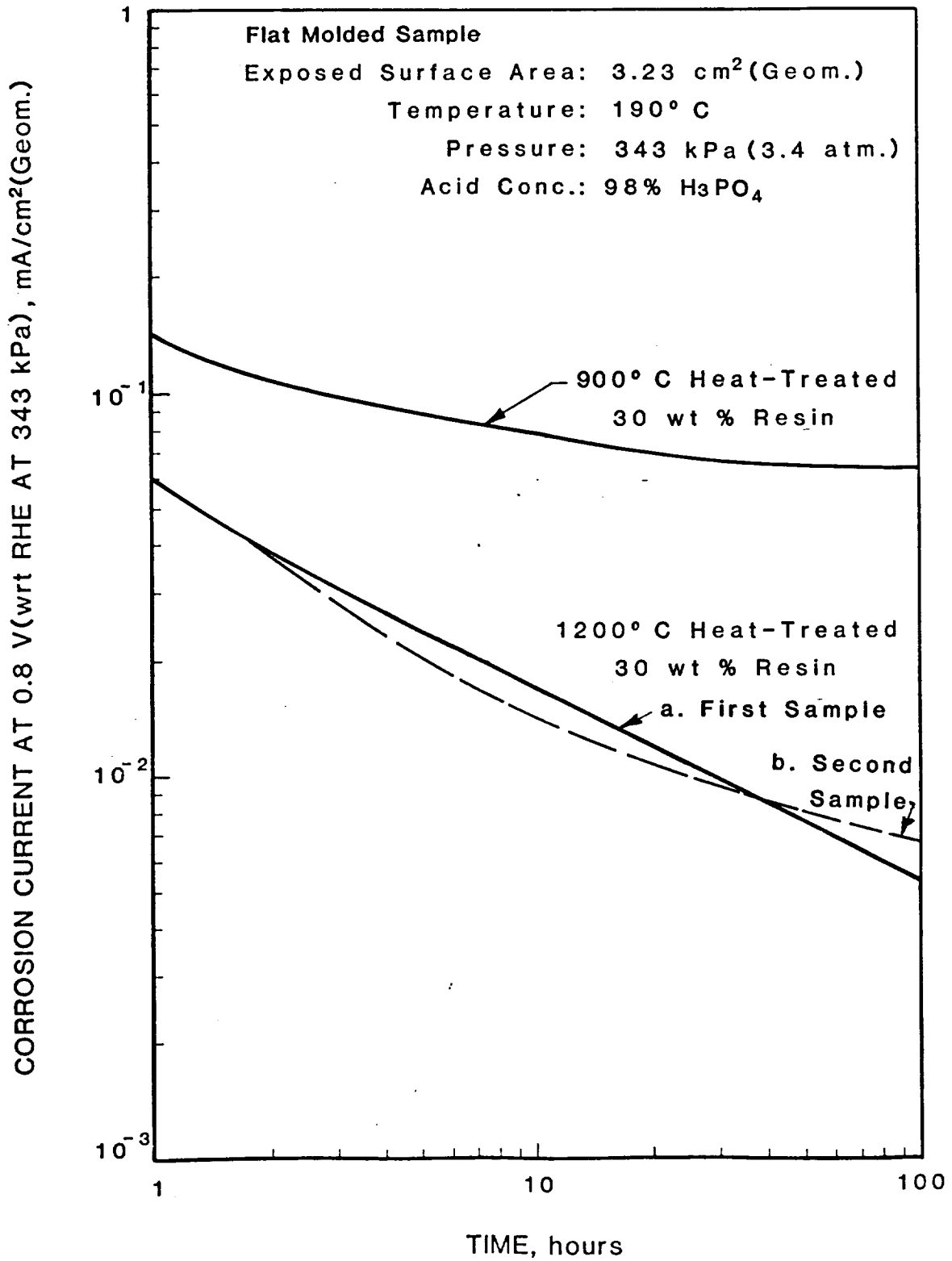
FIGURE 1.12   CORROSION RATES OF HEAT-TREATED BIPOLAR PLATE
             MATERIALS AT 0.8V (RHE) AND PRESSURE

ENERGY RESEARCH CORPORATION

under a microscope with 50X magnification and found to be defect free and structurally strong. Acid absorption and weight loss measurements for these samples are being conducted.

Pressurized corrosion experiments were performed using the 1600C heat-treated 30 w/o Varcum 29-703/A-99 graphite material. The effect of pressure appears to be much greater with this sample than was apparent with the 900°C material as shown in Figures 1.13 to 1.15. Futher work would be required to verify whether this is an experimental artifact or characteristic of the higher heat-treatment temperature.

The effect of acid concentration on the corrosion rate of bipolar plate material was evaluated using several acid concentrations between 100 w/o and 70 w/o H_3PO_4. The usual totally immersed sample was held for at least 24 hours at 0.8V, 190°C, 75 psia total pressure, and a known acid concentration. During this time, the corrosion current decreased and then stabilized. The stabilized corrosion current was taken as the corrosion rate for the specified acid concentration. The acid concentration was kept constant at the desired level by starting with a known concentration in the sealed pressure vessel and letting the pressure increase while heating to 190°C. If the pressure was less than 75 psia after heating, it was adjusted by adding N_2 to the vessel. For the 70% acid case, the total pressure was held at 85 psia. The observed corrosion currents shown in Figure 1.16 were very substantial. By decreasing the concentration from 100 to 70% the rate increases 18 fold. This suggests that if a mechanism for creating low acid concentration in the plate material were to occur, the plate may corrode very rapidly.

1.2 Analysis of Possible Poisons

Phosphoric acid from each of the corrosion experiments described above was retained for post-test examination. Visual examination revealed that the acid from 900°C heat-treated materials was discolored. As the heat-treatment temperature was increased, the discoloration decreased. Acid from experiments testing 2400 and 2700°C plates showed very slight coloration. Separation of the colored material by centrifugation was possible, but appeared to be droplets of
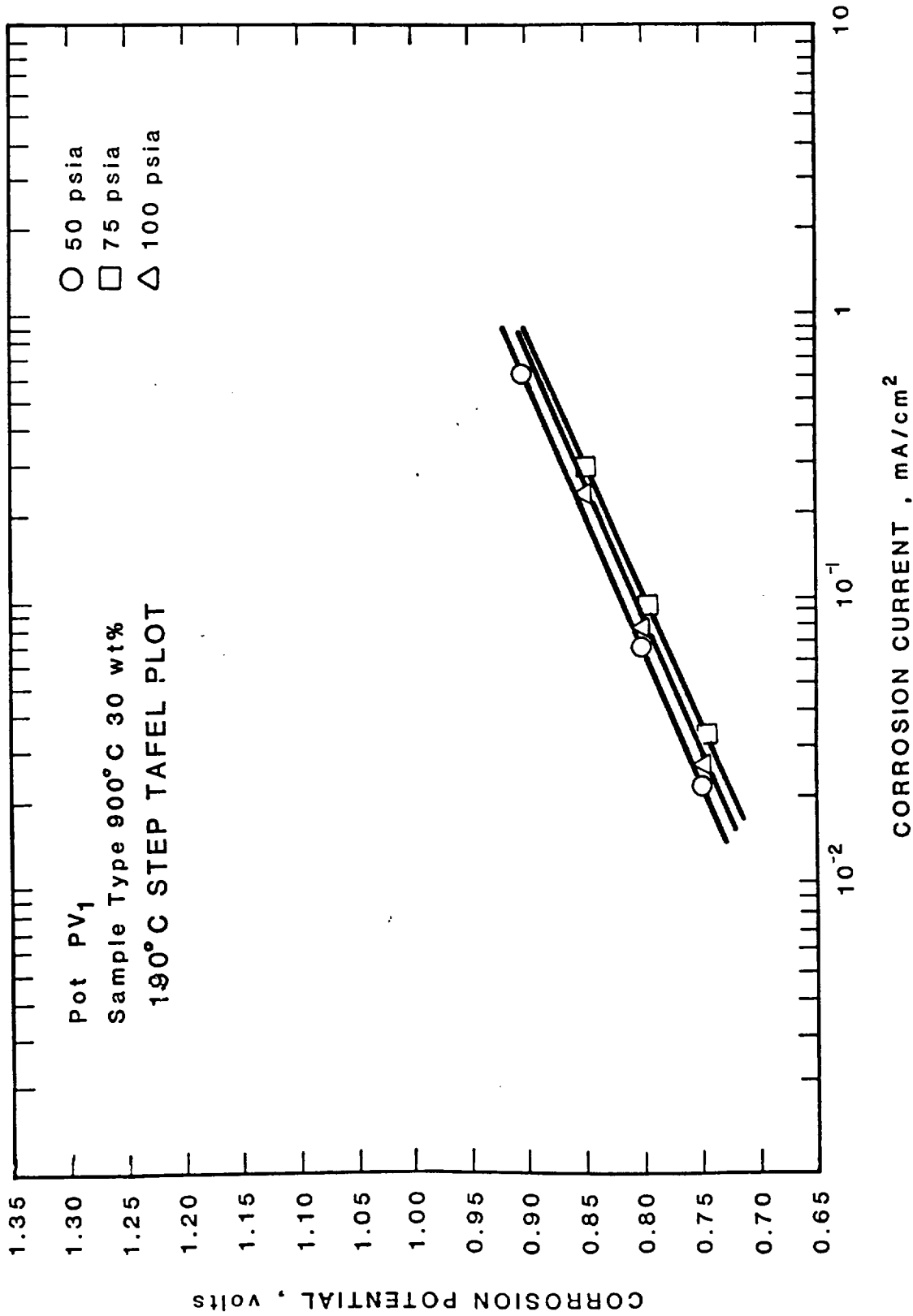
FIGURE 1.13   PRESSURIZED CORROSION FOR 900°C
HEAT-TREATED COMPOSITE AT 190°C
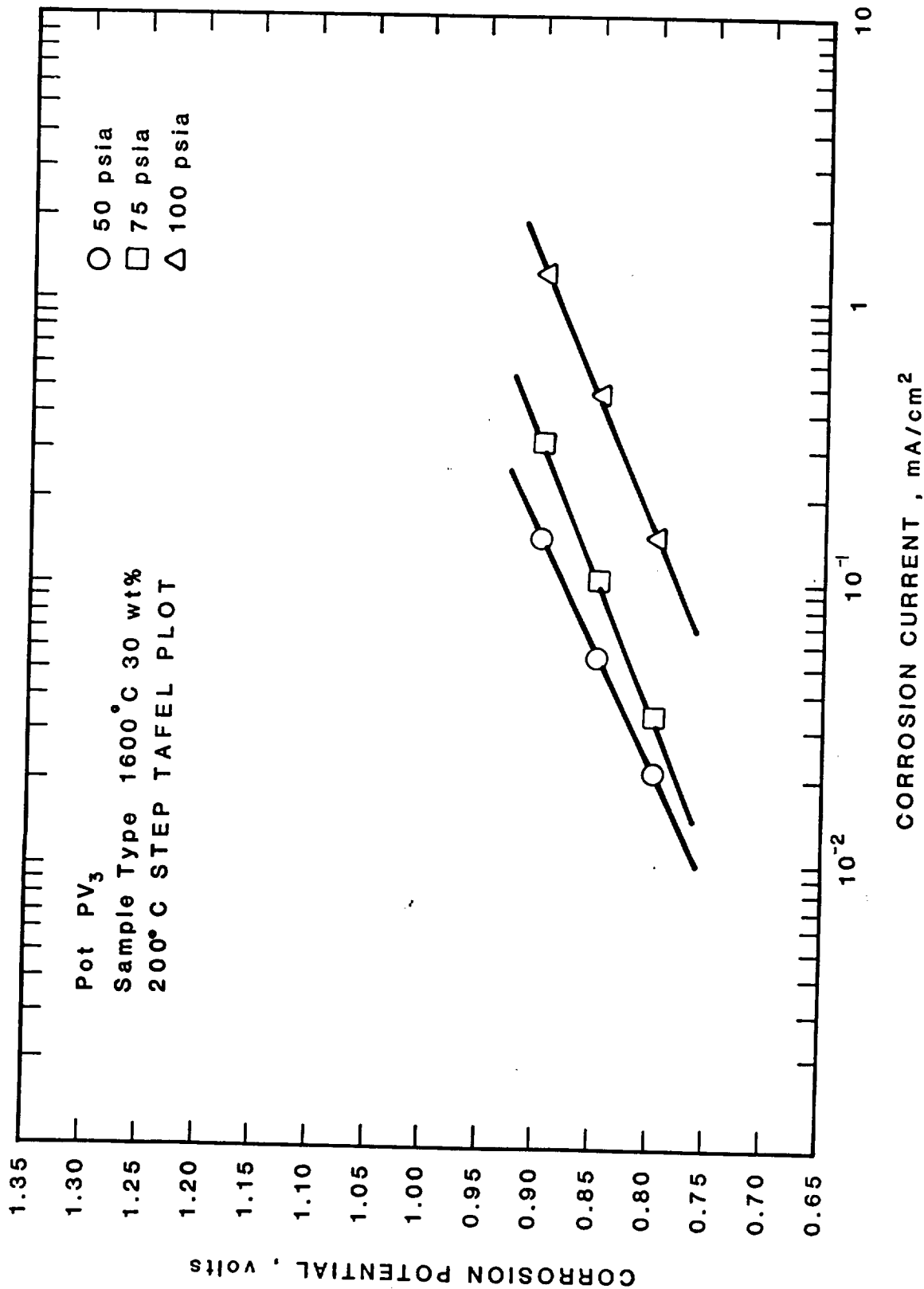
FIGURE 1.14   PRESSURIZED CORROSION FOR 1600°C
HEAT-TREATED COMPOSITE AT 190°C
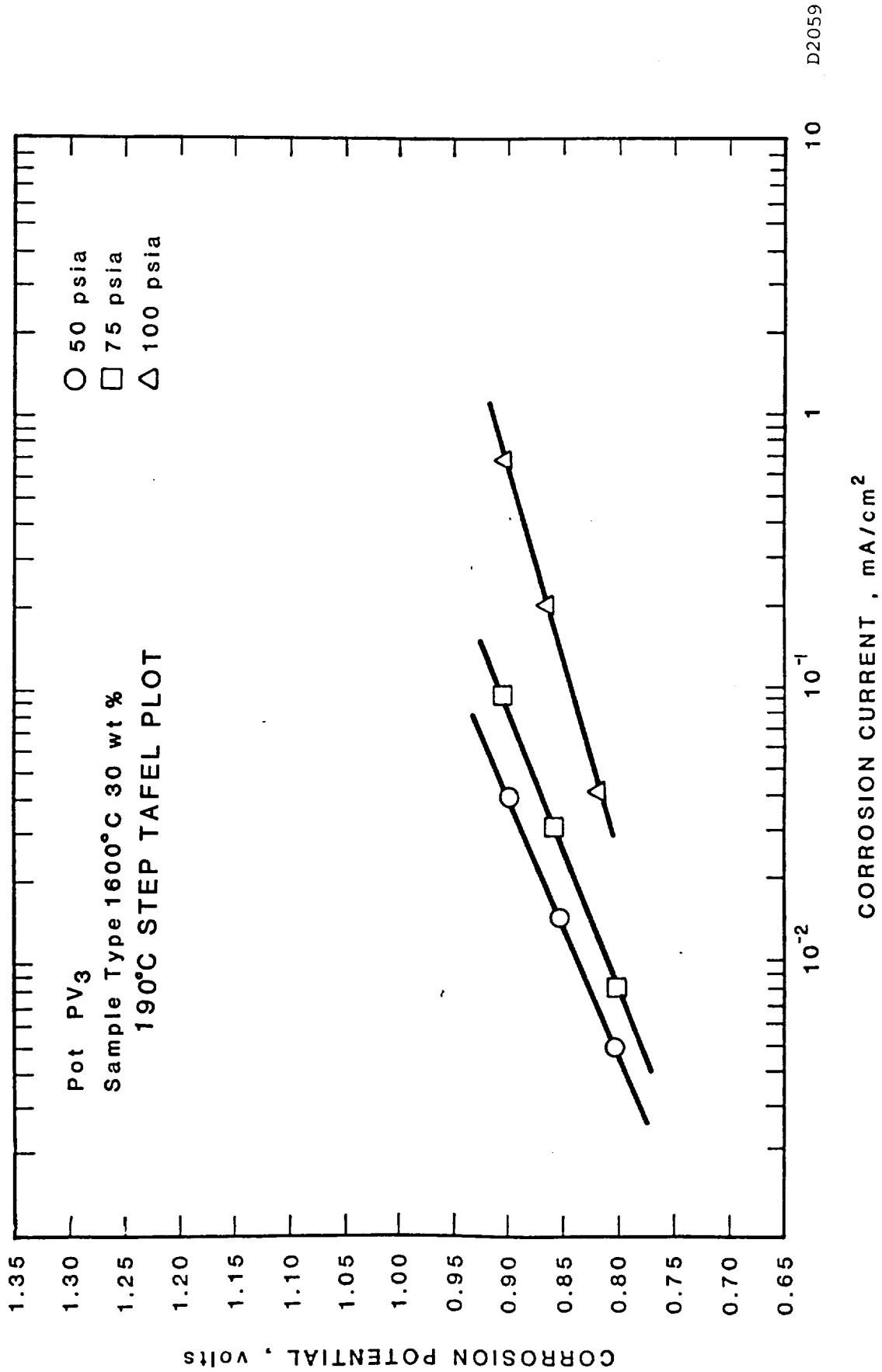
FIGURE 1.15   PRESSURIZED CORROSION FOR 1600°C
HEAT-TREATED COMPOSITE AT 200°C
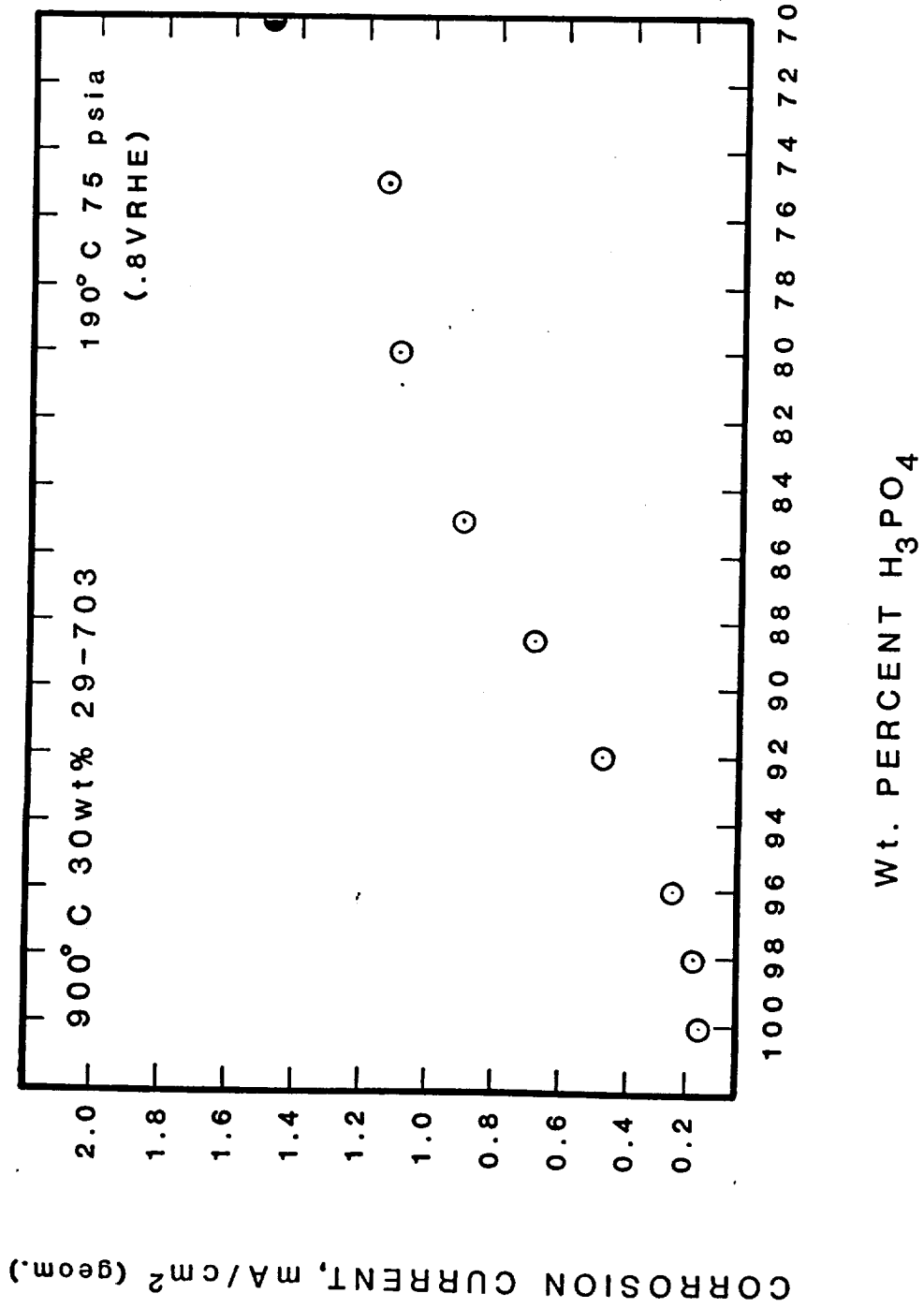
FIGURE 1.16 CORROSION RATE CONCENTRATION EFFECT

ENERGY RESEARCH CORPORATION

viscous liquid rather than colloidal solid particles. No further characterization of this liquid was performed. Future work should explore the composition of this material which is stable in hot phosphoric acid and may be a poison to the fuel cell electrodes.

1.3 Physical Properties Measurements

In addition to the corrosion measurements described in Section 1.1, materials heat-treated at different temperatures were characterized by measuring the following properties.

- carbon yield
- density
- porosity
- shrinkage

Heating of graphite/phenolic resin composites in an inert atmosphere decomposes the resin, leaving a glassy carbon residue. The chemical composition of this residue is known to vary with the heat-treatment temperature. It may depend on the amount of decomposition products which are trapped within the microporosity ($<50\overset{o}{A}$) that is not measured by mercury porosimetry. Average carbon yields were obtained to assess the changes which may occur when heating above 900°C. The values shown in Table 1.4 indicate that there is a measureable change when heating above 900°C, suggesting that materials are being removed by the additional heating. The change after 1200°C heat-treatment, however, appears relatively small.

During the initial 900°C heat-treatment the density of the material changes significantly. The as-molded material appears to be very close to the expected theroetical density at all the prepared resin contents. The density of heat-treated materials as shown in Figure 1.17 increases as the resin (1.3 g/cm^3) is converted to glassy carbon (1.5 g/cm^3). Heat-treating to 1600°C produces an additional small change. Going to 2400°C however, significantly changed the amount of porosity for all of the samples tested. A summary of the data

TABLE 1.4   CARBON YIELD AT DIFFERENT HEAT-
TREATMENT TEMPERATURES

Heat-Treatment Temperature, °C	Average Carbon Yield, %
900	67
1200	63
1600	62
2400	61
2700	61
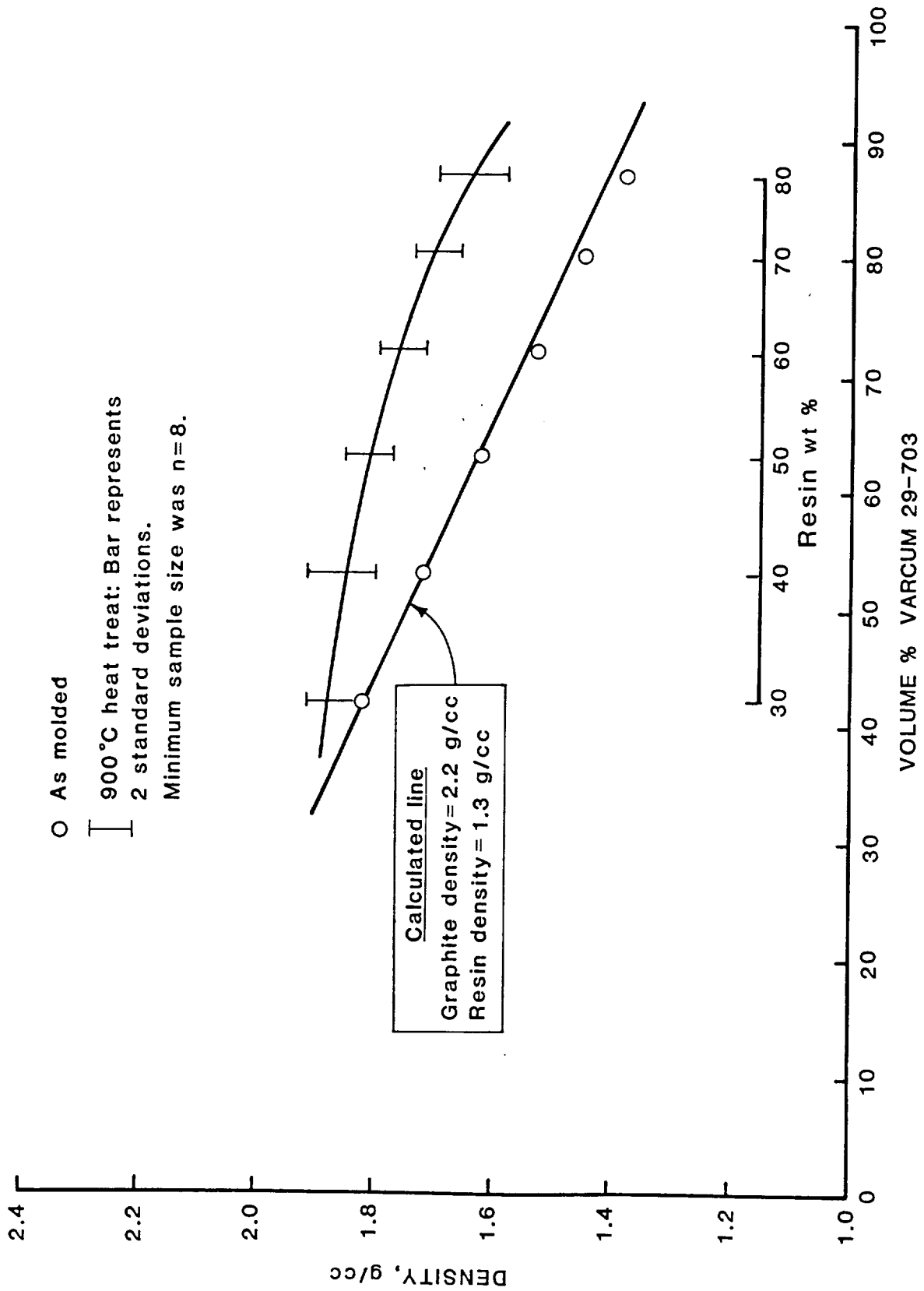
FIGURE 1.17 MEASURED DENSITY FOR VARCUM 29-703/ASBURY A-99 COMPOSITES

ENERGY RESEARCH CORPORATION

presented in Table 1.5 demonstrates that heating above 1600°C increases the porosity rather significantly. This probably occurs due to the differential thermal expansion between the graphite and glassy carbon. The analysis of the mercury porosimetry data indicates that the increased porosity mostly occurs in pores between 0.01 and 0.09 μm diameter. A graphical presentation of this is shown in Figures 1.18 and 1.19. These intermediate size pores are very likely small cracks. Porosity of this kind may be undesirable in the bipolar plates since it would absorb acid and promote degradation. Note that in Figure 1.18 (30 w/o resin), the porosity as a function of temperature goes through a maximum. This maximum is, however, not observed above 50% resin content (Figure 1.18 and Table 1.5).

During the heat-treating process, the material shrinks differently in the axial and planar directions. This anisotropic shrinkage may be a reflection of a basic compositional anisotropy as suggested by the apparent electrical anisotropy. Shrinkage variations result in bipolar plates that are not exactly the same size. Dimensional variations must therefore be accommodated by the cell and manifold seals. A summary of the shrinkage obtained with the composite plate material is shown in Table 1.6. The material continues to shrink as the heat-treatment temperature is increased but the change is less for temperatures in the 1200 to 1600°C range than in the 900 to 1200°C range. This provides an additional incentive for heat-treating to 1600°C.

1.4 Conclusions

Improvements in bipolar plate materials can be projected from the data obtained during this contract. Very dense parts can be prepared and heat-treated to 1600°C. This would decrease the corrosion rate with very little change in porosity. New manufacturing techniques may produce a composite material which does not increase its porosity upon heating above 1600°C, thereby allowing higher heat-treatment temperatures and lower corrosion rates. Additional improvements might also be achieved by applying a corrosion resistant coating.

TABLE 1.5 DENSITIES AND POROSITIES OF VARCUM 29-703 PHENOLIC RESIN/A-99 GRAPHITE COMPOSITES

INITIAL RESIN WT% (VOL%)	HEAT-TREAT (°C)	CALCULATED RESIN (WT%)	CALCULATED RESIN (VOL%)	RESIN DENSITY DC (G/CC)	WATER DENSITY MEAN DW (G/CC)	WATER S.DEV. (G/CC)	WATER NO. OF SAMPLES	BULK DENSITY MEAN DB (G/CC)	BULK S.DEV. (G/CC)	BULK NO. OF SAMPLES	MERCURY POROSITY SET#1 ((CC/G)*100)	MERCURY POROSITY SET#2 ((CC/G)*100)	MERCURY POROSITY AVERAGE	% POROSITY MERCURY PM F(DC,PM) (%)	% POROSITY WATER F(DC,DW) (%)	% POROSITY BULK F(DC,DB) (%)
30 (42)	160	29.58	41.55	1.83	1.82	0.01	18	1.80	0.01	12		0.61	0.61	1	<1	1
	900	22.05	28.65	2.01	1.88	0.02	17	1.83	0.02	10	1.19	2.36	1.78	3	7	9
	1200	20.99	27.39	2.02	1.83	0.03	9	1.86	0.02	8		1.44	1.44	3	9	8
	1600	20.72	27.06	2.02	1.86	0.02	10	1.86	0.01	10		1.89	1.89	4	8	8
	2400	20.45	26.74	2.03	1.63	0.03	8	1.60	0.03	6		13.96	13.96	22	20	21
	2700	20.45	26.74	2.03	1.82	0.02	10	1.69	0.03	8		8.57	8.57	15	10	17
40 (53)	160	39.52	52.51	1.73	1.72	0.01	9	1.69	0.02	6		0.69	0.69	1	0	2
	900	30.56	38.44	1.95	1.86	0.03	10	1.83	0.03	10	1.18	1.16	1.17	2	5	6
	1200	29.25	36.97	1.96	1.84	0.03	5	1.83	0.00	4		1.12	1.12	2	6	7
	1600	28.91	36.60	1.96	1.88	0.02	5	1.88	0.01	5		1.30	1.30	2	4	4
	2400	28.57	36.21	1.96	1.59	0.02	5	1.50	0.03	3		17.78	17.78	26	19	24
	2700	28.57	36.21	1.96	1.85	0.01	5	1.71	0.00	3		8.06	8.06	14	6	13
50 (63)	160	49.49	62.38	1.64	1.62	0.02	19	1.60	0.01	7		0.96	0.96	2	1	2
	900	39.76	48.37	1.89	1.82	0.02	18	1.76	0.05	10	0.71	1.51	1.11	2	3	7
	1200	38.27	46.81	1.90	1.80	0.02	8	1.78	0.04	8		1.03	1.03	2	5	6
	1600	37.89	46.40	1.90	1.83	0.02	8	1.81	0.04	7		1.14	1.14	2	4	5
	2400	37.50	45.99	1.90	1.50	0.05	8	1.44	0.03	6		19.91	19.91	27	21	24
	2700	37.50	45.99	1.90	1.74	0.03	8	1.56	0.05	10		9.98	9.98	16	8	18
60 (72)	160	59.51	71.33	1.56	1.53	0.00	9	1.52	0.01	5		0.79	0.79	1	2	2
	900	49.75	58.42	1.82	1.76	0.02	10	1.69	0.03	10	0.91	2.84	1.87	3	3	7
	1200	48.19	56.90	1.83	1.74	0.01	5	1.73	0.03	4		1.12	1.12	2	5	5
	1600	47.78	56.50	1.83	1.76	0.01	5	1.76	0.03	3		0.96	0.96	2	4	4
	2400	47.37	56.09	1.84	1.66	0.05	5	1.56	0.09	4		8.95	8.95	14	10	15
	2700	47.37	56.09	1.84	1.68	0.02	5	1.60	0.04	4	10.80	11.68	11.24	17	8	13
70 (80)	160	69.57	79.47	1.48	1.45	0.00	9	1.43	0.03	7		1.14	1.14	2	2	4
	900	60.63	68.61	1.75	1.70	0.02	10	1.65	0.03	10	0.83	0.93	0.88	2	3	6
	1200	59.13	67.25	1.76	1.69	0.01	5	1.67	0.06	5		0.79	0.79	1	4	5
	1600	58.73	66.89	1.77	1.71	0.01	5	1.70	0.03	3		0.95	0.95	2	3	4
	2400	58.33	66.52	1.77	1.60	0.04	5	1.57	0.03	2	9.02	12.65	10.83	16	9	11
	2700	58.33	66.52	1.77	1.57	0.06	5	1.48	0.00	4	13.04	20.51	16.78	23	11	16
80 (87)	160	79.67	86.90	1.42	1.38	0.01	19	1.38	0.02	12		0.96	0.96	1	3	3
	900	72.53	78.93	1.69	1.66	0.03	15	1.56	0.03	10	0.85	0.78	0.81	1	2	8
	1200	71.26	77.88	1.69	1.62	0.01	8	1.57	0.04	6		0.76	0.76	1	4	7
	1600	70.93	77.59	1.70	1.64	0.01	10	1.61	0.03	9		0.76	0.76	1	3	5
	2400	70.59	77.31	1.70	1.62	0.01	6	1.55	0.04	7	4.45	7.21	5.83	9	5	9
	2700	70.59	77.31	1.70	1.63	0.04	10	1.58	0.06	7	9.42	11.24	10.33	15	4	7

* Calculated values derived from resin weight losses and the following densities: 1.3 g/cm³ for the density of resin as molded (160°C heat-treatment), 1.55 g/cm³ for the density of resin heat-treatment of 900 to 2700°C, and 2.2 g/cm³ for the density of graphite.

** $F(DC, PM) = \dfrac{100\ PM}{1/DC + PM}$, $F(DC, DW) = 100\dfrac{(1-DW)}{DC}$, and $F(DC, DB) = 100\dfrac{(1-DB)}{DC}$.

F
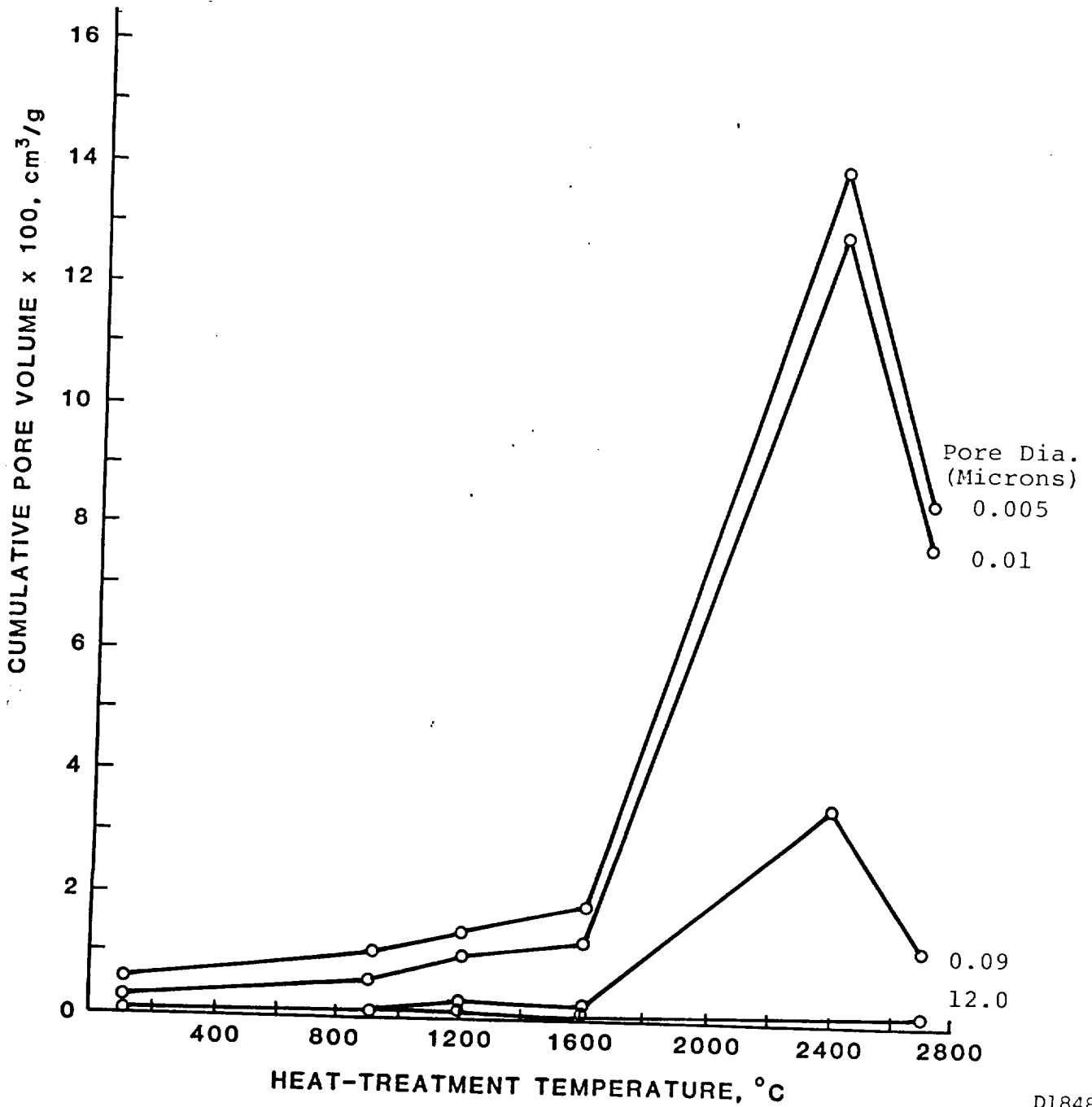
FIGURE 1.18   MERCURY POROSIMETRY OF 30 WT% VARCUM 29-703
RESIN AND 70 WT% A-99 GRAPHITE COMPOSITE
HEAT-TREATED AT DIFFERENT TEMPERATURES
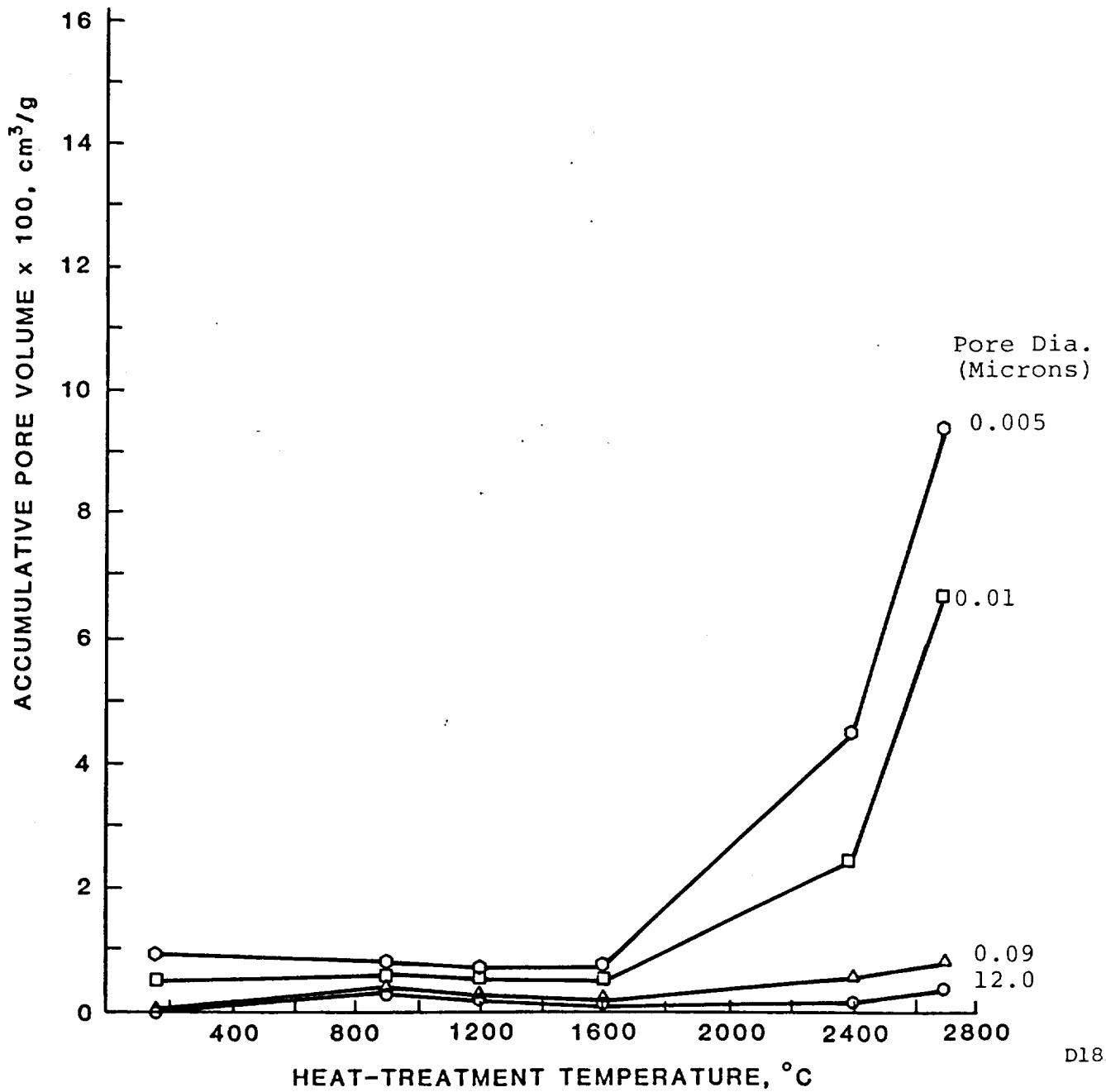
D1848R

FIGURE 1.19   MERCURY POROSIMETRY OF 80 WT% VARCUM 29-703
              RESIN AND 20 WT% A-99 GRAPHITE COMPOSITE
              HEAT-TREATED AT DIFFERENT TEMPERATURES

ENERGY RESEARCH CORPORATION

TABLE 1.6 SHRINKAGE OF VARCUM 29-703/A-99 MATERIALS FROM
AS-MOLDED TO FINAL HEAT-TREATMENT TEMPERATURE

| VOL% RESIN | HEAT-TREATMENT TEMP, °C | % SHRINKAGE | | | | | | NUMBER OF SAMPLES, N |
| | | LENGTH | | WIDTH | | THICKNESS | | |
		MEAN	S.DEV	MEAN	S.DEV	MEAN	S.DEV	
42 (30wt%)	900	3.32	0.18	3.32	0.23	5.94	0.81	68
	1200	3.58	0.17	3.54	0.36	8.71	0.64	8
	1600	3.64	0.20	3.58	0.27	7.51	0.97	20
	2400	3.06	0.31	3.01	0.42	-3.53	2.11	8
	2700	3.73	0.32	3.69	0.35	2.22	3.59	20
53 (40wt%)	900	5.13	0.35	5.12	0.55	10.93	1.30	32
	1200	5.52	0.05	5.55	0.14	12.80	1.30	5
	1600	5.66	0.16	5.78	0.10	14.59	0.66	5
	2400	5.01	0.09	4.50	0.48	-0.82	6.25	5
	2700	6.08	0.28	6.24	0.21	4.46	0.94	5
63 (50wt%)	900	6.87	0.45	6.93	0.66	13.20	1.20	68
	1200	6.97	0.38	7.22	0.21	13.79	1.80	8
	1600	7.28	0.30	7.34	0.48	16.20	0.72	20
	2400	5.36	0.50	5.12	0.25	-0.98	-1.29	8
	2700	7.50	0.46	7.32	0.70	2.14	3.05	20
72 (60wt%)	900	9.71	0.49	9.51	0.49	12.60	1.60	31
	1200	10.36	0.45	9.98	0.48	15.58	1.23	5
	1600	10.28	0.85	10.00	0.78	16.60	2.50	5
	2400	9.60	0.78	9.23	0.47	12.43	2.28	5
	2700	9.52	1.26	9.00	0.64	9.56	1.84	5
80 (70wt%)	900	11.50	0.57	11.5	0.74	15.10	1.30	30
	1200	11.93	0.28	11.80	0.97	16.98	0.69	4
	1600	12.38	0.90	12.65	0.73	18.32	1.21	4
	2400	11.11	0.59	10.97	0.61	6.15	9.40	5
	2700	11.42	0.68	11.23	0.47	8.00	3.75	5
87 (80wt%)	900	13.20	0.55	13.20	1.00	16.30	1.10	60
	1200	13.93	0.36	13.60	0.67	18.53	1.10	6
	1600	13.45	0.60	13.72	0.87	18.78	0.87	20
	2400	13.22	0.63	13.61	0.89	16.56	5.02	8
	2700	13.23	0.86	13.31	1.13	17.59	1.75	17

SECTION 2

COMPONENT/FABRICATION DEVELOPMENT

The objectives of the effort described in this section were to improve the component fabrication techniques by identifying methods which would increase production rates and/or decrease their expected cost. Three areas were emphasized which would significantly impact the manufacturing of fuel cell stacks. Bipolar plates, electrodes, and acid inventory control members were examined in some detail so that manufacturing recommendations could be made at the conclusion of this study.

2.1 Bipolar Plate Development

Phenolic resin/graphite composites of various compositions between 30 and 80 wt% resin were investigated to optimize the resin content. The molding trials, however, did not suggest an optimum composition. All resin contents could be molded quickly, but somewhat different conditions were required to satisfy dimensional tolerances requirements. The differences in molding conditions are not expected to affect the cost. Another factor which changes with resin content is the shrinkage during heat-treatment. Even though the shrinkage increases with higher resin content, this can be accounted for in the mold design; therefore, there does not appear to be an optimum resin content.

The molding cycle is a major contributor to the bipolar plate costs. ERC presently uses a five minute cycle time for compression molding a ribbed bipolar plate. This is the time spent from placing a preform in the press to removing the molded plate. To reduce this time, plates were molded using two minute, one minute and 45 second cycles. Plates molded in 45 seconds released from the mold easily, had good dimensions, and could be heat-treated satisfactorily, thus a very fast molding cycle was demonstrated.

ENERGY RESEARCH CORPORATION

2.2   Acid Inventory Control Members (AICM)

Acid volume changes during stack operation must be accommodated by the cell components. These volume changes depend on gas flows, cell temperature and temperature gradients, and the rate of acid equilibration. Transient operation can be an especially harsh condition. Energy Research Corporation has been developing a selectively wetproofed anode backing paper which can accommodate volume changes, store acid, and distribute the acid within a cell. The basic design of the material is shown in Figure 2.1. Initial development of this design and technique had been achieved on a previous contract (DEN3-67). The wetproofed dot pattern allows gas transport to the electrode, while the interconnected unwetproofed area allows transport of acid across the electrode face. Variation of dot size and spacing controls the amount of gas transport to the electrode.

Results of initial efforts to define the reproducibility and uniformity are summarized in Table 2.1.

TABLE 2.1   AICM REPRODUCIBILITY AND UNIFORMITY

APPLICATOR	SAMPLE TYPE	NO. OF SAMPLES	TEFLON CONTENT, %
2	1	5	30.9 ± 2.2
	2	20	27.5 ± 8.6
4	1	5	32.1 ± 2.4
	2	19	30.9 ± 8.9

Sample Type 1 is a piece of backing paper cut to the exact size of the applicator and weighed before and after application of the wetproofing agent. Sample Type 2 is a 2 inch x 2 inch wetproofed piece cut from a 5 inch x 15 inch backing paper requiring multiple applications. The higher variability of Sample Type 2 may be caused by variations in the weight per unit area of the fresh backing or variations in the cut sample.

CATALYST LAYER

BACKING

SELECTED WETPROOFED AREA

COMPLETELY WETPROOFED AREA
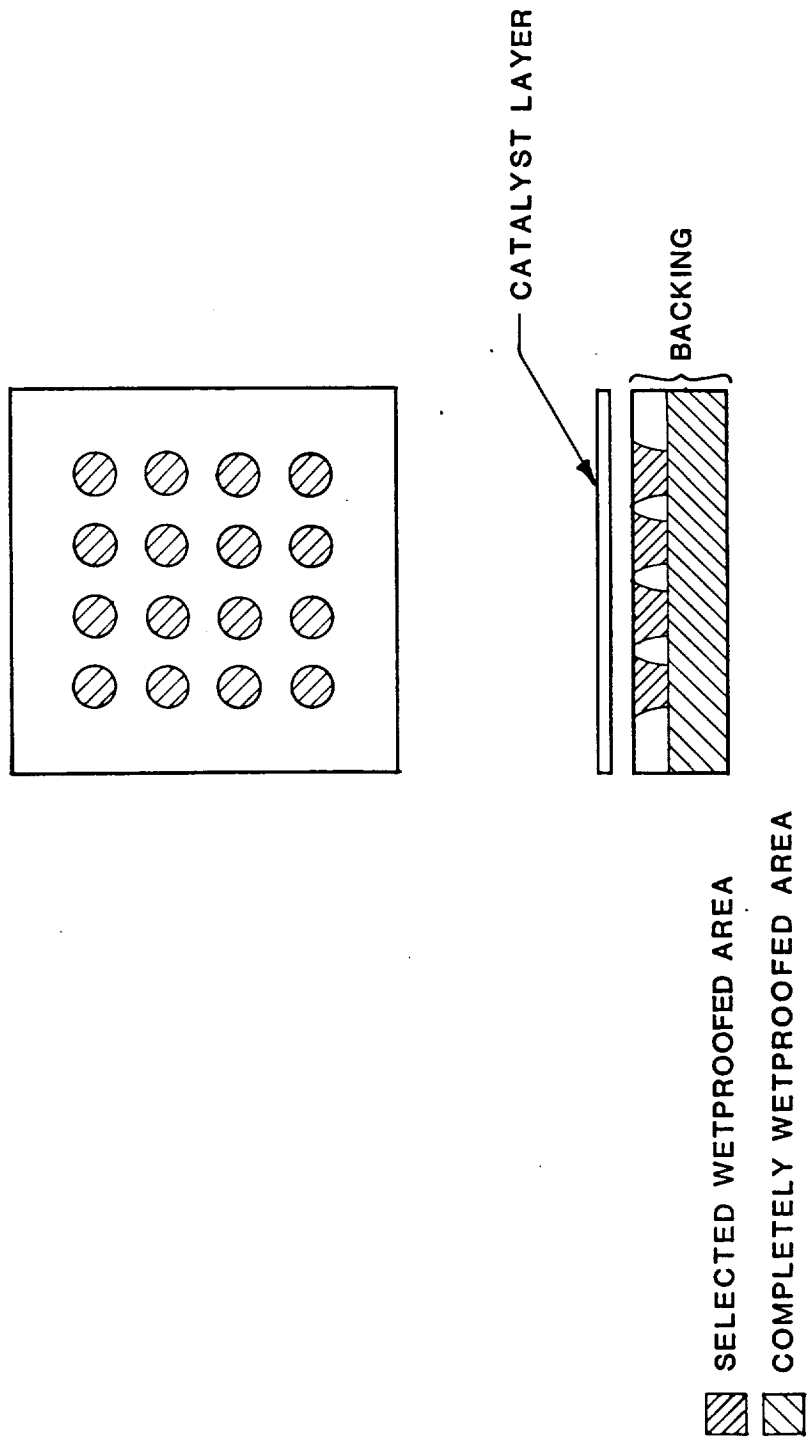
FIGURE 2.1 AICM-ANODE BACKING

ENERGY RESEARCH CORPORATION

Effort is continuing to optimize and characterize these materials in out-of-cell tests. Although this may define the material capacity, the final test is whether it performs in an operating stack. This phase of the development was curtailed because of a substantial reduction in contract funding. Results of a stack tested with AICM's are described in Section 3.

2.3 Electrode Development

Two aspects of electrode manufacturing were evaluated during this program: a) sintering, and b) platinum loading. Sintering is a very important operation in the manufacturing of electrodes and one that can be automated easily. A conveyor oven can be sized to match the production rate required. This type of oven was used to sinter a number of electrodes which were tested in 25 cm^2 cells. The cell performances are summarized in Tables 2.2 and 2.3.

The anodes in Cells 2007 through 2009 were sintered at $340^{\circ}C$ to define the minimum sintering temperature. As expected, the anodes sintered at $340^{\circ}C$ showed evidence of insufficient wetproofing while operating in a reverse mode. The SiC coated cathodes in these cells were also sintered at $340^{\circ}C$ followed by batch oven sintering at $330^{\circ}C$. Adequate wetproofing was attained because Teflon sinters at a lower temperature when it is reheated. Cell 2010, which also exhibited an acceptable performance, contained an anode conveyor-sintered at $350^{\circ}C$, and a cathode with its SiC layer that were simultaneously conveyor sintered at $350^{\circ}C$. The results of these tests indicate that electrodes and SiC matrices can be sintered in a conveyor oven at the same time.

Platinum loading of electrodes is one of the primary parameters which affects fuel cell stack cost and performance. Theoretically, an increased platinum loading on the cathode results in an increased performance. Therefore, platinum loading may be optimized to minimize the overall stack cost per kilowatt.

A series of cells was assembled with low-loaded cathodes to compare with the baseline cells. Some of these experimental electrodes were prepared at the 0.10 mg/cm^2 Pt loading level, while others were prepared at the .05 mg/cm^2 Pt

TABLE 2.2   ELECTRODE SINTERING CONDITIONS

CELL NUMBER	ELECTRODE	SINTERING CONDITIONS	DIFFUSION LIMITATION
2007	Anode	Conveyor Oven, 340°C	No loss as anode, moderate loss as cathode
	Cathode	Conveyor Oven, 340°C and Resintered with SiC Layer at 330°C in Batch Oven	No
2008	Anode	Conveyor Oven, 340°C and Resintered at 330°C in Batch Oven	No
	Cathode	Conveyor Oven, 340°C and Resintered with SiC Layer at 330°C in Batch Oven	No
2009	Anode	Conveyor Oven, 340°C	20 mV cell loss as anode, severe loss as cathode
	Cathode	Conveyor Oven, 340°C and Resintered with SiC Layer at 330°C in Batch Oven	No
2010	Anode	Conveyor Oven, 350°C	No
	Cathode	Conveyor Oven, 350°C Electrode and SiC Layer Sintered Together	No

ENERGY RESEARCH CORPORATION

TABLE 2.3   CELL TESTING SUMMARY

CELL NO.	2007	2008	2009	2010
TEST OBJECTIVE	Vulcan Catalyst	Vulcan Catalyst	Vulcan Catalyst	Vulcan Catalyst
CELL CHARACTERISTICS ANODE Type % TFE Loading,mg Pt/cm^2	Rolled 40 0.28	Rolled 40 0.30	Rolled 40 0.25	Rolled 40 0.42
CATHODE Type % TFE Loading,mg Pt/cm^2	Rolled 40 0.56	Rolled 40 0.56	Rolled 40 0.56	Rolled 40 0.47
CELL TEMPERATURE, °C	180	180	180	190
ANODE BACKING % FEP	34	37	33	35
CATHODE BACKING % FEP	33	33	33	38
PEAK PERFORMANCE IR-FREE, mV Air 100 mA/cm^2 200 mA/cm^2	707 664	711 663	697 643	716 674
O$_2$ 100 mA/cm^2 200 mA/cm^2	767 729	771 733	752 703	779 743
O$_2$ Gain 100 mA/cm^2 200 mA/cm^2	60 65	60 70	55 60	63 69
PRESENT PERFORMANCE IR-FREE, Air 200 mA/cm^2	Terminated 600 mV (Cell Short)	500 Hrs. 642 mV (Cell Short)	Terminated 200 mV (Cell Short)	400 Hrs. 674 mV

ENERGY RESEARCH CORPORATION

level.   Different electrocatalyst batches were utilized in preparing the respective cathodes. The catalyst batches are designated as either A, B, C or D. The peak performance level for each of the experimental cathodes is shown in Table 2.4.

TABLE 2.4   PERFORMANCE OF CELLS WITH VARIOUS CATALYST LOADINGS USING H_2 AND AIR

Cells	Catalyst	Cathode Loading, mg/cm^2	Average Peak Performance mV @ 200 mA/cm^2	Average Loss mV Actual	Predicted
2024, 2025	A	0.50	673	0	0
2026, 2027	C	0.11	615	58	60
2036, 2037	B	0.11	623	50	60
2039, 2040	A	0.10	608	65	64
2033, 2034	D	0.05	576	92	97

As shown, the actual performance losses due to the lower Pt loading did correlate reasonably well with the losses which are theoretically predictable. A summary of performance characteristics of these cells is shown in Table 2.5. From the peak performance data it appears that the amount of platinum on the carbon support (2, 5 or 10%) may alter the observed performance. It must be kept in mind that when the electrode loading is kept constant and the percent platinum on the carbon varies, the electrode thickness changes, leading to a high internal ohmic resistance. Thus the 5% platinum catalyst may provide a better thickness, porosity, and platinum particle size.

The lower percent platinum on carbon is generally assumed to decrease the platinum particle size and increase the performance. Finding the optimum of these variables is very difficult and can be easily confused by other variables.

ENERGY RESEARCH CORPORATION

TABLE 2.5 LOW-LOADED CATHODE PERFORMANCE

CELL NO.	CELL CATHODE* Catalyst % Pt on Carbon	Type	Pt mg/cm²	PTFE %	PEAK Oxygen 20 mA/cm²	Oxygen 200 mA/cm²	Air 200 mA/cm²	FINAL Oxygen 20 mA/cm²	Oxygen 200 mA/cm²	Air 200 mA/cm²	OXYGEN GAIN mV @ 200 mA/cm² @ Peak	Final	OPERATING HOURS	DECAY RATE mV/1000 hr.	REASON FOR TERMINATION
2026	2	C	0.11	45	788	680	609	767	678	590	71	88	5856	3	Voluntary
2027	2	C	0.11	45	789	694	620	764	676	597	74	79	5736	4	Voluntary
2036	5	B	0.11	45	783	690	625	761	670	604	65	66	4752	4	Crossover
2037	5	B	0.11	45	775	687	620	775	661	590	67	71	5568	5	Voluntary
2039	10	A	0.10	45	776	678	606	764	663	591	72	72	2332	6	Voluntary
2040	10	A	0.10	45	768	677	609	751	645	573	68	72	2352	15	Voluntary
2033	1	D	0.05	45	758	646	570	751	641	562	76	79	936	9	Voluntary
2034	1	D	0.05	45	755	659	582	757	665	582	77	83	1176	0	Voluntary

*Anodes are all 0.3 mg Pt/cm², 10% Pt/C, 40% PTFE

(190°C, H_2/Air, 1 atm)

ENERGY RESEARCH CORPORATION

The trend however, suggests that a 5% catalyst may produce a better electrode structure. The decay rates observed for these cells are within the range normally observed. There appears to be only a slight trend toward a lower rate with the 2% catalyst. Thus, there does not appear to be any major detrimental or beneficial effects of the low cathode loading.

Variations of anode platinum contents are not expected to alter cell performance to any great extent. However, if there were any anode poisons present in the system, the low loading could have resulted in significant decreases in initial performance and decay rates. The data shown in Table 2.6 demonstrates that this does not occur. Poisons, therefore, did not appear to affect the performance. The loss of performance (6 to 8 mV/1000 hrs) observed may be associated with a slow poison release, but this is clearly a speculation at this time.

Combining the low loaded anodes and cathodes did not show any particular problems. The performance and decay rates as shown in Table 2.7 were as expected. This demonstrates that the basic trade-off of platinum loading, cell performance, and cost can be made without any major detrimental problems with the initial performance. Effects of carbon monoxide poisoning were not evaluated with these low loaded electrodes due to programmatic constraints. The carbon monoxide is expected, however, to have a greater effect as the anode loading is decreased, and may limit the level at the anode.

A stack test with low-loaded electrodes is described in Section 3.

ENERGY RESEARCH CORPORATION

TABLE 2.6 LOW-LOADED ANODE PERFORMANCE

CELL NO.	CELL ANODE*				CELL PERFORMANCE LEVELS (IR-Free, mV)						OXYGEN GAIN mV @ 200 mA/cm²		OPERATING HOURS	DECAY RATE mV per 1000 hr.	REASON FOR TERMINATION
	Catalyst % Pt on Carbon	Type	Pt mg/cm²	PTFE %	PEAK			FINAL							
					Oxygen		Air	Oxygen		Air	Peak,	Final,			
					20 mA/cm²	200 mA/cm²	200 mA/cm²	20 mA/cm²	200 mA/cm²	200 mA/cm²					
2043	1	D	0.05	40	865	737	669	865	706	631	68	75	1560	-	Voluntary (Unknown Problem)
2044	1	D	0.05	40	864	730	660	838	723	660	70	63	1632		Voluntary
2032	2	C	0.10	40	859	740	663	812	700	623	77	77	6120	7	Voluntary
2035	2	C	0.10	40	861	745	672	819	613	501	73	112	5712	-	Test Stand Problem
2041	5	B	0.10	40	877	760	683	847	740	664	77	76	2328	8	Voluntary
2042	5	B	0.10	40	870	749	680	846	732	663	69	69	2328	7	Voluntary

*Cathodes are all 0.5 to 0.6 mg Pt/cm², 10% Pt/C, 40% PTFE

(190°C, H₂/Air, 1 atm)

ENERGY RESEARCH CORPORATION

TABLE 2.7 LOW-LOADED ANODES AND CATHODES

| CELL NO. | ANODE | | | CATHODE | | | CELL PERFORMANCE LEVELS (IR-Free, mV) | | | | | | OXYGEN GAIN @ 200 mA/cm² | | OPERATING HOURS | DECAY RATE | REASON FOR TERMINATION |
| | Catalyst Designation % Pt | Pt mg/cm² | PTFE % | Pt % | Pt mg/cm² | PTFE % | PEAK | | | FINAL | | | @ Peak, mV | Final, mV | | mV per 1000 hr. | |
							Oxygen 20 mA/cm²	Oxygen 200 mA/cm²	Air 200 mA/cm²	Oxygen 20 mA/cm²	Oxygen 200 mA/cm²	Air 200 mA/cm²					
2045	2	0.10	40	5	0.11	45	781	669	607	761	661	581	62	80	9000	3	Voluntary
2046	2	0.10	40	5	0.11	45	776	677	609	752	651	567	68	84	9168	5	Voluntary
2047	2	0.10	40	5	0.11	45	797	683	614	788	674	598	69	76	5064	3	Voluntary
2048	2	0.10	40	5	0.11	45	790	683	617	782	625	549	66	76	4728	15	Voluntary

(190°C, H_2/Air, 1 atm)

ENERGY RESEARCH CORPORATION

SECTION 3

NEW COMPONENT AND CELL ASSEMBLY TESTING

Testing of new materials and new components in multicell stacks was the primary objective of the effort described in this section. Long-term stability of these materials and components was critical for their acceptance as viable candidates. The four components listed below were tested to provide a basis for further development. Each will be described in this section along with the stack results.

- nonheat-treated bipolar plates

- heat-treated bipolar plates

- acid inventory control member

- low platinum loaded electrodes

3.1 Multicell Testing of Bipolar Plates

Bipolar plates have been manufactured for a considerable time using a phenolic resin/graphite mixture. This material had reasonably good electrical properties and short-term resistance to phosphoric acid. Out-of-cell and stack testing on ERC's NASA Contract DEN3-67 demonstrated the poisoning effect of this nonheat-treated composite. A heat-treatment of this composite at >900°C produced a more conductive and corrosion resistant plate which did not appear to poison the fuel cell. This development improved the fuel cell performance by at least 80 mV, as shown in Figure 3.1. However, only 5,000 hours of testing had been achieved during that program. Stacks with heat-treated plates (No. 620, 621, 431, and 432) and nonheat-treated plates (No. 428, 429, and 430) were continued on test during the present DEN3-205 program. In addition, a 23-cell stack (No. 433) containing heat-treated plates (molded ribs) was built and operated for 1,500 hours.
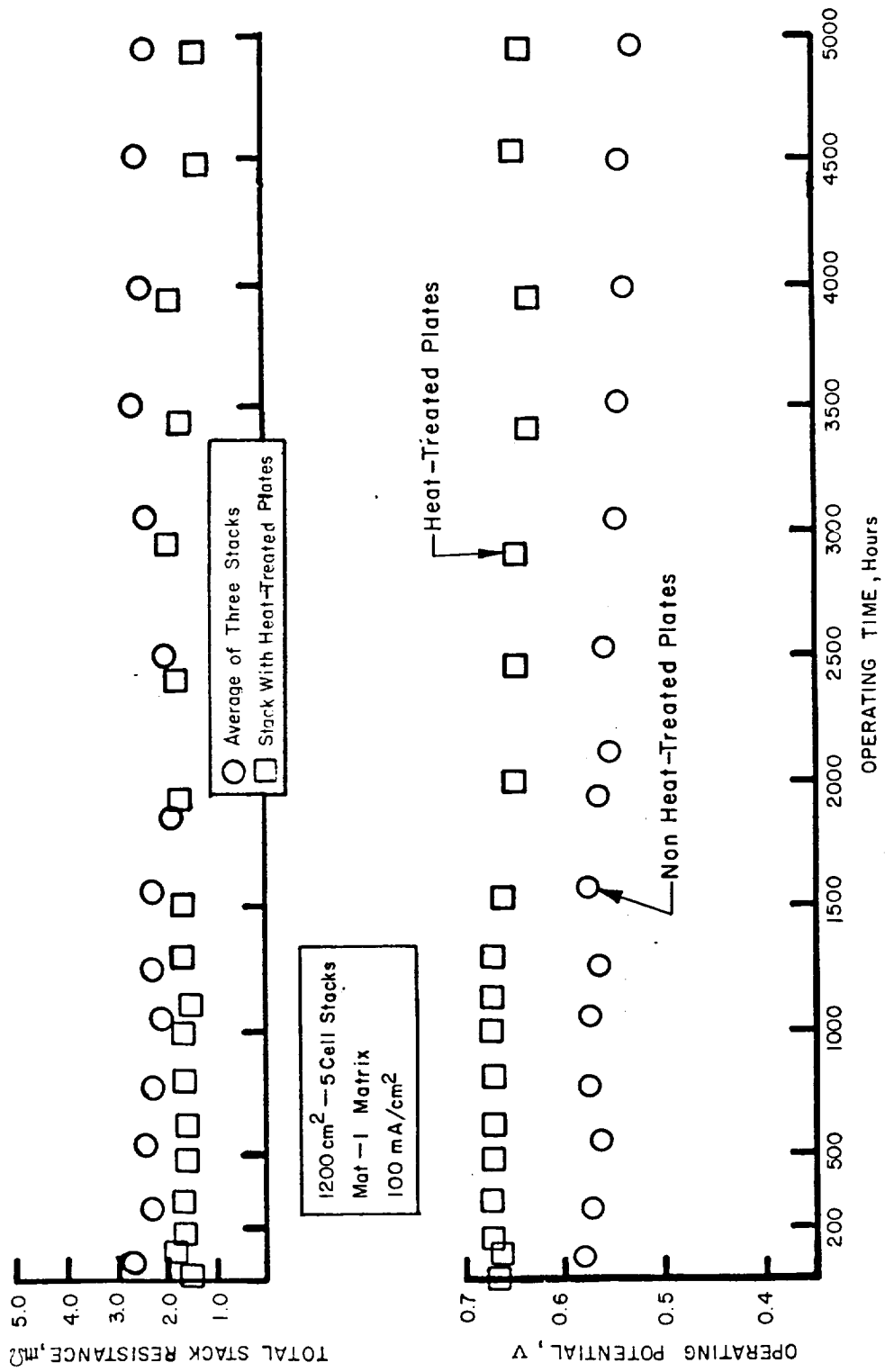
D1318AR1

FIGURE 3.1 PERFORMANCE OF STACKS WITH HEAT–TREATED AND NON HEAT–TREATED PLATES

ENERGY RESEARCH CORPORATION

Testing of nonheat-treated plate stacks continued during this program for an additional 2,000 to 3,000 hours. All stacks with the nonheat-treated plates had significant blockage of both the acid addition and flow channels after ~4,000 hours of operation. Upon disassembly of Stacks 428, 429, and 430, the nonheat-treated plates were found to be soft and swollen, primarily along the edges and corners.

Upon disassembly of Stack 432 (with heat-treated plates after 4,240 hours), the plates were very hard and were not swollen. There were, however, two soft spots on the cathode plates in Cells 1 and 2. Discoloration of the plate in these areas suggested that a crossleak had been present. Disassembly of Stack 433 also indicated that the plates were not attacked except at a hot spot that had existed in Cell 20 during most of the 1,500 hours of operation. The plate was slightly soft but not swollen in the hot spot region. This suggests that the corrosion process has a large activation energy, which is consistent with the values of 55 to 65 kcal/mol obtained in the out-of-cell test reported in Section 1, Table 1.3. Local hot spots may not only increase the corrosion rate, but also increase the degradation rate of the Teflon wetproofing in the backing paper. This could allow acid migration to the plate and result in corrosion. The mild corrosion apparent in Stack 432 suggests that the 900°C heat-treated bipolar plate may be satisfactory for long-term operation at 1 atm.

Operation of Stack 431 with heat-treated plates had achieved over 22,000 hours of operation by the completion of this program*. The degradation rate after 16,000 hours of operation had increased significantly. The stack was kept in operation, but observation of the stack faces during a manifold change indicated that the backing paper was sagging into the gas flow channels. The corners of the plate in Cell 5 were also becoming soft and limiting the ability to replenish the acid. This softness of corners appears to be associated with low density areas produced during molding. It seems apparent that the 900°C heat-treated plates will require additional development for use in stacks beyond ~15,000 hours. These improvements would include molding the plates with denser corners and edges, some surface treatment and/or higher temperature heat-treatment.

---

* The stack was operated further under in-house funds.

Post-test observation for Stacks 431 and 433 also indicated that the backing paper was crushed under the bipolar plate ribs within about 3 inches of the periphery. The center of the backing paper was not as heavily crushed. This is typical of long-term cells and was evident when the stack faces of Stack 431 were examined during a change of manifolds. After 19,000 hours of operation, the backings of Stack 431 were cracking and expanding into the gas flow channels. Thus is seems apparent that either the compression of the stack must be reduced or the strength of the backing paper needs to be improved for operation longer than ~15,000 hours.

The materials limitations just described are also reflected in Stack 431 performance, as shown in Figure 3.2 and Table 3.1. Replenishment of acid seems to be required about every 3,000 to 4,000 hours and, therefore, a blockage of the fill channels can be deleterious. This was not a problem with Stack 431 until after 16,000 hours when the average decay rate increased from 2 to 12 mV/1000 hr. Cell 5 was not responding to acid additions and the decay rate increased from 2 to 36 mV/1000 hr. Acid management is, therefore, crucial for long-term operation.

Optimum stack performance also requires good seals and low stack resistance. Bipolar plates must be flat to achieve these objectives and it is most important for stacks with many cells. Optimization of seals was not part of this program. The high resistance (9.4 mΩ/cell) of the 23-cell stack (No. 433), may be a result of nonuniform compression due to warpage of the bipolar plates. This may also account for the 30 mV lower performance as compared with the 5-cell stack (No. 431). The resistance and open circuit voltage shown in Figure 3.3 responded to acid addition, indicating good acid transport to the cells and electrodes.

The acid fill channel and seal design used in Stacks 431 and 433 is shown in Figure 3.4. This design allows contact of the matrix and cathode to the fill channel so that there is ample opportunity for the components to wick acid across the inside seal. Apparently this arrangement was still effective after 18,000 operations of operation, as shown by the responsiveness of the cell performance and open circuit voltage of Stack 431 to acid addition.

TABLE 3.1   PERFORMANCE OF INDIVIDUAL CELLS IN STACK 431 AT 100 mA/cm²

CELL NO.	INITIAL PERFORMANCE, V		PERFORMANCE, V										TERMINAL VOLTAGE PERFORMANCE DECAY RATE*	
			12,756 hr		14,655 hr		16,382 hr		19,678 hr				0-16,382 hr	16,382 hr – 19,678 hr
	TERMINAL	IR-FREE	TERMINAL	IR-FREE	TERMINAL	IR-FREE	TERMINAL	IR-FREE	TERMINAL	IR-FREE			TERMINAL	IR-FREE
1	0.67	0.70	0.64	0.67	0.63	0.66	0.63	0.66	0.61	0.64			2	6
2	0.66	0.70	0.64	0.67	0.63	0.66	0.63	0.66	0.61	0.64			2	6
3	0.67	0.70	0.64	0.67	0.63	0.66	0.62	0.66	0.60	0.63			3	6
4	0.67	0.70	0.65	0.66	0.64	0.67	0.63	0.66	0.61	0.64			2	6
5	0.65	0.68	0.64	0.67	0.63	0.66	0.63	0.66	0.51	0.54			1	36
Stack Avg.	0.66	0.69	0.642	0.67	0.63	0.66	0.63	0.66	0.59	0.62			2	12

Temp.: 180-185°C; Cell Size + 12" x 17" bipolar plates heat treated at 900°C, H_2/Air

* mV/1000 hours of operation
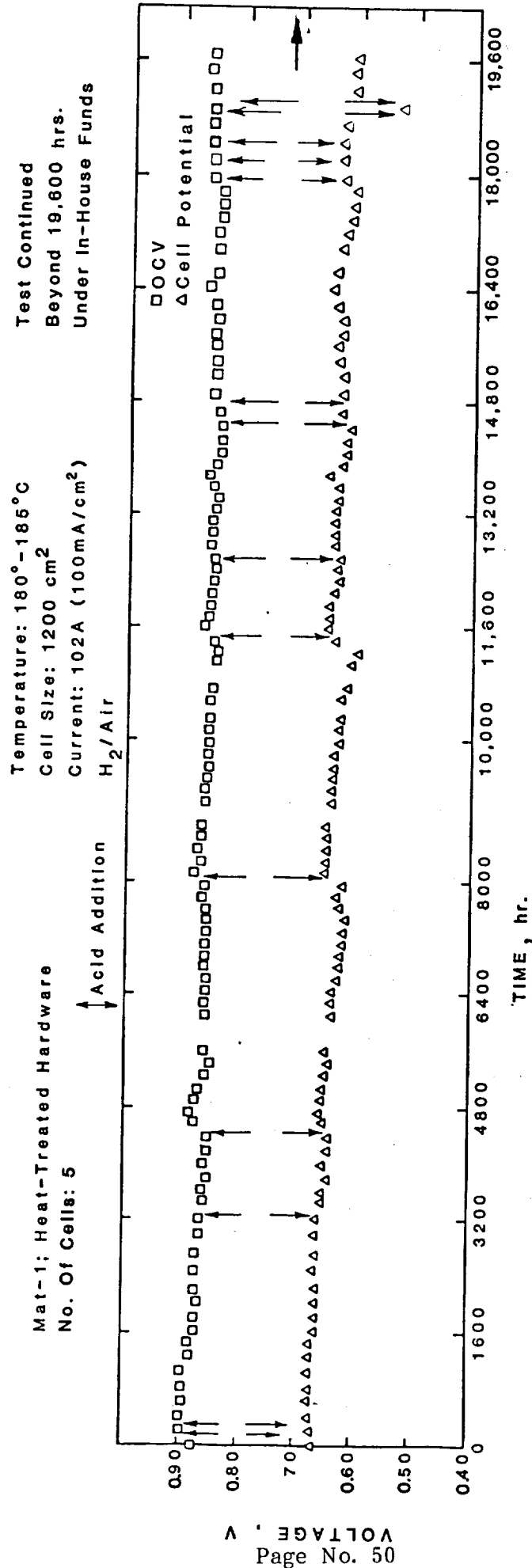
FIGURE 3.2   LIFEGRAPH OF STACK 431 WITH HEAT-TREATED PLATES
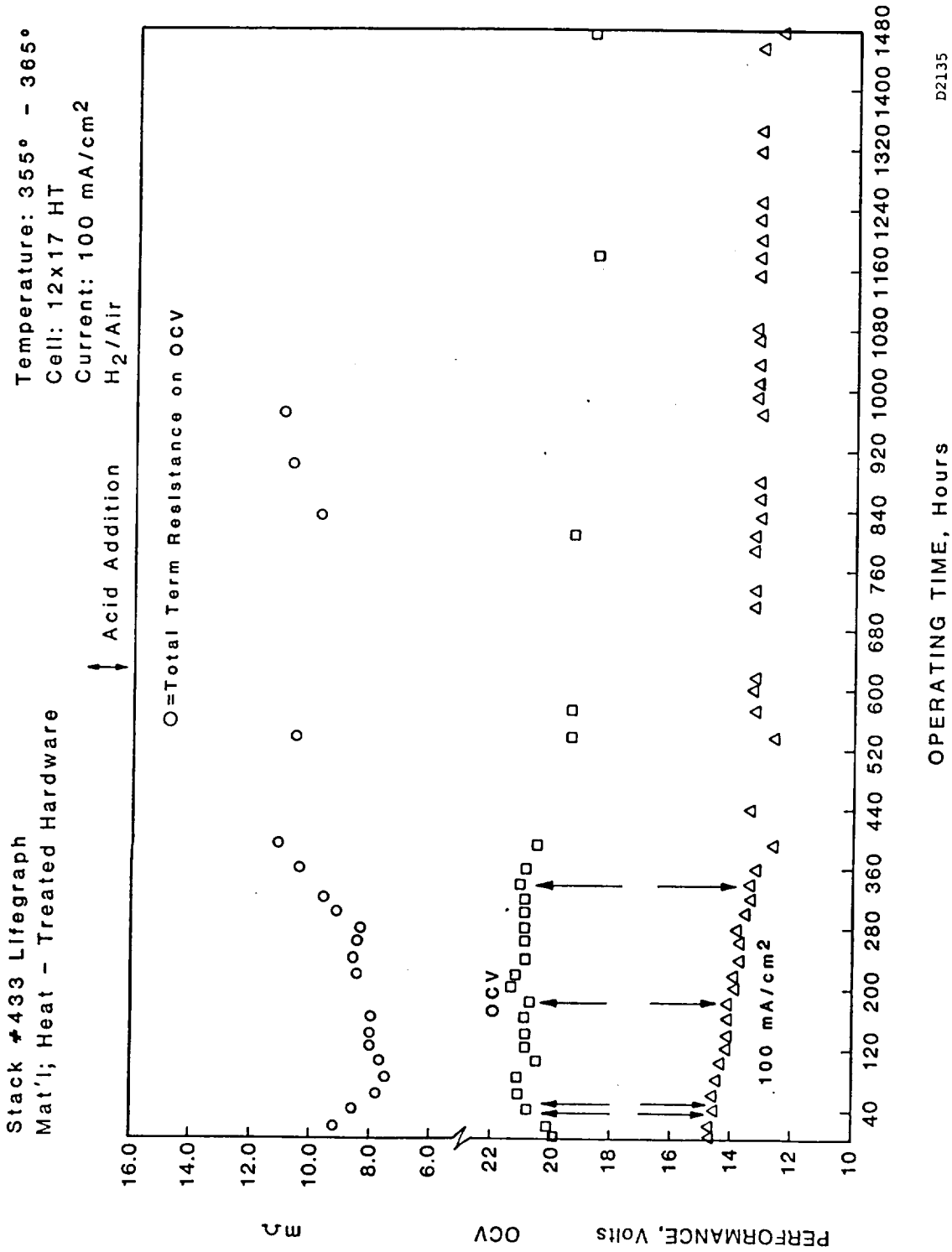
FIGURE 3.3 LIFE GRAPH OF STACK 433
(23-Cell with heat-treated plates)
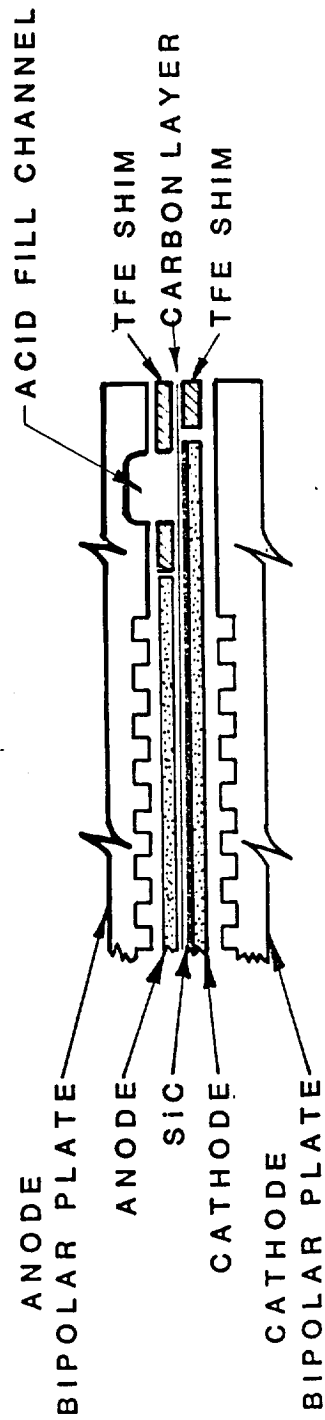
FIGURE 3.4 SCHEMATIC OF SEAL DESIGN USED IN STACKS 431 and 433

3.2 Stack Testing of Acid Management Control Member (AICM)

There are several aspects to acid management which require operational or component solutions. The AICM was designed to address the following situations:

1. Acid expansion and contraction during start-up, transients, and upsets.

2. Acid transport and lateral distribution in the anode backing to minimize resistance and gas diffusion.

3. Acid storage to decrease the performance loss betwen acid additions at normal maintenance intervals of approximately 4,000 hours.

Although additional optimization may be desirable, the state-of-the-art AICM (see Section 2) was tested in a stack to establish a baseline and identify areas for improvement. A 3-cell stack (No. 620) was built with 5 inch x 15 inch heat-treated bipolar plates and incorporated anode electrodes which had the selectively wetproofed backing papers (AICM). The primary objective was to determine if the wetproofing was sufficient to prevent excessive wetting of the anode backing, leading to a diffusion polarization. The performance shown in Figure 3.5 demonstrates the expected peak performance of 0.675 V at 100 mA/cm^2 and 180°C on H_2/air. Although the open circuit voltage and performance were responsive to acid additions at 3,400 and 6,400 hours, further additions resulted in a performance loss. Upon disassembly, the plates were found to be cracked. Extensive corrosion of cathode plate surfaces was found in the areas which appeared to have discolored. This discoloration was attributed to hot spots that occur when the anode and cathode gases mix. The bipolar plates were from a very early batch of heat-treated plates and may have been porous. Since that time, different resins and new molding procedures have improved the density. The cracked plates, however, probably allowed extensive crossleaks to occur, which caused the localized overheating. Over 10,000 hours of operation was still achieved with an average decay rate from the peak performance of ~12 mV/1000 hr. The amount of acid added during the operation of this stack was monitored, but the numbers are not representative because of cell design considerations. The AICM does not appear to need any extensive manufacturing changes, however, additional testing would be desirable with the improved plates which were available at the end of this program.
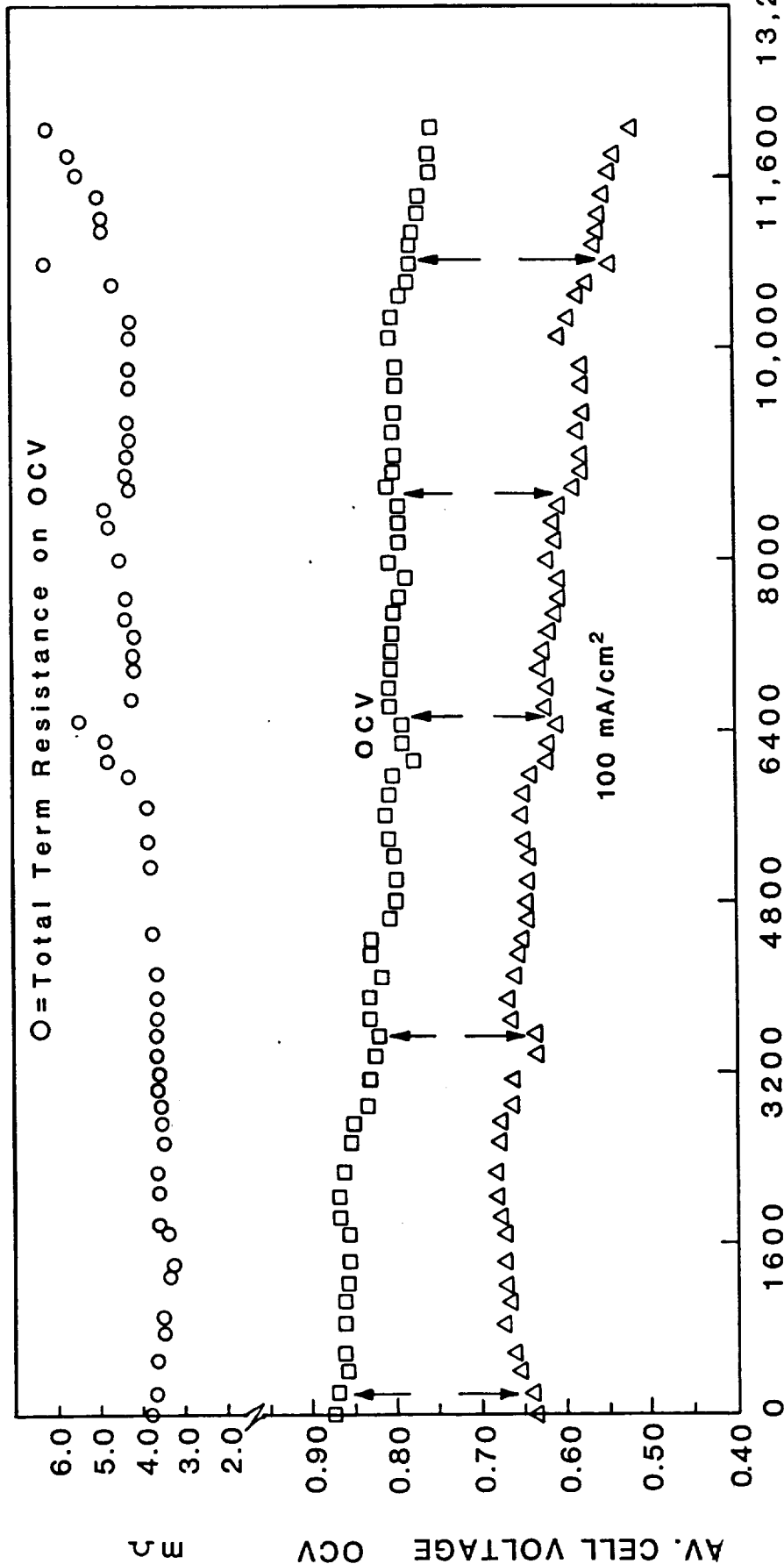
FIGURE 3.5 LIFEGRAPH OF STACK 620 WITH AICM AND HEAT-TREATED BIPOLAR PLATES

ENERGY RESEARCH CORPORATION

3.3   Low-Loaded Electrodes

Powerplant costs and performance can be affected by the amount of platinum used in the electrodes. This program examined the effect of platinum loading and the results from single 25 cm^2 cells are reported in Section 2 of this report. The next large test vehicle used by ERC for evaluation was a 3-cell, 5 inch x 15 inch stack. A 3-cell stack (No. 621) was assembled using heat-treated bipolar plates and electrodes containing ~0.12 and ~0.25 mg Pt/cm^2 in the anodes and cathodes, respectively. The matrix was MAT-1 and the seals were ERC's standard Teflon. The stack responded to acid additions as indicated in Figure 3.6, again confirming the fast transport of acid with the cathode and matrix exposed to the acid fill channel.

Performance of this stack was slightly higher than expected with a peak of 0.66 V on H_2/air at 180°C. The stack had a reasonable performance for about 15,000 hours with a decay rate of approximately 6 mV/1000 hr. per cell @ 100 mA/cm^2. This decay behavior was within the range of standard cells (2 to 8 mV/1000 hr). After 15,000 hours of operation, the stack performance was decaying at a faster rate. A broken current collector and higher crossleak of H_2 across the cell may have contributed to this decay. At 18,200 hours of operation, the performance of this stack dropped significantly after a hydrogen supply interruption.

Post-test analyses showed that one of the terminal bolts connected to the current collector was broken in two pieces, making it impossible to connect the stack back to the load. Bipolar plates were found structurally strong and the ribs were intact, showing no sign of corrosion. However, large cracks were detected on the bipolar plates, mainly at air exits. The anodes and anode backings of the stack were found to be wet. The cathode and cathode backings were dry. Matrices of the cells appeared dry. Acid channels were also dry, hard, and slightly clogged.

3.4   Conclusions from Stack Testing

The primary objective of this program was to demonstrate long-term endurance of 900°C heat-treated bipolar plates and to identify areas for

F

Temperature: 179° – 185°C

Cell Size: 5x15

Current: 32.8A (100mA/cm²)

H₂/Air

Mat-1; Heat-Treated Hardware
Low Loaded Electrodes

Acid Addition

□ OCV

△ Cell Potential

VOLTAGE , volts

0.90 0.80 0.70 0.60 0.50 0.40

TIME , hr.

0 1600 3200 4800 6400 8000 10,000 11,600 13,200 14,800 16,400 18,000 19,600

D1863f
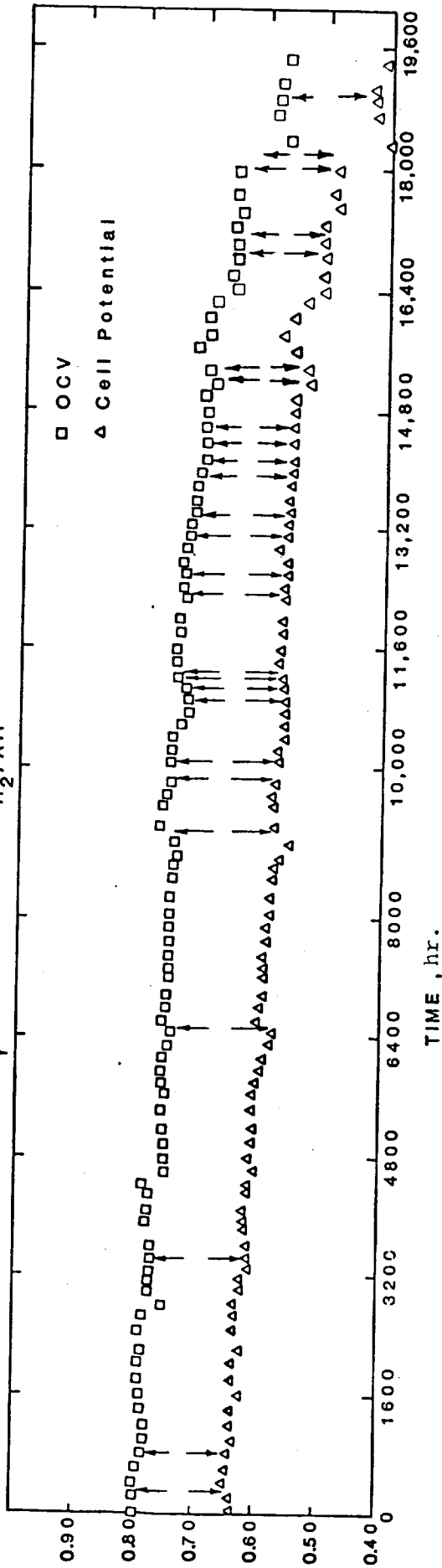
LIFEGRAPH OF STACK 621

FIGURE 3.6   LIFEGRAPH OF STACK 621 WITH LOW-LOADED ELECTRODES

improvement. The summary of stacks in Table 3.2 demonstrates the achievement of this objective. Especially Stack 431, which has achieved over 22,000 hours of operation and is continuing to be operated under in-house funds. Although there was not sufficient time or funding to test the improved bipolar plates available at the conclusion of this program, it seems reasonable to expect even longer life with less softening and channel blockage from these materials. Improvements in plate flatness, thickness uniformity, and density should lead to a decrease in the occurrence of cracked plates and crossleaks.

The long-term testing also revealed that low-loaded electrodes can indeed operate with the present components without being poisoned by long-term degradation products. If any poisons still exist in the components, they continue to produce effects very early in the operation, as they did with nonheat-treated bipolar plates.

AICM testing revealed the need to seal the edges of the anode AICM backing so that acid does not weep out. As might be expected, the acid addition procedure may also require modification to maintain a partially filled AICM. These procedures remain for future development.

Post-test examination of the backing papers suggested that this component lost its strength with time, possibly due to corrosion of the fiber bonds. Improvements in its strength without sacrificing porosity would definitely be desirable.

ENERGY RESEARCH CORPORATION

TABLE 3.2   SUMMARY OF LONG-TERM STACK TESTS

Stack No.	Test Purpose	No. of Cells	Nominal Cell Size, In.	Hours Operated, 12/31/82	Peak Perf., V @ 100 mA/cm²	Peak OCV, V
620	H.T. Plates w/AICM	3	5 x 15	12,050	0.683	0.870
621	H.T. Plates w/Low Pt Elec.	3	5 x 15	19,261	0.656	0.810
428	Non H.T. Plates - Endurance	5	12 x 17	8,574	0.638	0.906
429	Non H.T. Plates - Endurance	5	12 x 17	8,699	0.584	0.824
430	Non H.T. Plates - Endurance	5	12 x 17	8,615	0.634	0.880
431	H.T. Plates - Endurance	5	12 x 17	22,044*	0.680	0.900
432	H.T. Plates - Endurance	5	12 x 17	4,240	0.620	0.940
433	Molded H.T. Plates - Multicell	23	12 x 17	1,480	0.641	0.865

*Test continuing

SECTION 4

HIGH PRESSURE TECHNOLOGY DEVELOPMENT

Large phosphoric acid fuel cell powerplants are expected to be pressurized to achieve greater efficiencies. The pressurization also results in compact reactors, heat exchangers and ducting. The higher pressure operation, however, poses additional constraints on technology development. The increased pressure may lead to an increased corrosion of the carbon catalyst support and bipolar plate materials. Improved and cost-effective catalyst materials are desirable for an efficient powerplant operation. Some of these issues are addressed in this section. The construction of a pressurized stack facility was also initiated during this program.

4.1 <u>Development of Electrodes Suitable for Pressurized Operation</u>

Three aspects of electrode development were investigated:

1. Development of more corrosion resistant catalyst support materials.

2. Investigation of heat-treated platinum catalysts.

3. Development of alloy catalysts for greater performance and stability.

Results obtained in these areas are summarized in Sections 4.1.1 to 4.1.3.

4.1.1   Development of Catalyst Support Materials

Corrosion characteristics of different support materials were compared in out-of-cell corrosion tests as well as in laboratory-scale cells at high operating potentials. In addition, 8 laboratory cells were operated under normal conditions to compare long-term decay associated with different catalyst supports.

ENERGY RESEARCH CORPORATION

Out-of-Cell Corrosion Characteristics

The corrosion characteristics of the following catalyst support materials were evaluated at atmospheric conditions to establish a preliminary ranking:

- As-received Shawinigan carbon black (acetylene black)

- Shawinigan carbon black, heat-treated at $1800^{\circ}C$

- Vulcan, XC-72 carbon black, heat-treated at $1800^{\circ}C$

- Vulcan, XC-72 carbon black, heat-treated at $2500^{\circ}C$

The test apparatus and procedure used for these samples are discussed in Section 1. The samples were corroded initially at 1.05V (RHE) for 100 hours and then a slow sweep polarization test was conducted. The potentiostatic corrosion rates (mA/mg) at 1.05V (RHE) are compared in Figure 4.1. The heat-treated samples have comparable corrosion rates and are about three times less than the as-received Shawinigan. The Tafel slope and the Critical Corrosion Potential (a potential above which corrosion current increases rapidly) measured during sweep polarization are reported in Table 4.1. The Tafel slopes for these samples are comparable to each other and lie between 95 and 111 mV. The critical corrosion potential for as-received Shawinigan is somewhat lower as compared with the heat-treated Shawinigan. In an earlier study,* an as-received Vulcan XC-72 support showed the corrosion rate (mA/mg) at 0.8V of 7 to 10 times greater than an as-received Shawinigan carbon black. This may have been observed because Shawinigan is a pure carbon relative to XC-72 or to incomplete stabilization. It should also be noted here that if one compares the corrosion rates in terms of $mA/(cm^2$ of real surface area), the comparison may be somewhat different. However, the overall qualitative rating (in terms of stability) may remain as follows:

Vulcan XC-72 (as-received) less than,

Shawinigan (as-received) less than,

Vulcan (1800 HT, 2500 HT) and

Shawinigan (1800 HT)

* Christner, L. and George, M., "Electrode Optimization for Phosphoric Acid Fuel Cells,"Final Report for DOE Contr. No. DE-AC-03-78ET13114, Energy Research Corp., Danbury, CT, 1981.
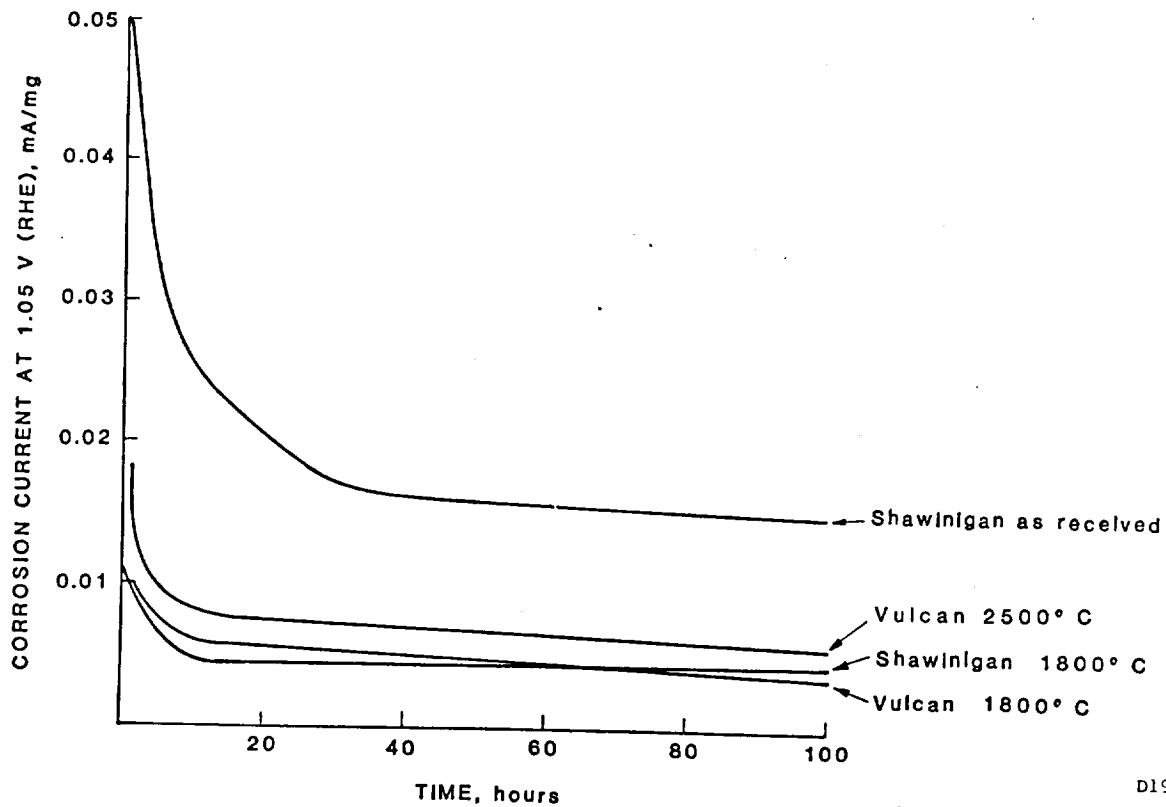
FIGURE 4.1   CATALYST SUPPORT CORROSION CURRENT AT 1.05V (RHE)
(190°C and 100 Wt% H_3PO_4)

TABLE 4.1   CORROSION CHARACTERISTICS OF VARIOUS
CATALYST SUPPORT MATERIALS

Acid Conc.:   100-102% H_3PO_4 Temperature = 190°C   Pressure = 1 Atmosphere

Sample	Heat-Treatment Temperature °C	Tafel Slope mV/Decade @ 190°C Sweep Tafel	Critical* Corrosion Potential, V Anod Sweep	Cath Sweep	Corrosion Current @ 1.05 V and 190°C mA/mg
Vulcan XC-72	1800	95	1.06	1.08	4.6 x 10^{-3}
Vulcan XC-72	2500	111	1.19	1.25	6.0 x 10^{-3}
Shawinigan	As-Received	100	1.02	1.04	15 x 10^{-3}
Shawinigan	1800	110	1.24	1.28	4.6 x 10^{-3}

*Critical corrosion potential is a potential above which the corrosion current increases rapidly.

ENERGY RESEARCH CORPORATION

Stress Testing in Laboratory Cells

The as-received Vulcan and Shawinigan materials were further stress tested at ~875 mV cathode potential in laboratory-scale cells (Cells 2083 and 2085) for approximately 1,850 hours (11 weeks). The purpose of these cells was to intentionally corrode the catalyst support, and see the effect of such a corrosion on cell performance. The results also provide information on cell performance decay under part-load conditions where operating potentials are expected to be high.

Two control cells (Cells 2084 and 2082) with the same cathodes were operated at normal operating potentials (~660 to 680 mV, 200 mA/cm^2). The Vulcan-type cathodes contained 40% PTFE and Shawinigan-type cathodes contained 30% PTFE. Cathodes with these levels of wetproofing had exhibited acceptable stability in the past at normal operating conditions.

All four cells were operated at normal conditions (200 mA/cm^2 on air) for a minimum period of 400 hours. During this break-in period, the cells were allowed to reach peak performance. The stressed cells were operated on oxygen at ~875 mV and on a once-a-week basis, performance was checked at 200 mA/cm^2 on both air and oxygen to determine the cell performance. The control cells were operated continuously at 200 mA/cm^2 on air. The peak performance of all cells was within -3.5 to +4.5 mV of each other. The oxygen gains at peak performance were 75 $\pm$ 5 mV, thus showing comparable wetproofing. The weekly performance levels for both the stress and control cells are shown in Table 4.2. The "0" time data corresponds to performance levels just prior to initiation of the stress testing.

The performance changes during the stress test period are summarized in Table 4.3. While additional repeat cells are needed to obtain definitive conclusions, the following observations may be made from the data:

TABLE 4.2   PERFORMANCE HISTORY OF CELLS WITH VULCAN AND SHAWINIGAN SUPPORTS*

WEEKS ON TEST	CELL 2084 VULCAN-CONTROL (0.54,40)[+]				CELL 2083 VULCAN-STRESS (0.54,40)[+]				CELL 2082 SHAWINIGAN-CONTROL (0.5,30)[+]				CELL 2085 SHAWINIGAN-STRESS (0.57,30)[+]			
	OXYGEN 20 mA/cm²	200 mA/cm²	AIR 200 mA/cm²	O_2 GAIN	OXYGEN 20 mA/cm²	200 mA/cm²	AIR 200 mA/cm²	O_2 GAIN	OXYGEN 20 mA/cm²	200 mA/cm²	AIR 200 mA/cm²	O_2 GAIN	OXYGEN 20 mA/cm²	200 mA/cm²	AIR 200 mA/cm²	O_2 GAIN
0	873	762	688	74	870	757	689	68	875	756	678	78	882	761	684	77
1	864	757	685	72	856	746	677	69	855	748	674	74	877	761	681	80
2	860	755	685	70	855	750	678	72	846	743	671	72	873	754	675	79
3	866	757	684	73	849	733	659	74	853	746	673	73	869	746	666	80
4	870	763	689	74	846	729	652	77	864	749	673	76	864	741	660	81
5	854	749	675	74	843	725	644	81	842	736	664	72	861	739	656	83
6	851	742	667	75	838	716	633	83	842	737	664	73	852	731	647	84
7	845	745	672	73	836	717	630	87	838	734	662	72	851	726	638	88
8	855	749	676	73	833	710	624	86	846	737	664	73	850	722	637	85
9	845	747	674	73	829	704	617	87	834	734	663	71	845	716	630	86
10	864	758	681	77	826	696	607	89	854	745	666	79	839	714	625	89
11	858	752	677	75	820	687	596	91	844	727	651	76	835	706	619	87

* The control cells continuously operated at 200 mA/cm² on air (660 to 680 mV). The stressed cells continuously operated at ≈875 mV on oxygen (400 hours break-in period for all four cells). Operating temp. 190°C.

[+] Parentheses show cathode Pt loading in mg/cm² and % PTFE content respectively. 1.25 stoich H_2, 3 stoich air, 14 stoich O_2.

TABLE 4.3   SUMMARY OF PERFORMANCE CHANGES FOR VULCAN AND SHAWINIGAN
SUPPORTS DURING THE 11 WEEK TEST PERIOD

CELL NO	CATALYST SUPPORT	mV CHANGES DURING STRES TEST				
		20 mA/cm^2, O_2	200 mA/cm^2, O_2	200 mA/cm^2, O_2	200 mA/cm^2, AIR	O_2 Gain
2084	Vulcan, Control	-15	-10		-11	+ 1
2083	Vulcan, Stress	-50	-70		-93	+21
2082	Shawinigan, Control	-31	-27		-27	- 2
2085	Shawinigan, Stress	-47	-55		-65	+10

- There is indeed a significantly greater decay in all the cells operated at ~ 875 mV. If one assumes that performance changes at 20 mA/cm^2 are indicative of inherent catalytic activity, a significant portion of the decay appears to be related to changes in the activity. Oxygen gain, indicative of diffusion polarization, registered only a small increase for the stressed cells. The observed changes in activation polarization may be related to carbon corrosion leading to a loss of platinum or to a greater platinum coarsening at the higher cathode potential. The former mechanism is more likely.

- Based on the limited data, it appears that Shawinigan black is a somewhat better candidate support for higher pressure and temperature operation where higher cell voltages are expected. Also, Shawinigan black has far less impurities as compared with Vulcan XC-72.

Long-Term Endurance Testing of Different Supports

Four cells (No's. 2067, 2068, 2065 and 2066) with heat-treated Vulcan and Shawinigan supports were endurance tested and their performance behavior was compared with that of standard Pt/Vulcan XC-72 supports. Table 4.4 summarizes the peak and final performance of the above mentioned cells along with standard cathode cells.

Two of the cells (No's. 2067 and 2068) had cathodes with Vulcan supports heat-treated at 1800°C and wetproofed with 35% PTFE. The other two cells (No's. 2065 and 2066) had cathodes with Shawinigan supports heat-treated at 1800°C and wetproofed with 25% PTFE. The wetproofing levels were chosen on the basis of past experience, but further optimization may be necessary as evidenced by the somewhat high oxygen gains for these electrodes. The standard cells (No's. 2024, 2025, 1490 and 2084) had cathodes with as-received Vulcan support, wetproofed with 40% PTFE. As can be observed in Table 4.4, the IR-free peak performance on air at 200 mA/cm^2 for the standard cells was 682 $\pm$ 13 mV. The peak performance for the cells with heat-treated cathodes was on the lower end of the standard cells, 673 $\pm$ 3 mV. Thus there is a reasonable basis for comparison of their long-term behavior. Peak performance for all the cells described here was achieved in a normal break-in period of 100 to 400 hours. The observed decay rates at 20 mA/cm^2 (O_2) and 200 mA/cm^2 (O_2 and air) are summarized in Table 4.5. As can be seen in this table, the air performance decay rates for heat-treated supports are somewhat lower than the corresponding decay rates for standard cells. The trends are reversed for 20

TABLE 4.4 SUMMARY OF 25-cm² CELLS TESTED WITH DIFFERENT CATALYST SUPPORTS

	CELL CATHODE			CELL PERFORMANCE LEVELS (IR-FREE, mV)						Oxygen Gain @ 200 mA/cm², mV		Operating Hours	Comments (Reason for termination)
				PEAK			FINAL						
				Oxygen		Air	Oxygen		Air				
	Cell No.	Pt mg/cm²	PTFL, %	@ 20 mA/cm²	@ 200 mA/cm²	@ 200 mA/cm²	@ 20 mA/cm²	@ 200 mA/cm²	@ 200 mA/cm²	@ Peak	Final		
STANDARD Pt CELLS	2024	.50	40	865	754	671	834 / 834	720 / 731	639 / 646	83	81 / 85	5164 / 6408	Voluntary
	2025	.50	40	875	759	675	836 / 836	722 / 731	644 / 643	84	78 / 88	4880 / 5876	Voluntary
	1490	.65	40	889	776	695	863	755	680	81	75	5136	Still Operating
	2084	.54	40	873	762	688	845 / 843 / 844	732 / 732 / 729	657 / 655 / 646	74	75 / 77 / 83	5376 / 7032 / 8904	Still operating
Pt/VULCAN 1800 HT	2067	.56	35	888	765	674	841	735	663	91	72	5544	Voluntary
	2068	.56	35	880	753	670	847	736	656	83	80	3624	Voluntary
Pt/SHAWINIGAN 1800 HT	2065	.48	25	881	764	675	837	737	661	89	76	5232	Voluntary
	2066	.48	25	881	759	673	840	737	655	86	82	3672	Voluntary

TABLE 4.5 SUMMARY OF DECAY RATES OBSERVED FOR DIFFERENT
CATALYST SUPPORTS IN 25-cm^2 CELLS

	mV/1000 hr (first 5000 hrs)		
	20 mA/cm^2 O_2	200 mA/cm^2 O_2	200 mA/cm^2 Air
Std Pt/Vulcan			
2024	6	7	6
2025	8	8	6
1490	5	4	3
2084	5	6	6
Pt/Vulcan 1800			
2067	9	6	2
2068	10	5	4
Pt/Shaw 1800			
2065	8	5	3
2066	11	6	5

mA/cm^2 (O_2) decay rates. The differences in the internal structure of electrodes and acid film thicknesses for the standard and the unoptimized heat-treated electrodes may be responsible for this reversal in trends. On the basis of 200 mA/cm^2 air performance and the results of out-of-cell and stress tests, however, heat-treated carbons appear preferable to the as-received Vulcan support. Further testing, and post-test characterization is recommended to clearly differentiate and rationalize the behavior of different supports.

4.1.2 Investigation of Heat-Treated Platinum Catalyst

The standard cathode utilizes as-received Vulcan XC-72 as the support material, and no special post-catalyzation treatment is employed. As shown in Section 1, decay rates for this type of cathode vary between 3 and 6 mV, and greater decay rates may be expected at a higher pressure and voltage. In the previous section, we discussed the improved catalyst support for minimizing the performance decay. In this section, we will discuss the possibility of stabilizing the catalyst by a post-catalyzation heat-treatment. The possibility of improving the initial cell performance by such a treatment was also investigated.

The standard Pt/Vulcan catalyst was heat-treated in a N_2 atmosphere at $900^{\circ}C$. The possible benefits of the heat-treatment are threefold:

1. The platinum crystalline size increases and approaches a near-optimum size.

2. The carbon support becomes somewhat better stabilized and some of the impurities may be removed.

3. Variability of the carbon surface and surface groups is minimized.

The platinum surface area of the sintered electrode for this batch (designated as CAT-6-A) was 60 m^2/g Pt as compared to a normal surface area of 120 m^2/g Pt. Performance of two 25-cm^2 cells (No's. 2061 and 2062) tested with this catalyst is shown in Table 4.6. The initial performance of these two cells was in the same range as the typical standard cells (See Table 4.4, Cells 2024, 2025, 1490 and 2084). Cell 2061 was terminated voluntarily after 5,856 hours, showing an overall performance decay rate of ~3 mV/1000 hr. The

ENERGY RESEARCH CORPORATION

TABLE 4. 6 SUMMARY OF 25-cm² CELLS TESTED WITH DIFFERENT ALLOY CATALYSTS

Page 1 of 2

Cell No.	Catalyst Designation	Alloying Element	Pt mg/cm²	PTFE %	PEAK Oxygen @ 20 mA/cm²	PEAK Oxygen @ 200 mA/cm²	PEAK Air @ 200 mA/cm²	FINAL Oxygen @ 20 mA/cm²	FINAL Oxygen @ 200 mA/cm²	FINAL Air @ 200 mA/cm²	Oxygen Gain @ Peak	Oxygen Gain Final	Operating Hours	Comments (Reason for termination)
2061	CAT-6-A	None	.50	40	880	758	687	848 / 840	734 / 740	657 / 668	71	77 / 72	5040 / 5856	Voluntary
2062	CAT-6-A	None	.50	40	871	758	684	809	717	645	74	72	4800	Crossover
2049	CAT-1-A	V	.50	40	894	767	691	853	743	650	76	93	4992	Voluntary
2053	CAT-2-A	V	.57	40	904	782	708	842	739	643	74	96	4944	Voluntary
2054	CAT-2-A	V	.57	40	911	783	709	854	742	649	74	93	4872	Voluntary
2055	CAT-3-A	V	.50	40	903	771	693	850	734.	654	78	80	5376	Voluntary
2056	CAT-3-A	V	.50	40	892	769	693	837	736	664	76	72	5544	Voluntary
2071	CAT-2-A	V	.55	45	890	761	682	850	734	661	79	73	5376	Voluntary
2072	CAT-2-A	V	.55	45	896	762	686	846	734	655	76	79	5256	Voluntary
2057	CAT-4-A	Ta	.55	40	895	772	689	828 / 836	730 / 734	652 / 657	83	78 / 77	256 / 6600	Voluntary
2058	CAT-4-A	Ta	.55	40	889	764	685	845 / 846	738 / 744	663 / 670	79	75 / 74	4992 / 6576	Voluntary
2073	CAT-8-A	Ta	.60	45	891	764	682	863 / 857	750 / 745	669 / 661	82	81 / 84	4872 / 5856	Voluntary
2074	CAT-8-A	Ta	.60	45	894	764	681	849 / 843	752 / 741	674 / 670	83	78 / 71	5064 / 5864	Voluntary
2090	CAT-12-A	Ta	.59	45	797	763	687	855 / 848	738 / 736	661 / 655	76	77 / 81	4896 / 6744	Voluntary
2091	CAT-12-A	Ta	.59	45	899	764	692	841 / 827	723 / 700	642 / 621	72	81 / 79	5064 / 6768	Voluntary

........(continued)

ENERGY RESEARCH CORPORATION

TABLE 4.6 SUMMARY OF 25 cm² CELLS TESTED WITH DIFFERENT ALLOY CATALYSTS   ....(Concluded)

| Cell No. | CELL CATHODE | | | | CELL PERFORMANCE LEVELS (IR-FREE, mV) | | | | | | | | Operating Hours | Comments (Reason for termination) |
| | Catalyst Designation | Alloying Element | Pt mg/cm² | PTFE % | PEAK | | | FINAL | | | Oxygen Gain @ 200 mA/cm², mV | | | |
					Oxygen @ 20 mA/cm²	Oxygen @ 200 mA/cm²	Air @ 200 mA/cm²	Oxygen @ 20 mA/cm²	Oxygen @ 200 mA/cm²	Air @ 200 mA/cm²	@ Peak	Final		
2063	CAT-7-A	Cr	.48	40	855	695	604	855	695	604	91	91	600	Low Initial Performance
2064	CAT-7-A	Cr	.48	40	861	696	602	861	696	602	94	94	480	Low Initial Performance
2086	CAT-7-A	Cr	.48	45	879	756	684	841	736·	664	72	72	888	Voluntary Low Performance
2087	CAT-7-A	Cr	.48	45	879	753	680	844	733	665	73	68	1776	Voluntary Low Performance
2079	CAT-10-A	Cr	.54	45	900	772··	698	866 840	748 726	671 650	74	77 76	5352 8448	Voluntary
2080	CAT-10-A	Cr	.54	45	901	769··	695	854	746	672	74	74	1824	Voluntary
2081	CAT-10-A	Cr	.54	45	895	770	695	860 857	748 737	674 644	75	74 93	4920 8400	Voluntary
2088	CAT-11-A	Cr	.60	45	904	775	699	848 843	735 739	658 658	76	77 81	5352 6168	Voluntary
2089	CAT-11-A	Cr	.60	45	900	770	697	874 866	743 749	660 673	73	83 76	5136 6984	Voluntary

performance decay for Cell 2062 was considerably greater because of a gas crossover in the cell. Other cells operated at ERC, with a similar heat-treated cathode, have shown results similar to Cell 2061 (within the variability range). Thus the heat-treated Pt-on-Vulcan catalyst appears only marginally better than a standard, unheat-treated cathode.

4.1.3 Development of "Alloy" Catalysts

Alloying the platinum catalyst with nonnoble metals may improve the oxygen reduction activity and possibly also improve the catalyst stability. Performance improvements of approximately 25 mV were sought under this program. Binary "alloys" were prepared using three alloying elements (vanadium, tantalum, and chromium) with varying compositions. The alloys or intermetallic compounds were prepared by impregnating suitable chemicals on a platinum-supported-on-Vulcan catalyst.

A complete list of the twelve catalyst batches prepared during this program is shown in Table 4.7. The table also lists the intended atomic percentage of the alloying element, surface area of the active material, lattice parameter and other characteristics, whenever measured. In some cases, corrosion testing and differential calorimetry were also performed to characterize the stability of these catalysts.

A total of 29 laboratory-scale cells with different "alloy" electrode structures were assembled and tested during the program. A goal of 5,000 hours of testing at 1 atm was set for these cells. The cells were operated at 200 mA/cm^2 on air, but for comparison of catalytic activity, IR-free performance at 20 and 200 mA/cm^2 on O_2 was measured periodically. Although, the measurement of ohmic resistance is somewhat uncertain, the IR-free performance at 20 mA/cm^2 (O_2) appears to be a reasonable indicator of inherent catalytic activity. The catalytic activity of the "alloys" was compared with that of a standard platinum-on-Vulcan catalyst. Because of the experimental nature of these electrodes, not all of the electrode structures provided acceptable performance or endurance levels. Performance behavior of a selected number of cells is included in Table 4.6. Results of the platinum-vanadium, platinum-tantalum and platinum-chromium catalysts are discussed below.

TABLE 4.7 CHARACTERISTICS OF ALLOY CATALYSTS PREPARED DURING THIS PROGRAM

Catalyst	Desired Composition	Composition of Alloying Element in Catalyst Atomic %	Composition in Sintered Electrode Atomic %	Lattice Structure	Lattice Parameter*	Electrochemical Surface Area of Sintered Electrode m²/g$_{Pt}$	XRD Crystallite Size Å	Accelerated Corrosion Test at 0.9V, 100% H₃PO₄, 190°C, 50 hr
CAT-1-A	PtV₃	74	26	Cubic	3.88	49	42	
CAT-2-A	Pt₃V	16	13	Cubic	3.87	101	40	87% of V dissolved
CAT-3-A	PtV	40	22	Ortho-rhombic		66		
CAT-9-A	Pt₃V			–		50		
CAT-4-A	Pt₂Ta			Ortho-rhombic	3.94	78		65% Ta dissolved
CAT-5-A	PtTa₂			–				
CAT-8-A	Pt₃Ta			Mono-clinic	3.95		141	
CAT-12-A	PtTa				3.92			
CAT-7-A	PtCr₃			Cubic		73		
CAT-10-A	PtCr₃	∿75	∿75		3.88	74	39	
CAT-11-A	PtCr₃				3.91		43	
CAT-13-A	PtCr₃					<40	69	

* Lattice parameter for pure platinum is 3.916 Å.

ENERGY RESEARCH CORPORATION

Platinum-Vanadium Catalysts

Four batches of this type of catalyst, CAT-1-A, CAT-2-A, CAT-3-A and CAT-9-A were prepared. Although the preparations were carried out with the intention of obtaining specific atomic percentages, the sintered electrodes showed compositions similar to Pt_3V. The measured lattice parameter and structural analysis confirmed that a Pt_3V intermetallic was formed by these preparations. Electrochemical Area (ECA) measurements showed catalyst surface areas of 50 to 100 m^2/g on the basis of platinum weight. An accelerated corrosion test in 100% H_3PO_4 at 0.9V (RHE) and 190°C showed that 87% of the alloying element from CAT-2-A was dissolved after 50 hours.

Cell testing showed that initial activity (as measured by IR-free voltage at 20 mA/cm^2 on O_2) was as much as 40 mV greater than a typical Pt/Vulcan cell. A lifegraph of Cell 2054, assembled with CAT-2-A is shown in Figure 4.2 along with a "typical" lifegraph of a baseline cell. After 5,000 hours of cell testing, this cell appears only marginally better than the baseline performance. The reason for the greater decay in activity as compared to the standard Pt catalyst appears to be related to dissolution of the alloying element, as discussed above. Upon disassembly, only trace amounts of vanadium were found in the cathode.

Platinum-Tantalum Catalysts

Four batches of this type of catalyst, CAT-4-A, CAT-5-A, CAT-8-A and CAT-12-A were prepared. Reasonably high surface areas were obtained with these preparations. Tantalum is expected to be more corrosion resistant to phosphoric acid as compared with vanadium. The accelerated corrosion testing showed that while tantalum was more stable as compared with vanadium, approximately 65% of Ta dissolved in 50 hours.

Cell testing of different catalyst batches with Tantalum as the alloying element showed as much as 30 mV improvement in initial activity over the "standard" cathode activity, but at 5,000 hours, the electrode activity was only slightly better than the standard (Table 4.6). Oxygen gains were reasonable all throughout, indicating an acceptable level of wetproofing. An example of cell performance behavior with catalyst CAT-4-A is shown in Figure 4.3.
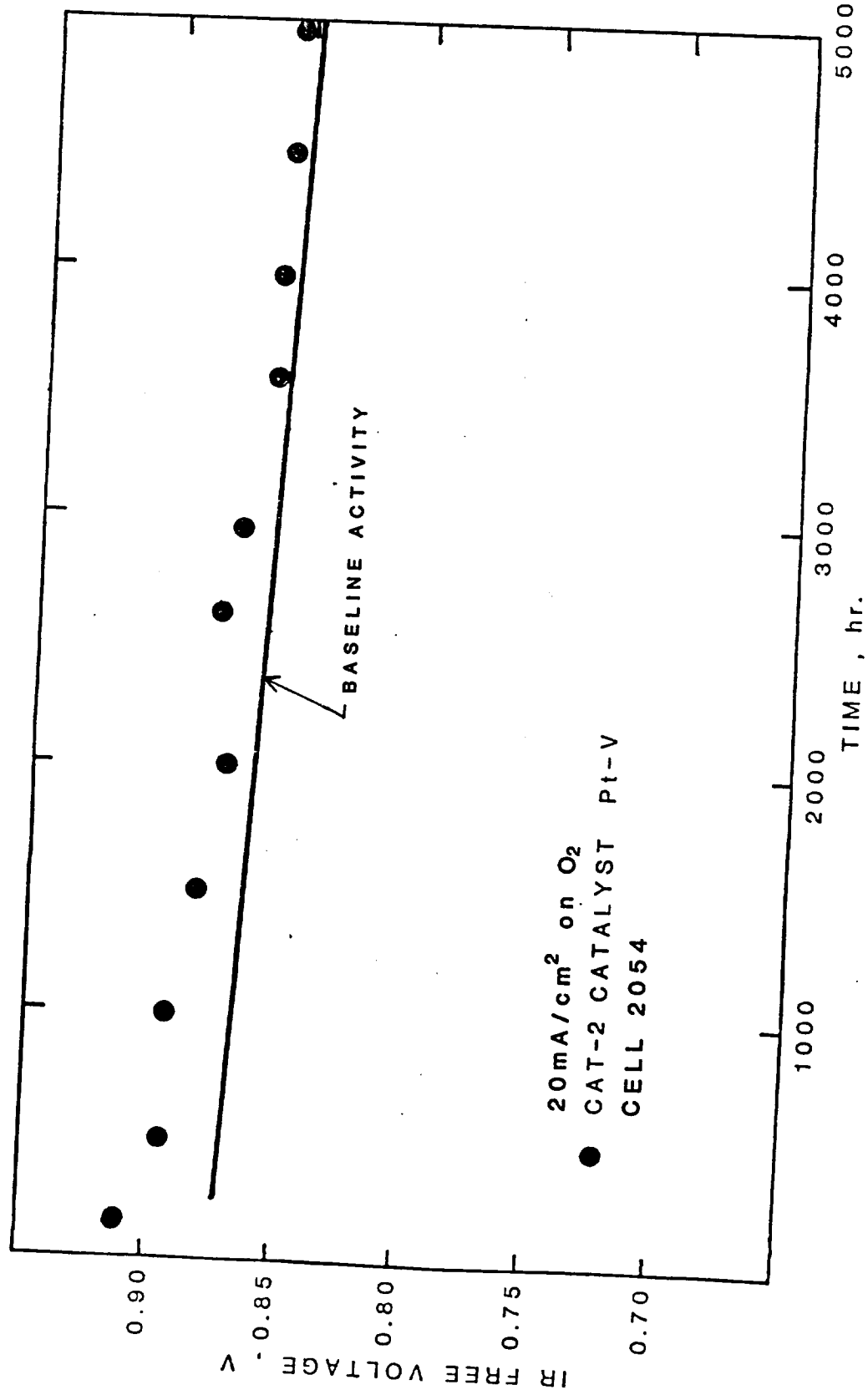
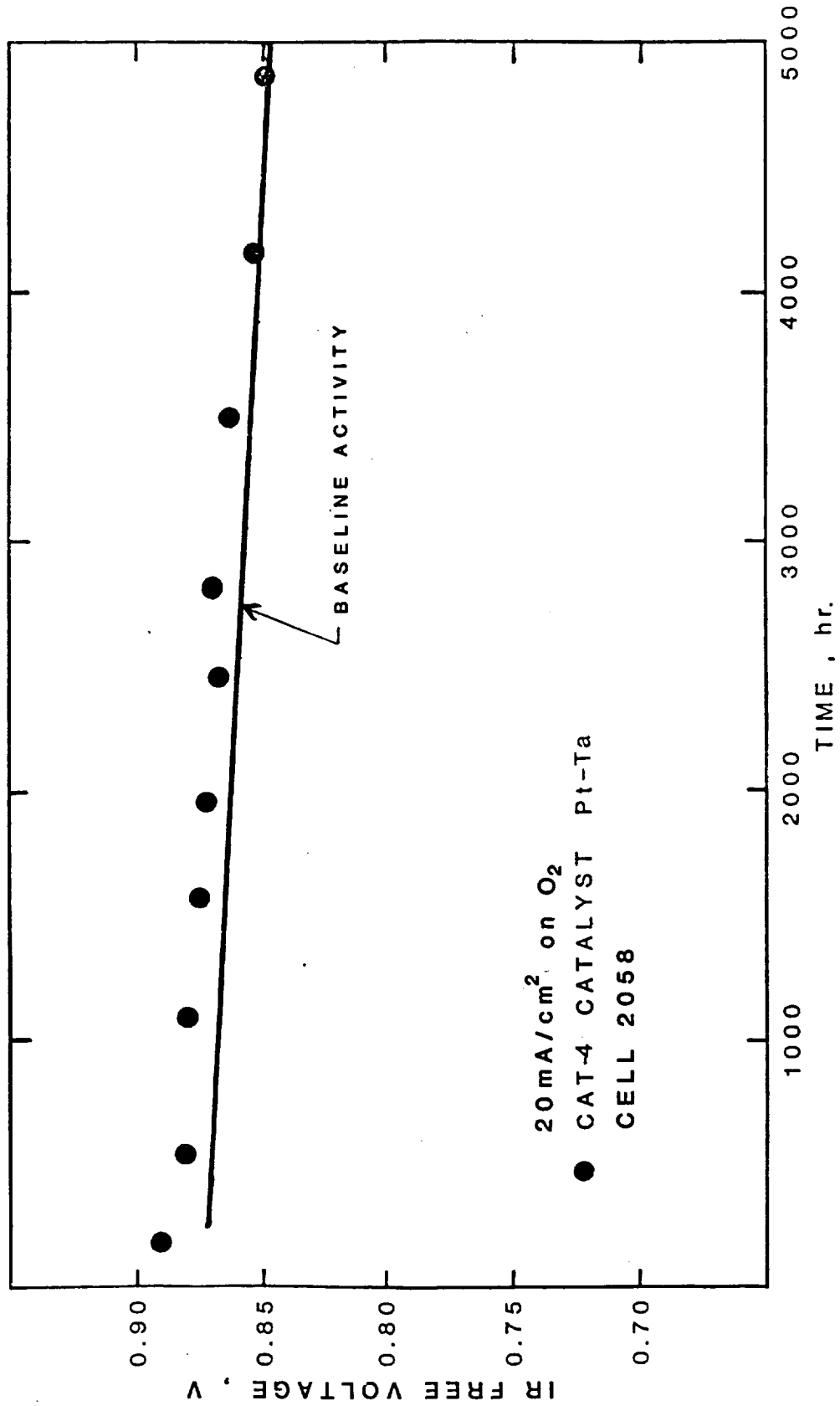FIGURE 4.2 LIFEGRAPH OF CELL 2054 WITH A Pt-V CATHODE

D2002**R**

FIGURE 4.3 LIFEGRAPH OF CELL 2058 WITH A Pt-Ta CATHODE

ENERGY RESEARCH CORPORATION

Platinum-Chromium Catalysts

Four batches of this catalyst, CAT-7-A, CAT-10-A, CAT-11-A and CAT-13-A were prepared during the program. The Electrochemical Area (ECA) of Batches CAT-7-A and CAT-10-A was ~75 m^2/g_{Pt}, but Batch CAT-13-A showed only a 40 m^2/g_{Pt} surface area. X-ray diffraction measurements showed the lattice parameters of 3.88 and 3.91 for Batches CAT-10-A and CAT-11-A respectively, indicating that an alloy was indeed formed.

Some electrodes with this type of catalyst were wetproofed with 40% PTFE (Cells 2063 and 2064) but showed high oxygen gains. Therefore, most of the electrodes were wetproofed with 45% PTFE. Initial activity with these catalysts were as much as 30 to 35 mV better than the standard activity. A signigicant portion (~1/2) of this activity advantage was still observable for some of the cells at 5,000 hours, as shown in Table 4.6 and Figure 4.4. Thus it appears that among the alloying elements tested, chromium is the most promising candidate. Further optimization of this preparation procedure, electrode fabrication and long-term testing are, therefore, recommended.

4.2 Pressurized Test Facility Development

High pressure stack technology development requires the capability for testing full size plate multicell stacks. Since component behavior can be tested reasonably well in 3 to 5 cell stacks, as it has been done for 1 atm operation, a facility was designed for this size stack. Only a brief description will be provided in this section for the rather complex system required for testing at pressure. The operating variables such as pressure limit, current, air and fuel flow, temperature, etc., were chosen somewhat arbitrarily, since an optimum had not been identified. Initial component testing did not require this knowledge; however, future systems to obtain engineering design information would need to be more specifically oriented toward a particular fuel cell system design.
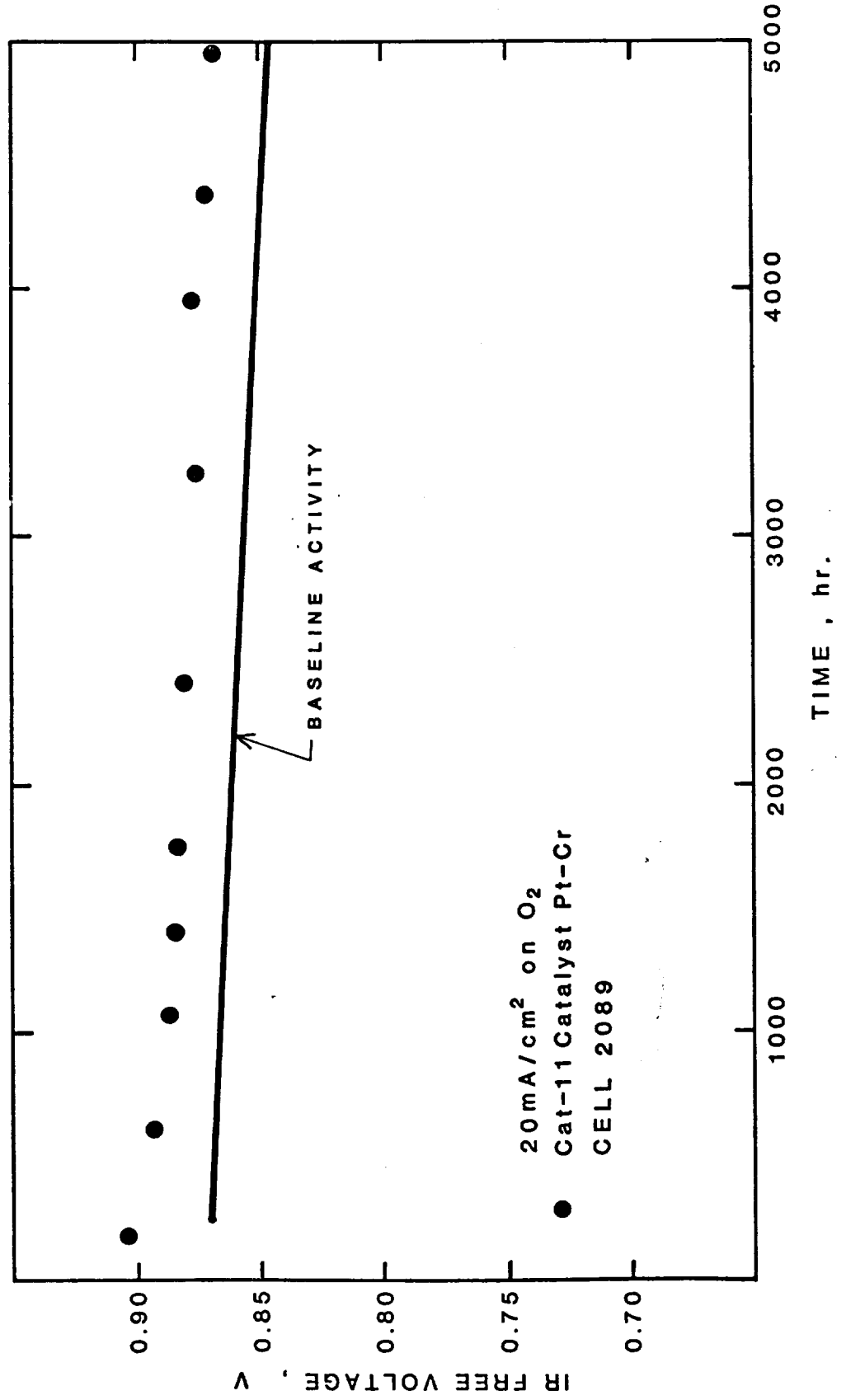
FIGURE 4.4   LIFEGRAPH OF CELL 2089 WITH A Pt-Cr CATHODE

The pressure vessel as shown in Figure 4.5 was designed for operation up to 120 psia with all penetrations through the flat bottom flange. Ease of access to the connections and the stack was achieved by setting the height of the flange at 36 inches. This was very important during the system check-out when plumbing and wiring modifications were necessary. Flexible connections were also made between the self-contained control panel (see Figure 4.6) and the pressure vessel which resulted in a compact and accessible system.

A schematic of the system is shown in Figure 4.7. The control scheme uses mass flow controllers in conjunction with pneumatic differential transmitters and controllers to keep the system at the set point. Using the vessel pressure as reference, the anode and cathode streams were controlled to the desired pressure differential by adjusting the rate at which gas exited the system. A summary of the basic operating characteristics is shown in Table 4.8.

A process control and automatic data acquisition system was assembled which monitored several operating parameters continuously. The basic features included in this test facility are outlined below:

Operation

- 100 to 1000 kPa and 50 to 200 mA/cm^2 testing

- Data scanning and recording by an automatic data acquisition system

- Unattended round-the-clock pressurized operation

- Reactants simulating actual fuel cell operating compositions

Safety and Stack Protection Features

- Stack overheating protection

- Low cell-voltage protection

- Electric power failure protection

- H_2 level monitor in the vessel and room

- CO monitor in room

- Automatic shutdown (maintaining differential pressures of $\pm$ 13 cm of water)
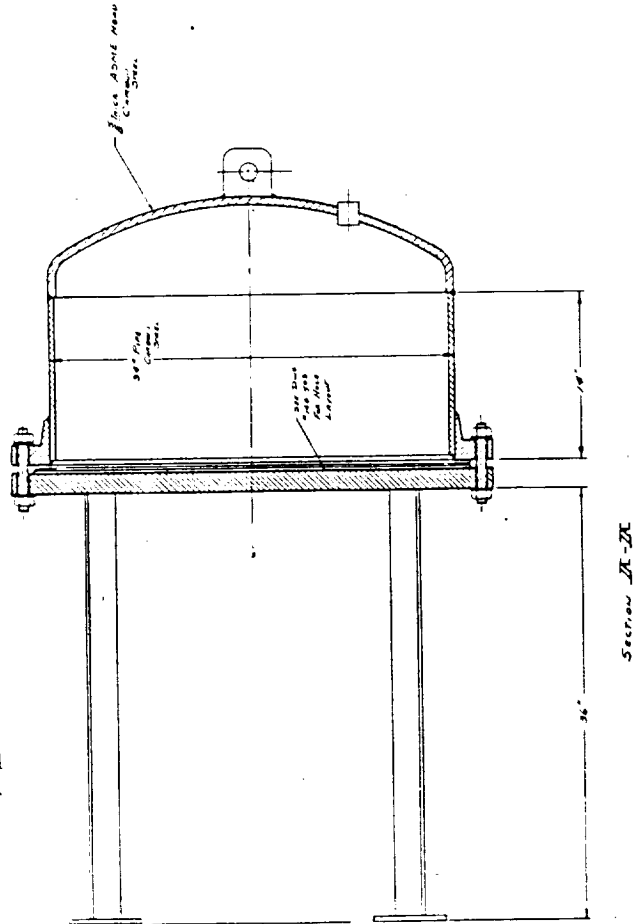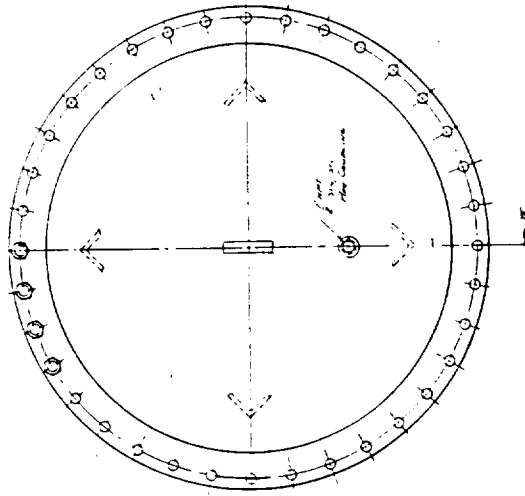
Designed & built to Section
 VIII of ASME code & stamped
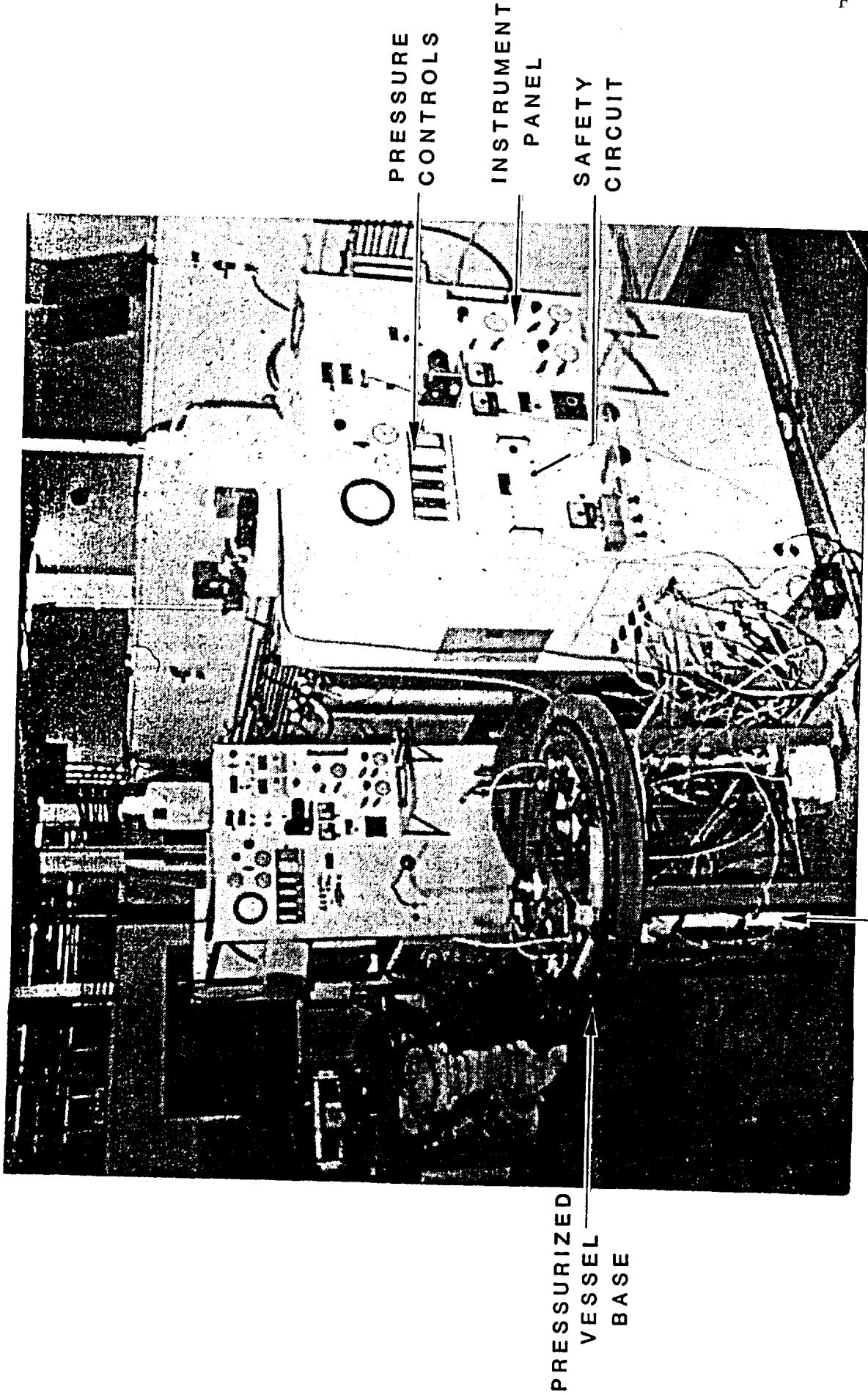All welds to be fully radio-
 grammed
Design Pressure 300 PSI
Working Pressure 200 PSI
Temperature 350°F

D2137

FIGURE 4.5   VESSEL FOR PRESSURIZED STACK TESTING

Page No. 80

F

P0657

PRESSURE CONTROLS

INSTRUMENT PANEL

SAFETY CIRCUIT

VAPORIZER

PRESSURIZED VESSEL BASE

FIGURE 4.6   COMPLETED TEST FACILITY FOR PRESSURIZED STACK TESTING

D1447

FIGURE 4.7 PRESSURIZED FLOW SCHEMATIC FOR 12 x 7 IN. CELL
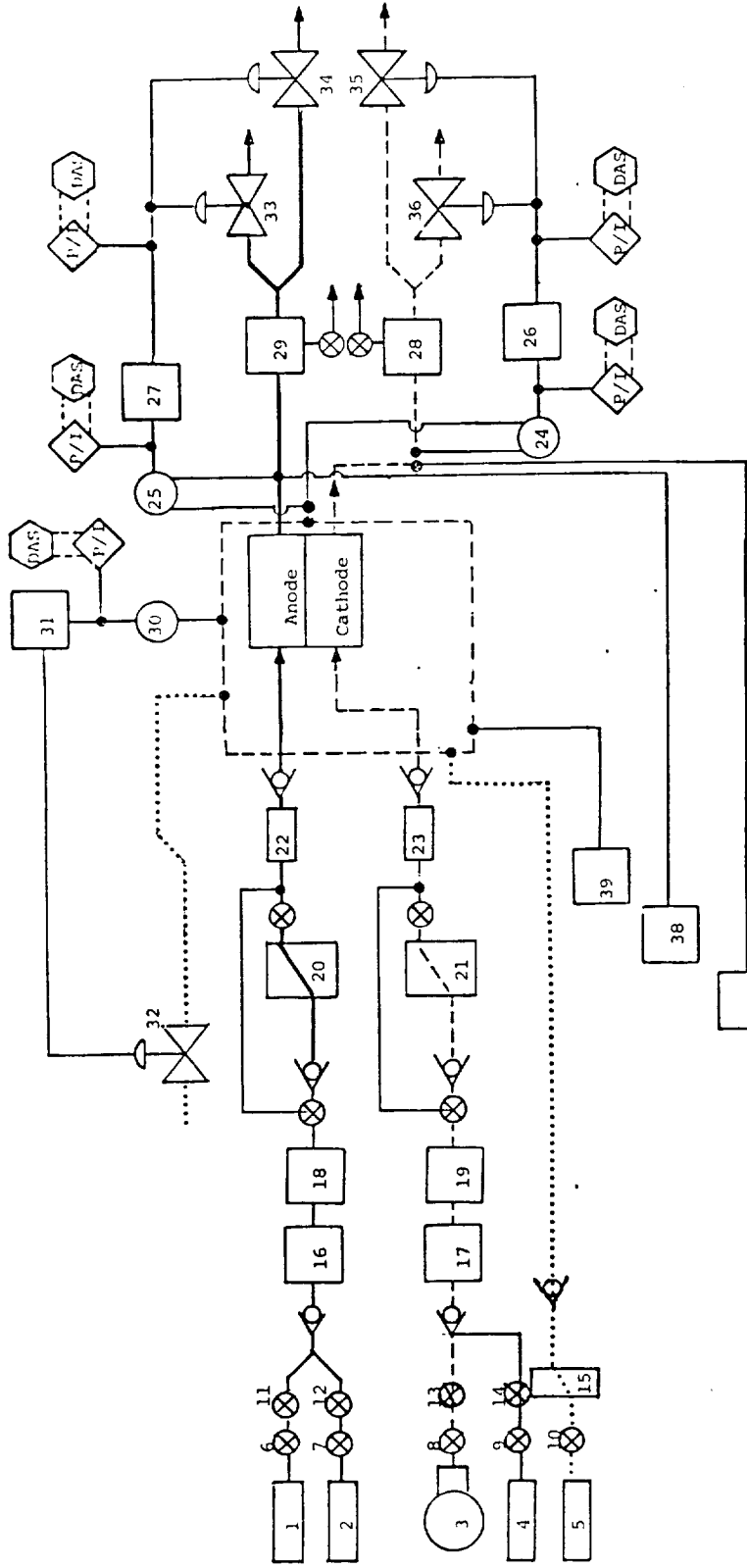
1	Fuel Supply	11-14	Valves	24-25	Differential Pressure Transmitters
2	External Fuel Supply	15	Rotameter	26-27	Differential Pressure Controllers
3	Air Compressor	16-17	Mass Flow Transducers	28-29	Condensers
4	External Oxidant Supply	18-19	Mass Flow Controllers	30	Pressure Transmitter
5	Vessel Atmosphere Supply	20-21	Humidifiers	31	Pressure Controller
6-10	Pressure Regulators	22-23	Preheaters	32-36	Pressure Control Valves
				37-39	Pressure Gauges

TABLE 4.8   OPERATIONAL CHARACTERISTICS OF PRESSURIZED TEST FACILITY FOR 5-CELL STACK

Pressure Range	:	100 to 1000 kPa
Standard Gases	:	H_2 fuel, air oxidant, auxiliary inputs for special gases
Current Range	:	0 to 200 mA/cm^2
Fuel Flow Range	:	Up to 80% utilization at 50 mA/cm^2
Vaporizer Capacity	:	Up to 6 SLM of water vapor
Oxidant Flow Range	:	Up to 50% utilization at 50 mA/cm^2 20% to 100% utilization at 600 mA/cm^2
Temperature Range	:	30 to 250°C

Controlled Operating Parameters

- Vessel pressure (pneumatic control)

- Current (manual)

- Temperatures: air, fuel, cooling and cell (temperature controller)

- Fuel compositions (manual)

- Air and fuel flow rates (manual)

- Cathode to vessel and anode to vessel differential pressures (pneumatic control)

- Water level in the condenser water trap (automatic)

Performance Measurements

- Cell Voltage

- Temperature distribution

- Pressure drop across stack in all streams (only one stream per test)

The design details of some of the important subsystem components are discussed below.

- Pressure Vessel: A pressure vessel fitted with a blind flange was designed according to the ASME code to operate at 2200 kPa and 177°C and to test up to 52-cm tall 1200-cm^2 (12 inch x 17 inch) size fuel cell stacks. The vessel was made of carbon steel; the vessel bottom and the flanges were faced with SS-316.

- Pressure Fittings: Voltage leads, thermocouple wires and solid conductors penetrating into the pressure vessel from the test panels are to be sealed against the operating pressure of the vessel. Conax type sealant glands are commercially available. An alternate, simpler means for sealing electrical wires, thermocouples and solid conductors was developed and successfully implemented.

- Fuel Humidifier: Dry fuel (a mixture of H_2, CO and CO_2) was humidified to simulate the fuel composition obtained from a fuel processor. A positive displacement pump was used in combination with an electrically heated vaporizer.

- <u>Data Acquisition System (DAS)</u>: A Kaye Instruments scanner was used for reading the measured variables (current, flow rates, temperatures, voltages, pressure, and differential pressures). An Apple II Plus microcomputer was used for data recording and data manipulation. The system used a floppy disk for data storage.

Facility check out and stack operation could not be performed during this program because of a reduction in funding.

THIS PAGE INTENTIONALLY LEFT BLANK

1. Report No. NASA CR- 174660	2. Government Accession No.	3. Recipient's Catalog No.
4. Title and Subtitle Full Scale Phosphoric Acid Fuel Cell Stack Technology Development		5. Report Date
		6. Performing Organization Code
7. Author(s) L. Christner, M. Farooque		8. Performing Organization Report No. Final Technical Report
9. Performing Organization Name and Address Energy Research Corporation 3 Great Pasture Road Danbury, CT 06810		10. Work Unit No.
		11. Contract or Grant No. DEN3-205
12. Sponsoring Agency Name and Address U.S. Department of Energy Division of Fossil Fuel Utilization Washington, DC 20545		13. Type of Report and Period Covered
		14. Sponsoring Agency Code DOE/NASA/0205-8

15. Supplementary Notes

Final Technical Report prepared under interagency agreement DE-A101-80ET17088. Project Manager, Robert B. King, Solar and Electrochemistry Division, NASA Lewis Research Center, Cleveland, OH 44135

16. Abstract

This report summarizes the technology development for phosphoric acid fuel cells on NASA contract DEN3-205, which is an extension of contract DEN3-67. The effort was limited due to a funding decrease; however, several topics were investigated: preparation, heat treatment, and characterization of carbon composites used as bipolar separator plates was carried on. The molded materials contained 30 to 80% resin and were heat treated between 900 and 2700°C. Characterization included resistivity, porosity, and electrochemical corrosion. These high density glassy carbon/graphite composites worked well in long term (>22,000 hours) fuel cell endurance tests.

Platinum alloy cathode catalysts and low-loaded platinum electrodes were evaluated in 25-cm^2 cells. Although the alloys show an initial improvement, some of this improvement is diminished after few thousand hours. These materials looked promising for future development. Low platinum loading (0.12 mg/cm^2 anodes and 0.3 mg/cm^2 cathodes) performed about the same as twice this loading.

A selectively wetproofed anode backing paper was tested in 5 inch x 15 inch 3-cell stack. This material may provide for acid volume expansion, acid storage, and acid lateral distribution.

17. Key Words (Suggested by Author(s)) Fuel Cells, Phosphoric Acid, Carbon Corrosion, Alloy Catalysts, Carbon Composites.	18. Distribution Statement Unclassified Unlimited STAR Category 44 DOE Category UC97d
19. Security Classif. (of this report)	20. Security Classif. (of this page)	21. No of Pages	22. Price*

* For sale by the National Technical Information Service, Springfield, Virginia 22161

NASA-C-168 (Rev. 10-75)

FINAL DISTRIBUTION LIST FOR CONTRACT NO. DEN3-205

Mr. Charles Pax	1	Mr. R. P. Stickles	1
Mr. Graham Hagey	1	Arthur D. Little, Inc.	1
U.S. Dept. of Energy		32-126 Acorn Park	
20 Massachusetts Ave., NW		Cambridge, MA 02140	
Washington, DC 20545			

Mr. W. O'Grady   1
Brookhaven National Laboratory
Upton, NY 11973

Dr. A. J. Appleby   1
Mr. E. Gillis   1
Electric Power Research
  Institute
3412 Hillview Avenue
P.O. Box 10412
Palo Alto, CA 94304

Professor E. Yeager   1
Case Western Reserve University
Electrochemistry Laboratory
University Circle
Cleveland, OH 44106

Ms. Diane T. Hooie   1
Mr. Richard R. Woods   1
Mr. John Cuttica   1.
Gas Research Institute
8600 W. Bryn Mawr Avenue
Chicago, IL 60631

Dr. James Cusamano   1
Catalytics Associates, Inc.
3255 Scott Boulevard
Suite 7-E
Santa Clara, CA 95051

Dr. Gerald Voecks   1
MS 125-159
Jet Propulsion Laboratory
4800 Oak Grove Drive
Pasadena, CA 91103

Dr. Fraser Walsh   1
ECO, Inc.
225 Needham Street
Newton, MA 02164

Dr. S. B. Brummer   1
EIC Laboratories, Inc.
55 Chapel Street
Newton, MA 02158

Dr. J. Stuart Fordyce   1
Mr. Robert B. King   5
M.S. 5-5
NASA-Lewis Research Center
21000 Brookpark Road
Cleveland, OH 44135

Dr. Bernard S. Baker   1
Dr. Larry Christner   1
Energy Research Corporation
3 Great Pasture Road
Danbury, CT 06810

Dr. R. R. Barthelemy   1
Air Force Aero Propulsion
  Laboratory
Wright-Patterson AFB, OH 45433

Dr. Arthur Kaufman   1
Engelhard Industries Division
Menlo Park
Edison, NJ 08817

Dr. John Ackerman   1
  CEN, D-205
Argonne National Laboratory
9700 South Cass Avenue
Argonne, IL 60439

Mr. J. Surfess   1
Fuel Cell User's Group
Energy Transition Corporation
1101 Connecticut Avenue, N.W.
Washington, DC 20036

Dr. Johann Joebstel   1
U.S. Army MERADCOM
DRDME-EC
Fort Belvoir, VA 22060

FINAL DISTRIBUTION LIST FOR CONTRACT NO. DEN3-205 (Continued)

Dr. Vinod Jalan   1
Giner, Inc.
14 Spring Street
Waltham, MA 02154

Mr. Elias H. Camara   1
Institute of Gas Technology
3424 S. State Street
Chicago, IL 60616

Dr. P.N. Ross   1
Materials & Molecular
   Research Division
Lawrence Berkeley Laboratories
Berkeley, CA 94720

Dr. Ross Lemons   1
Dr. James Huff   1
Los Alamos Scientific Laboratory
P.O. Box 1662
Los Alamos, NM 87545

Mr. Dan Schnyer   1
Code REC-14
NASA Headquarters
Washington, DC 20546

Dr. R. Fernandes   1
Niagra Mohawk Power
300 ERie Blvd., West
Bldg. C-3
Syracuse, NY 13202

Dr. Paul Stonehart   1
Stonehart Associates
P.O. Box 1220
Madison, CT 06443

Mr. Bernard Jackson   1
TVA
Division of Energy Demo. & Tech.
Office of Power, 501 CEB
Muscle Shoals, AL 35660

Dr. Lawrence B. Welsh   1
Universal Oil Products
10 UOP Plaza
Des Plaines, IL 60016

Mr. John Bett   1
United Technologies Corporation
P.O. Box 109
South Windsor, CT 06074

Dr. J. Brown   1
Westinghouse R&D Center
1310 Beulah Road
Pittsburgh, PA 15235

Mr. J.J. Buggy   1
Mr. J.M. Feret   1
Westinghouse Electric Corporation
Advanced Energy Systems Division
P.O. Box 10864
Pittsburgh, PA 15236

Editor   1
A.G.A. Monthly
American Gas Association
1515 Wilson Boulevard
Arlington, VA 22209

Dr. R. Eric Leber   1
American Public Power Assoc.
2600 Virginia Avenue, NW
Washington, DC 20037

Professor R. T. Foley   1
The American University
Department of Chemistry
Nebraska & Massachusetts Ave., NW
Washington, DC 20546

Mr. Earle H. Knowles   1
Arizona Public Service Company
P.O. Box 21666, Station 1332
Phoenix, AZ 85036

Mr. M. L. Deviney   1
Ashland Chemical Company
Res. & Develop. Center
P.O. Box 2219
Columbus, OH 43216

Mr. David D. Marchant   1
Ceramics & Graphite Section
Battelle Pacific Northwest Labs.
P.O. Box 999
Richland, WA 99352

FINAL DISTRIBUTION LIST FOR CONTRACT NO. DEN3-205 (Continued)

Mr. Sidney Gross   1
Boeing Company
M.S. 8C-62
P.O. Box 3999
Seattle, WA 98124

Mr. Kenneth R. Dow, Jr.   1
R-234
Boston Edison
800 Boylston Street
Boston, MA 02199

Mr. Peter Steitz   1
Power Division
Burns & McDonnell
P.O. Box 1763
Kansas City, MO 64141

Dr. Stephan A. Fogelson   1
Burns & Roe, Inc.
185 Crossways Park Drive
Woodbury, NY 11797

Mr. David Wang   1
California Energy Commission
1111 Howe Avenue, MS-68
Sacramento, CA 95825

Mr. William F. Morse   1
Director of Research
Columbia Gas System
Columbus, OH 43202

Dr. Robert A. Bell   1
Consolidated Edison Company
4 Irving Place - Rm. 14146
New York, NY 10003

Dr. M. Eisenberg   1
Electrochemica Corporation
21485 Charleston Road
Mountain View, CA 94040

Dr. Theodore R. Beck   1
Electrochemical Technology Corp.
3935 Leary Way, N.W.
Seattle, WA 98107

Mr. T. C. Weaver   1
Florida Power Corporation
P.O. Box 14042
St. Petersburg, FL 33733

Mr. D. Chatterji   1
General Electric Company DECP
50 Fordham Road
Wilmington, MA 01887

Mr. J. Peterson   1
General Electric Company
#1 River Road
Bldg. 23, Room 290
Schnectady, NY 12345

Dr. John C. Cutting   1
Gilbert Associates, Inc.
P.O. Box 1498
Reading, PA 19603

Mr. Joseph A. Orlando   1
GKCO Consultants
Suite 328
4600 Duke Street
Alexandria, VA 22304

Mr. Ed Thellman   1
Dept. 741
Gould Inc.
Ocean Systems Division
18901 Euclid Avenue
Cleveland, OH 44117

Mr. Krishna Chandra   1
Holmes & Narver, Inc.
9999 Town & Country Road
Orange, CA 92668

Dr. Dirk Pouli   1
Hooker Chemicals & Plastic Corp.
Research Ctr., Grand Islands
Niagara Falls, NY 14302

Dr. Thomas J. Hirt   1
Vice President
InterNorth, Inc.
4840 F Street
Omaha, NE 68102

Dr. A. M. Moos   1
Leesona Moos Laboratories
Leesona, Inc.
Strawberry Field Road
Warwick, RI 02886

FINAL DISTRIBUTION LIST FOR CONTRACT NO. DEN3-205 (Continued)

Dr. J. J. Rasmussen   1
Montana Energy & MHD Research
  and Develop. Institute, Inc.
P.O. Box 3809
Butte, MT 59702

Dr. R. A. Goffe   1
Monstanto Co.
800 N. Lindbergh Blvd.
St. Louis, NO 63166

Mr. S. J. Schneider   1
Deputy Chief, Div. 561
A 257 Materials Bldg.
National Bureau of Standards
Washington, DC 20234

Mr. Albert Himy   1
Electrochemical Power Sources
Naval Sea Systems Command
NAVSEA 5433
Washington, DC 20362

Dr. George Neece   1
Code 472
Office of Naval Research
800 N. Quincy Street
Arlington, VA 22217

Mr. S. H. Law   1
Northeast Utilities Service Co.
P.O. Box 270
Hartford, CT 06101

Mr. William Mixon   1
Oak Ridge National Laboratory
P.O. Box X
Oak Ridge, TN 37830

Mr. John Kekela   1
Ohio Edison Company
76 South Main Street
Akron, OH 44308

Dr. Leonard G. Austin   1
Mineral Processing Sec.
108 Steidle Bldg.
Pennsylvania State Univ.
University Park, PA 16802

Mr. J.P. Gibbons   1
Energy Conversion Research
Philadelphia Electric Co.
S10-1, 2301 Market Street
Philadelphia, PA 19101

Mr. P. A. Lewis   1
Mr. W. Wood   1
PSE & G
80 Park Plaza, T-14A
Neward, NJ 07101

Professor O. Lindstrom   1
Dept. of Chemical Technology
Royal Institute of Technology
S-100 44 Stockholm
SWEDEN

Mr. J. G. Montgomery   1
San Diego Gas & Electric
P.O. Box 1831
San Diego, CA 92112

Mr. Barry R. Flynn   1
Santa Clara Municipal
  Electric Department
1500 Warburton Drive
Santa Clara, CA 95050

Mr. Craig R. Cummings   1
Science Applications, Inc.
1200 Prospect Street
LaJolla, CA 92037

Mr. K. R. Williams   1
PAI, Shell Int'l, Petro. Co.
Shell Center
SE1-7NA London
ENGLAND

Mr. R. D. Weaver   1
Stanford Research Institute
333 Ravenswood Avenue
Menlo Park, CA 94025

Professor David M. Mason   1
Dept. of Chemical Engineering
Stanford University
Stanford, CA 94305

ENERGY RESEARCH CORPORATION

<u>FINAL DISTRIBUTION LIST FOR CONTRACT NO. DEN3-205 (Concluded)</u>

Mr. Guido E. Guazzoni   .1
Power Sources Division
DELET/PE
Fort Monmouth, NJ   07703

Mr. Lloyd M. Pernela   1
Dept. of Comm. for State of
  Alaska
338 Denali Street
Anchorage, AK   99501

Dr. Nehemiah Margalite   1
C.E. Power Systems
Combustion Engineering, Inc.
Mail Drop 9452-LA04
1000 Prospect Hill Road
Windsor, CT   06095